Kinetochore activation of the spindle checkpoint by the kinase Mps1

Nitobe London

A dissertation

submitted in partial fulfillment of the

requirements for the degree of

Doctor of Philosophy

University of Washington

2015

Reading Committee:

Sue Biggins, Chair

Toshi Tsukiyama

Linda Wordeman

Program Authorized to Offer Degree:

Molecular and Cellular Biology

University of Washington

Abstract

Kinetochore activation of the spindle checkpoint by the kinase Mps1

Nitobe London

Chair of the Supervisory Committee:
Dr. Sue Biggins, Full Member
Division of Basic Sciences

Chromosome segregation is essential for faithful cell division and missegregation is associated with birth defects and cancer. Missegregation is prevented by the spindle checkpoint, which monitors attachments between microtubules and kinetochores prior to anaphase. Kinetochores are protein complexes that mediate microtubule-chromosome attachments and also signal the checkpoint by generating a soluble inhibitor of an ubiquitin-ligase that is necessary for anaphase onset. Checkpoint signaling is accomplished through localizing checkpoint proteins to kinetochores and requires activity of the conserved kinetochore kinase Mps1. These checkpoint proteins include Bub1 and Bub3, which perform additional functions to support chromosome segregation, as well as the checkpoint proteins Mad1, Mad2, and Mps1. Kinetochore localization of Mad1 and Mad2 is strictly correlated with checkpoint signaling. How these checkpoint proteins localize to kinetochores as well as the function of Mps1 activity in the spindle checkpoint was unknown. Here, I utilized purified kinetochore particles to address the role of Mps1 in checkpoint function. I first determined that Mps1 kinase activity was the dominant

activity on kinetochores in vitro, even though the kinase Bub1 and phosphatases also copurify. I was then able to reconstitute Bub1 and Bub3 binding to kinetochores in vitro and demonstrated that this binding was dependent upon Mps1 phosphorylation of the core kinetochore protein Spc105 on conserved MELT-like motifs. Similarly, I reconstituted the downstream Mad1 kinetochore binding event with native kinetochores as well as with recombinant proteins. Translational fusion experiments indicated that a domain of Bub1 is sufficient for Mad1 kinetochore binding, and this binding required Mps1 activity towards Bub1. *MPS1* overexpression arrested cells independently of Spc105 MELT phosphorylation but not Bub1 phosphorylation, highlighting the significance of Bub1 phosphorylation in checkpoint signaling. Together, this data reveals the deterministic role for Mps1 kinase activity in kinetochore checkpoint activation and clarifies the steps that must be taken to inactivate the checkpoint upon microtubule attachment to kinetochores.

ACKNOWLEDGEMENTS

I am deeply indebted to members of the Biggins lab and the local research community for constructive feedback, ideas, and technical assistance. Special thanks go out to Bungo Akiyoshi for instruction in the methods he developed to purify kinetochore particles and to Steven Ceto for experimental contributions. Valuable critical comments on manuscripts were provided by Bungo, Chip Asbury, Gary Deyter, Erica Hildebrand, and Matt Miller. I am greatly indebted to my advisor, Dr. Sue Biggins for endless support, inspiration, and a limitless supply of stimulating ideas. I also thank Chip Asbury and Geert Kops for significant critical contributions to my research, and am very grateful for help with mass spectrometry experiments by members of the Ranish lab - Jeff Ranish, Jie Luo, and Bong Kim - as well as Phil Gafken. Reagent requests were kindly answered by the labs of Trisha Davis, Arshad Desai, Kevin Hardwick, Prasad Jallepalli, Adele Marston, David Morgan, Andrew Murray, Andrea Musacchio, Karsten Weis and Mark Winey. I am further grateful for the input of the constituent members of the Seattle mitosis club, particularly the Asbury, Davis, and Wordeman labs. Finally, the contributions of my thesis committee, consisting of Sue Biggins Jim Priess, Jeff Ranish, Susan Parkhurst, and Toshi Tsukiyama have been an invaluable asset to my projects. I would also like to thank Sue, Toshi, Linda, and Lori Koch for providing insightful comments on this manuscript.

DEDICATION

This work is dedicated to my dog Sedona in loving memory.

TABLE OF CONTENTS

LIST OF FIGURES

LIST OF TABLES

Chapter I: Introduction

Chromosome segregation is an essential process in eukaryotic cells that allows faithful transmission of genetic material. Inaccurate segregation results in aneuploid daughter cells, which are associated with genetic instability and disease including cancer and birth defects. Aneuploidy is a distinguishing feature of most cancer cells that is exploited by chemotherapies that have harmful side effects, so the study of chromosome segregation can potentially lead to improved cancer treatments.

Segregation is preceded by chromosome replication during S-phase. To hold the replicated chromosomes together with their parental chromosomes, the cohesin protein complex is loaded concomitantly with DNA synthesis, forming linked sister chromatids. During mitosis, chromosomes attach to spindle microtubules through protein super-complexes called kinetochores, which bind to centromeric chromatin. Kinetochores can attach to microtubules emanating from either pole, but accurate segregation requires the correct attachment configuration. That is, sister kinetochores must be attached to microtubules from opposite spindle poles in a bioriented, or amphitelic, configuration (Fig I.A). Upon anaphase onset, the cohesin linkage is proteolytically cleaved and sister chromatids are physically separated to opposite poles by pulling forces from spindle microtubules. Proper execution of these events relies upon a mechanism, here referred to as the spindle checkpoint, which couples kinetochore-microtubule attachment status to cell cycle progression. The checkpoint is exquisitely sensitive in that a single unattached kinetochore is sufficient for a robust arrest of the cell cycle (Rieder et al., 1995), although the checkpoint response is enhanced by additional errors (Collin, 2013, Dick, 2013, Weaver, 2003, Reider, 2004).

Biorientation and microtubule attachment

Microtubules sporadically switch between polymerization and depolymerization in a process termed dynamic instability (Mitchison and Kirschner, 1994). This allows spindle microtubules to search space between the spindle poles and eventually contact a kinetochore. However, kinetochores cannot distinguish microtubules from either pole upon initial contact, so attachment errors are common. Cells must ensure both that attachments occur and that they are equivalent between opposite spindle poles, preventing monotelic and syntelic attachments, respectively (Fig I.A). An additional attachment state is

possible, merotelic attachments, where a single kinetochore is attached to multiple microtubules from opposite poles. However, these do not occur in budding yeast where kinetochores only bind to a single microtubule per kinetochore (Winey et al., 1995).

Incorrect microtubule attachment configurations can cause missegregation if they endure into anaphase, so cells employ several mechanisms that ensure biorientation prior to anaphase. Particularly well studied are a mechanism called the spindle checkpoint and a closely related function called error correction. Both of these mechanisms depend on kinase activity towards kinetochore proteins. The spindle checkpoint is initiated by signaling events at kinetochores and ultimately results in a metaphase arrest. This arrest allows time for error correction to occur. Error correction is the destabilization of incorrect kinetochore-microtubule attachments, formation of new attachments, and the stabilization of correct attachments. Both of these mechanisms are signaled by incorrect microtubule attachments. Additional mechanisms may also contribute to correct biorientation, such as a geometric bias of sister kinetochores to attach to opposite poles (Indjeian and Murray, 2007), although these mechanisms are less well understood.

Kinetochore composition and function

Central to all of these segregation functions is the kinetochore. Composed of over 45 unique proteins, the kinetochore is a highly complex protein assembly with numerous functions that are dynamically regulated. A large number of proteins comprise the inner kinetochore, which binds centromeric chromatin and specifies centromeric identity in most organisms. Many of these proteins perform redundant functions, while several are strictly required for DNA binding or for scaffolding the kinetochore (Fig I.B) (Biggins, 2013; Musacchio and Salmon, 2007). Linkages between the inner and outer kinetochore proteins are complex and may be subject to cell cycle-driven phosphoregulation (Akiyoshi et al., 2013; Bock et al., 2012; Emanuele et al., 2008; Thapa et al., 2015; Yang et al., 2008). However, the Mtw1^{Mis12} complex seems to function as a nexus point between nearly all inner and outer kinetochore proteins. (A recently discovered interaction between the inner kinetochore protein Cnn1 and the outer kinetochore protein Ndc80 bypasses Mis12c, but the significance of this interaction is still unclear (Bock et al., 2012; Malvezzi and Westermann, 2014; Schleiffer et al., 2012; Thapa et al., 2015).)

The outer kinetochore attaches to microtubules through three subcomplexes, Ndc80c, Spc105, and Dam1c, although the Spc105-microtubule interaction has not been conclusively demonstrated in budding yeast with recombinant proteins (Fig I.B)(Pagliuca et al., 2009). Together, these three subcomplexes comprise the KMN network (for the metazoan subcomplexes Knl1^{Spc105}, Mtw1^{Mis12}, Ndc80)(Cheeseman et al., 2006). Each of the proteins within these subcomplexes are present in multiple copies, with approximately 8 Ndc80c subcomplexes and 16 Dam1c subcomplexes per kinetochore (Joglekar et al., 2008). Ndc80 provides a major microtubule-binding activity that is important for initial attachments as well as load-bearing attachments (Biggins, 2013). Dam1c provides a processivity function for the kinetochore to stay attached to depolymerizing microtubules. It is not conserved across eukaryotes, but appears instead to be functionally similar to the human Ska complex (Welburn et al., 2009). Spc105^{Knl1} appears to contribute to microtubule affinity of the other subcomplexes with human proteins in vitro (Welburn et al., 2009), but may not be important for robust attachments in vivo in *C. elegans*. Instead, the microtubule-binding function of *C. elegans* Spc105^{Knl1} may play a role in checkpoint silencing (Espeut et al., 2012).

Phosphoregulation of kinetochore functions

Both error correction and the spindle checkpoint are regulated by phosphorylation at the kinetochore, and a major line of research has been to unravel the kinases and substrates involved and the molecular mechanisms that allow the processes to occur and to respond to microtubule attachment. Initial successes were achieved in elucidating Ipl1 as the error correction kinase (Biggins et al., 1999; Tanaka et al., 2002). Pioneering work identifying Ipl1 targets by mass spectrometry helped determine a high-fidelity consensus target motif for Ipl1, rendering identification of additional phosphorylation sites reasonably straightforward (Cheeseman et al., 2002). Phosphorylation of KMN proteins by Ipl1^{AuroraB}, particularly Ndc80 and Dam1, contributes to destabilization of microtubule attachments (Funabiki and Wynne, 2013), promoting microtubule release. Meanwhile, Ipl1 phosphorylation of Spc105^{Knl1} opposes localization of the phosphatase PP1. Kinetochore-associated PP1, and potentially other phosphatases including PP2A, restores microtubule affinity, permitting new attachments to form (Foley and Kapoor, 2012; Funabiki and Wynne, 2013). Tension-bearing microtubule attachments seem to reduce Ipl1 activity

towards the outer kinetochore, enhancing PP1 binding and decreasing Ndc80 and Dam1 phosphorylation and thereby stabilizing attachments. Ipl1 and PP1 therefore form part of a feedback loop that enables a switch-like response to incorrect attachment (Nijenhuis et al., 2014).

Exactly how the activity of Ipl1 towards outer kinetochore substrates is determined by microtubule attachments is a longstanding question in the field. Recent work has led to the current view that this activity is related to the ability of the kinetochore to stretch when bound to a pulling microtubule (Maresca and Salmon, 2009). This is an attractive explanation for the ability of kinetochores to monitor tension in addition to attachment and makes intuitive sense because Ipl1 localizes to centromeric chromatin, distal from the outer kinetochore. Nonetheless, the magnitude of kinetochore stretch is very small and may be more consistent with other mechanisms (Maresca and Salmon, 2010).

In addition to error correction, Ipl1 is also necessary to activate the checkpoint when kinetochores are attached to microtubules that are not under tension (Biggins, 2001). In contrast, the kinetochore kinase Mps1 is required for the checkpoint under all conditions. Mps1, which binds to the outer kinetochore (Kemmler, 2009), also promotes biorientation through an unknown mechanism (Jones et al., 2005; Maure et al., 2007). Ipl1^{AuroraB} enhances Mps1 kinetochore localization and activation in human cells (Nijenhuis et al., 2013; Santaguida et al., 2010; Saurin et al., 2011), but evidence for this function has not been found in yeast (Maure et al., 2007). The tension-specific requirement for Ipl1 may reflect an indirect role for Ipl1 in checkpoint activation through disrupting tensionless microtubule attachments, generating unattached kinetochores that stimulate signaling (Pinsky et al., 2006).

In addition to its strict requirement for the checkpoint, Mps1 is the only kinase that leads to checkpoint arrest when overexpressed. Despite its clear importance, the basis for Mps1 checkpoint function remained unknown because of difficulty identifying relevant substrates. Part of this difficulty is due to the promiscuity of Mps1, which does not adhere to a strict substrate consensus motif, as does Ipl1 (Mok et al., 2010). This promiscuity also suggests that Mps1 is likely to have multiple functionally redundant targets and leads to weak substrate specificity in vitro, further complicating traditional identification approaches. An additional difficulty is the complexity of the kinetochore, which contains many potential substrates. Mps1 appears to bind to kinetochores through the Ndc80 protein, although additional receptors may exist (Kemmler et al., 2009). In addition, budding yeast Mps1 is required for

spindle pole body duplication, an essential process, making kinetochore functions challenging to study specifically in vivo. To aid in the study of Mps1 function, an analog-sensitive allele, *mps1-as1* was developed (Jones et al., 2005) that can be specifically inhibited with an ATP analog compound, and this has been used for phenotypic analysis of Mps1 as well as substrate identification (Jones et al., 2005; London et al., 2012; Maciejowski et al., 2010). Numerous temperature-sensitive alleles of Mps1 also exist in yeast, including the highly destabilizing *mps1-1* allele (Castillo et al., 2002; Lauzé et al., 1995; Schutz and Winey, 1998), and chemical inhibitors can be utilized in human cells (Lan and Cleveland, 2010).

Like Ipl1 and Mps1, Bub1 is a checkpoint protein and kinase that localizes to kinetochores. It is required for tension-responsive checkpoint activation, presumably because it is necessary to localize Ipl1 (Funabiki and Wynne, 2013; Kawashima et al., 2010). Bub1 also serves an additional function in chromosome segregation because *bub1*Δ cells display reduced viability relative to *MAD* gene deletions that also override the checkpoint (Fig IV.5A). Bub1 kinase activity promotes centromeric localization of the protein Sgo1 through phosphorylation of histone H2A (Kawashima et al., 2010). Sgo1 is necessary for Ipl1 localization as well as additional mechanism(s) that promote biorientation (Storchová et al., 2011). Bub1 has also been reported to phosphorylate the checkpoint protein Cdc20 in human cells, although it is not clear precisely how this contributes to checkpoint activity (Tang et al., 2004). In any case, Bub1 kinase activity is not required for a spindle checkpoint response due to lack of attachment whereas the presence of the Bub1 protein is (Fernius and Hardwick, 2007), so the Bub1 protein has multiple functions in the checkpoint.

Several, additional kinases and phosphatases localize or are active at kinetochores (Funabiki and Wynne, 2013). In humans, the phosphatase PP2A also functions in both error correction (Foley and Kapoor, 2012) and in checkpoint silencing through promoting PP1 kinetochore association (Nijenhuis et al., 2014). These functions for PP2A may not be conserved in yeast because the PP2A receptor homolog, $Mad3^{BubR1}$, does not localize to kinetochores in budding yeast and does not have the PP2A recognition consensus motif (Gillett, 2004; Suijkerbuijk et al., 2012a). The phosphatase Cdc14 promotes mitotic exit by opposing Cdk1/cyclin B phosphorylation, but it is thought to remain tightly sequestered prior to early anaphase and so is likely to be downstream of checkpoint-silencing phosphatases (Wurzenberger and Gerlich, 2011). Polo kinase localizes to kinetochores in most eukaryotes and

performs functions important for mitotic entry and exit, but the yeast homolog, Cdc5, does not appear to localize to kinetochores (Funabiki and Wynne, 2013). Finally, the mitotic master regulator Cdk1 phosphorylates kinetochore substrates, but has not been found to stably associate with the kinetochore (Funabiki and Wynne, 2013).

The spindle checkpoint

Historically, the kinetochore has been viewed as generating a "wait anaphase" signal in response to incorrect attachments (London and Biggins, 2014a). Anaphase onset occurs upon the destruction of cyclin B, the mitotic cofactor of Cdk1 which stimulates numerous mitotic events, as well as the cohesin complex that holds sister chromatids together (London and Biggins, 2014a). The securin protein inhibits proteolytic cleavage of cohesion and thereby inhibits anaphase onset. Proteolysis of both cyclin B and securin is mediated by an ubiquitin-ligase complex called the Anaphase Promoting Complex/Cyclosome (APC/C). The APC/C depends upon the cofactor Cdc20 that targets cyclin B and securin for ubiqituitylation through degron motifs. To promote a metaphase arrest, the spindle checkpoint stabilizes cyclin B and securin by inhibiting activity of the APC/C.

Proper function of the spindle checkpoint requires numerous genes, most of which were identified in budding yeast in screens for mutants that did not arrest in response to microtubule-destabilizing drugs (Hoyt et al., 1991; Li and Murray, 1991). The checkpoint proteins Bub1, Bub3, Mad1, Mad2, Mad3^{BubR1}, and Mps1, all localize to kinetochores upon checkpoint activation in most organisms, except Mad3^{BubR1} localization has not been detected in budding yeast (Gillett, 2004). Cdc20 also localizes to mammalian kinetochores, although this may be transient in budding yeast (Yang et al., 2015). Kinetochore localization of these proteins leads to the generation of the Mitotic Checkpoint Complex (MCC) (Fig I.C), which inhibits the APC/C by numerous mechanisms (Primorac and Musacchio, 2013) and can be considered the soluble "wait anaphase" signal. Pioneering photobleaching experiments demonstrated that localization of checkpoint proteins is dynamic, with one pool of Mad2 exhibiting rapid turnover (Howell et al., 2004; Shah et al., 2004). Biochemical experiments, including copurification and gel filtration of checkpoint proteins, defined interactions between checkpoint proteins and determined that the MCC is the major inhibitor of anaphase (London and Biggins, 2014a). These and related experiments indicated

that Bub1 and Bub3 form a constitutive complex (Bub1/3) and that Mad1 forms a constitutive complex with Mad2 (Mad1/2). In contrast, Mad3^{BubR1} forms a regulated complex with Bub3, and Mad2 forms a regulated complex with Cdc20 (Brady and Hardwick, 2000; Hwang et al., 1998; Kim et al., 1998). Together, these four proteins - Mad2, Cdc20, Bub3, and Mad3^{BubR1} - assemble into the MCC through an unresolved pathway. Although the checkpoint proteins show high functional conservation across eukaryotes, Mad3^{BubR1} has diverged significantly across evolution, with Bub3 binding remaining conserved (Suijkerbuijk et al., 2012b).

Generation of the MCC is ultimately directed by kinetochores, but the details of how this occurs are complex and are still being elucidated. Recent progress has helped clarify the roles of the four MCC proteins in MCC function. Cdc20 interactions with Mad2 and Mad3^{BubR1} both play important roles, with Mad3^{BubR1} perhaps functioning as the dominant inhibitor of Cdc20 (Han et al., 2013). Bub3, however, may serve to mediate Mad3^{BubR1}-Cdc20 interactions (Han et al., 2014). The MCC is continuously disassembled, so kinetochores must promote its assembly at a greater rate in order to successfully inhibit the APC/C (Primorac and Musacchio, 2013) and MCC assembly likely involves clustering of MCC components. One important event is the kinetochore localization of Cdc20, which binds to Bub1 and BubR1 on human kinetochores through newly elucidated short linear motifs (Diaz-Martinez et al., 2014; Di Fiore et al., 2015; Lischetti et al., 2014). The key dynamic event in checkpoint activation, however, is believed to be catalytic activation of Mad2. Mad2 exists in a higher energy open form (O-Mad2) and more stable closed form (C-Mad2). C-Mad2 binds to Mad1 or Cdc20, while O-Mad2 cannot bind to these proteins but can dimerize with C-Mad2 (Luo and Yu, 2008; Mapelli and Musacchio, 2007). The prevailing model is that a kinetochore-bound pool of Mad1/C-Mad2 recruits O-Mad2 through Mad2 dimerization and converts it to C-Mad2, which binds to Cdc20 and forms part of the MCC. The critical regulatory step in this process is believed to be the kinetochore localization of Mad1/2. Mad1/2 complexes are always present in the cell, but for unknown reasons the kinetochore pool of Mad1/2 seems to be necessary to activate the checkpoint. Mad1/2 kinetochore localization is strictly correlated to checkpoint activity and requires the function of upstream checkpoint proteins Bub1/3 and Mps1. In this hierarchy, Mps1 kinase activity is required for localization of Bub1/3 and all other checkpoint proteins, with the potential exception of Ipl1^{AuroraB} (Abrieu et al., 2001; Heinrich et al., 2012; Nijenhuis et al., 2013; Tighe et al., 2008).

Recent advances, such as those detailed above, have propelled our understanding of kinetochore function forward dramatically in recent years. Biochemical and structural work, including new super-resolution microscopy approaches (Joglekar et al., 2009; Varma et al., 2013; Wan et al., 2009), have illuminated the architecture of the kinetochore as a whole and the interactions of the individual subcomplexes. Of particular note, a method was recently developed to purify intact native kinetochore particles (Akiyoshi et al., 2010). This advance has so far aided in defining the core composition of kinetochores, elucidating the biophysical properties of kinetochore-microtubule binding, and providing high resolution electron microscopy of the kinetochore (Akiyoshi et al., 2010; Gonen et al., 2012; Sarangapani et al., 2013). It also opens the door to investigating the dynamic biochemical events at the kinetochore in vitro.

To overcome existing limitations with in vitro approaches, I set out to reconstitute checkpoint protein binding events to kinetochores with native kinetochore particles. I found that Mps1 kinase activity specifically copurifies with kinetochore particles and is capable of promoting checkpoint protein-kinetochore binding in vitro. I then used this to identify the relevant Mps1 substrates. I determined that Mps1 activity recruits both Bub1/3 and Mad1/2 to kinetochores in separate phosphorylation events. Thus, Mps1 activity drives checkpoint signaling at kinetochores and this activity is a probable target for regulation of checkpoint activation by microtubule binding.

Figures

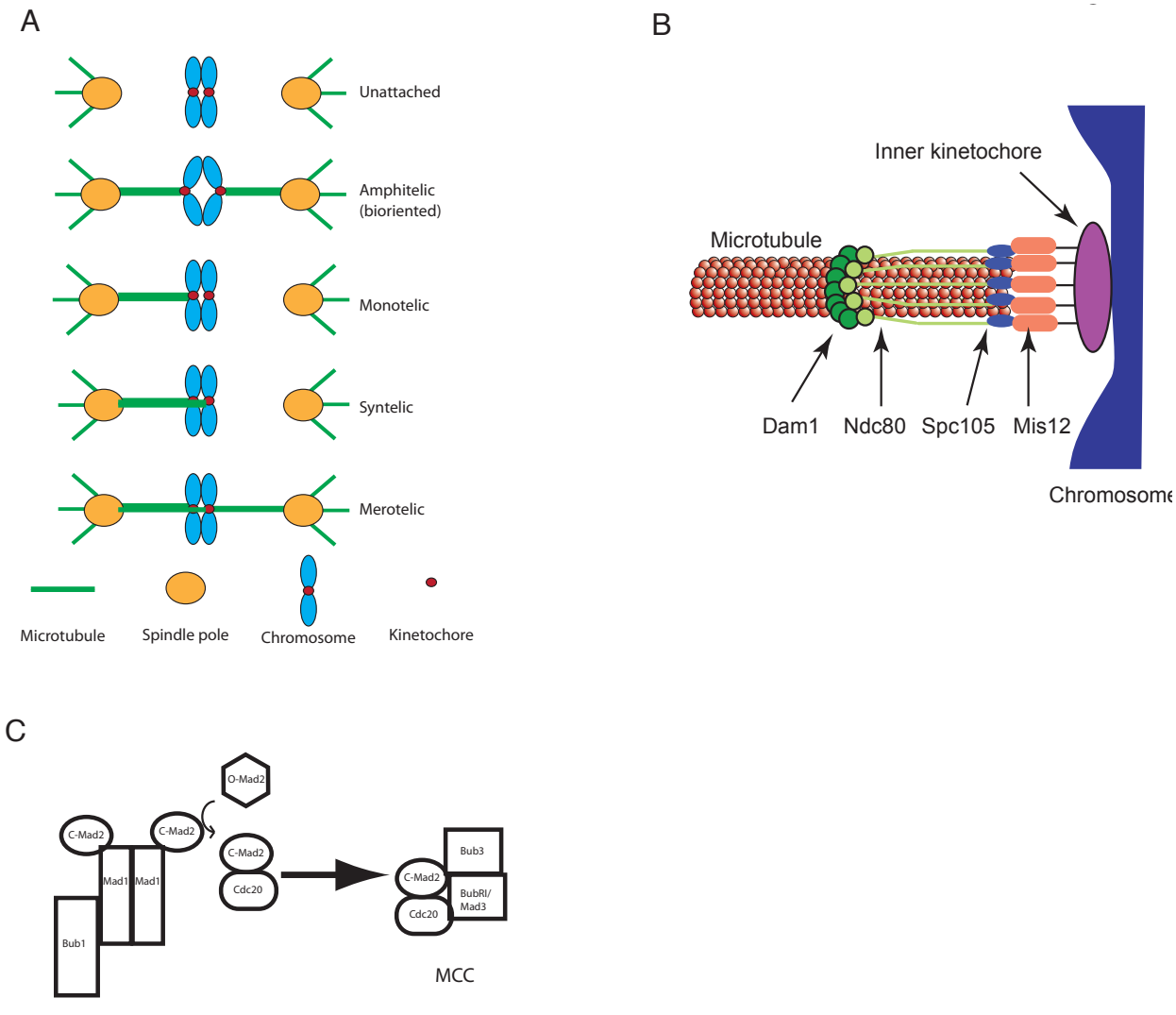

Figure I Accurate chromosome segregation is promoted by kinetochores and the spindle checkpoint

(A) Different microtubule attachment states to kinetochores are possible. Spindle microtubules (green) are anchored at spindle poles (yellow) and attach to chromosomes (blue) through kinetochores (red). Kinetochores can capture microtubules from either pole, resulting in one of several attachment states. Incorrect attachments include monotelics and syntelics, which fail to generate tension by opposing microtubule pulling forces. Merotelics are also incorrect and will result in reduced tension. Accurate segregation is only ensured upon formation of amphitelic (bioriented) microtubule attachments, which generate equal tension across sister chromatids. (B) The kinetochore is composed of numerous protein

subcomplexes. Diagramed are the outer kinetochore subcomplexes Dam1c, Ndc80c, Spc105c, and Mis12c. A large number of kinetochore proteins are present in the inner kinetochore, which associates with centromeric DNA and scaffolds the outer kinetochore. Outer kinetochore proteins bind to microtubules and function as signaling hubs for the spindle checkpoint. (C) The Mitotic Checkpoint Complex (MCC) is generated by kinetochores that catalyze conformational conversion of Mad2 from “open” (O-Mad2) to Cdc20-bound “closed” (C-Mad2). Cdc20-Mad2 is incorporated into the MCC, which inhibits the APC/C to prevent mitotic progression. Bub1 recruits Mad1 to budding yeast kinetochores to facilitate activation of Mad2.

Chapter II: Identification of Kinetochore Kinase and Phosphatase Activities

Summary

Regulation of kinetochore functions through kinase activity has been well established but progress identifying specific substrates has been limited. In vivo experiments, for instance, have been unable to determine which kinases and phosphatases interact directly with the kinetochore. I therefore analyzed purified kinetochore particles for copurifying kinases and phosphatases and tested for corresponding activity. I found that the Mps1 kinase copurifies strongly with kinetochores and represents the major catalytic activity in my assays.

Introduction

Kinase and phosphatase activity is crucial for regulating kinetochore functions, such as spindle checkpoint signaling (see Introduction and (Funabiki and Wynne, 2013)). Consistent with this, a host of kinases and phosphatases exhibit in vivo kinetochore localization, including Ipl1, Mps1, Bub1, and PP1. Ipl1 localization likely occurs through a distinct DNA-binding kinetochore subcomplex, Cbf3, although an outer-kinetochore pool of $Ipl1^{AuroraB}$ may exist (Caldas and DeLuca, 2013). Ipl1 and PP2A also localize to the pericentromere. In contrast, the mitotic master regulatory kinase Cdk1 targets kinetochore substrates, but has not been localized to kinetochores. Similarly, the phosphatase Cdc14 reverses Cdk1 phosphorylation at the kinetochore, but does not have an established kinetochore receptor (Wurzenberger and Gerlich, 2011). In higher eukaryotes, the Polo-like kinase $Cdc5^{Plk1}$ localizes to kinetochores and performs mitotic functions, but this has not been observed in budding yeast.

To study the binding partners and regulatory mechanisms of these enzymes, as well as to better understand their activity at the kinetochore, I analyzed purified kinetochores for copurifying enzymes. I found that Mps1, Bub1, PP1, Cdc14, and possibly Cdc5 copurify with kinetochores. Mps1 is the most

abundant copurifying protein from this set and represents the dominant kinase activity on purified kinetochores.

Results

Mass spectrometry on purified kinetochores identifies copurifying Mps1, Bub1, Glc7, Cdc5, and Cdc14

I performed mass spectrometry (MS) on purified kinetochore particles to identify copurifying proteins. MS identified Mps1 and Bub1 as copurifying in relatively high abundance, as inferred from the relative proportion of spectra belonging to each protein (Table I, see "Percent share spectral IDs"). The phosphatases Glc7 and Cdc14, as well as the kinase Cdc5, copurified at apparently lower abundance, while the kinase Ipl1 was not confidently identified, indicating it is likely not present at significant levels (Table I). The kinase Cdk1 and the phosphatase PP2A were not detected. I confirmed these results by Western blotting for all interactions except for Cdc5, Cdk1, and Ipl1 (Fig II.1A).

Cdc14 exhibits cell-cycle independent association with kinetochores

In order to determine how Cdc14 associates with kinetochores, I analyzed the kinetochore-Cdc14 CoIP during different cell-cycle arrests. At G1, S-phase, and mitotic (metaphase and anaphase) arrests, the Cdc14 interaction was detectable but reduced relative to asynchronously prepared kinetochore particles (Fig II.1B and data not shown). I next addressed whether compromising the function of various kinetochore proteins would abrogate the Cdc14 interaction. Deletion of Slk19, a kinetochore-associated protein implicated in Cdc14 localization (Faust et al., 2013; Stegmeier et al., 2002), did not reduce the interaction (Fig II.1C). I attempted to assay the interaction in temperature-sensitive mutants of other essential kinetochore proteins but found the interaction was not detectable at the restrictive temperature in *wild type* cells (data not shown).

Mps1 comprises the dominant catalytic activity on purified kinetochores

I next tested for kinase activity on kinetochores by incubating bead-bound kinetochore particles with radiolabeled ATP. Several substrates were highly phosphorylated in this assay (Fig II.2A), indicating that kinase activity copurifies. To identify the kinase(s) responsible, I utilized temperature-sensitive

mutants of the mitotic kinases Cdk1 (*cdc28-1*), Ipl1 (*ipl1-321*) or Mps1 (*mps1-1*), and a tetracycline-repressible form of Bub1 (*Ubi-r-TetR-Bub1*). Inactivation of these kinases did not grossly perturb kinetochore composition as determined by silver staining and Western blotting, except that Dam1 protein levels were significantly reduced in *mps1-1* kinetochores (Fig II.2A and II.2B and data not shown). Only inactivation of Mps1 abolished kinase activity, indicating it is the major source of activity (Fig II.2A). Because Mps1 is necessary for Bub1 kinetochore association (see section III), I further tested whether kinetochores that retained Bub1 and Mps1 were still active when Mps1 was specifically inhibited in vitro. Treatment of *mps-as1* kinetochores, which retained Bub1 (Fig II.2C), with the ATP analog 1NM-PP1 abolished kinase activity, confirming that Bub1 is not a major source of the observed phosphorylation (Fig II.2D). Finally, addition of recombinant GST-Mps1 restored the phosphorylation pattern of kinetochore proteins to *mps1-1* kinetochores, albeit to lower levels (Fig II.2E).

Copurifying phosphatase activity on kinetochore particles is negligible

Phosphatase inhibitors were included during preparation of the above experiments. To test if copurifying phosphatases could be active in my assays I omitted phosphatase inhibitors from all steps and incubated kinetochores in buffer lacking ATP. The checkpoint protein Mad1 dissociates from kinetochores upon treatment with recombinant PP1 in vitro (see section IV), so I tested Mad1 dissociation to assay phosphatase activity. I did not detect robust and specific dissociation (data not shown), indicating that copurifying endogenous phosphatases had little or no activity in my assays. This may reflect inhibition of the phosphatase, low phosphatase levels, or incompatible buffer conditions with phosphatase requirements. Although phosphatases exhibit very poor specificity in vitro, substrate specificity could also account for an inability to detect activity.

Discussion

The kinetochore association of kinases and phosphatases that I determined by CoIP corresponds to the reported in vivo localization patterns in all cases except for Cdc14. Cdc14 is proposed to be strictly sequestered to the nucleolus until anaphase initiation (Wurzenberger and Gerlich, 2011). It is therefore surprising that Cdc14 kinetochore association is found during all cell cycle stages in my experiments.

Identifying the Cdc14-interacting proteins at the kinetochore has not proven successful so far (Fig I.1C and data not shown), making it difficult to ascertain the binding requirements. Future work will be necessary to characterize the Cdc14-kinetochore protein interaction interface to facilitate mutagenesis and functional analysis. It is further possible that Cdc14-kinetochore association is a secondary effect of the kinetochore purification method. Alternative purification strategies, such as variations in lysis procedure, should clarify this.

Kinetochore composition from wild type or kinase mutant strains was broadly similar, although minor differences were detected (data not shown). Most strikingly, a reduction in Dam1 levels at kinetochores was observed upon Mps1 inactivation, consistent with a recent report (Meyer et al., 2013). The cause for this reduction, as well as its functional consequences, are not yet clear, although this may relate to a potential function for Mps1 in promoting biorientation through regulating microtubule affinity (Maure et al., 2007 and data not shown).

Regulation of Mps1 and Glc7 kinetochore association are under active investigation. Mps1 association is dynamic and is likely a key event in checkpoint regulation. Its ability to dissociate upon activation may be a critical feature of dynamic cycling of Mps1 at the kinetochore, although the factors contributing to dynamic cycling remains unclear (Hewitt et al., 2010; Jelluma et al., 2010; Nijenhuis et al., 2013). Kinetochore association of Bub1 will be discussed in section III.

Materials and Methods

Yeast strains, plasmids and microbial techniques

Media and genetic and microbial techniques were essentially as described (Rose et al., 1990). The construction of yeast strains and plasmids used in this study and the experimental growth conditions are described in (London et al., 2012) Yeast strains are listed in the strain table.

Yeast growth conditions

For experiments with temperature sensitive mutants, cells were shifted to 37 ˚C for 2 hours and harvested at an OD_{600} of approximately 2.0. Tetracycline-repressible *Ubi-R-TetR-BUB1* was inactivated

by treatment with 25 mg/mL doxycycline for 4 hours. Cells died within one cell cycle after tetracycline addition as indicated by a viability assay. 1NM-PP1 was used at 10 mM.

Kinetochore particle assays

Kinetochore particles were isolated by affinity-purifying Dsn1-6His-3Flag protein as previously described (Akiyoshi et al., 2009). Kinetochores were eluted from beads with 0.5 mg/mL 3x-Flag peptide in lysis buffer for kinase assays and kinetochore composition experiments, or into SDS-PAGE sample buffer for all other experiments. For kinase assays, bead-bound kinetochores were washed into kinase buffer (50 mM Tris-HCl pH 7.5, 75 mM NaCl, 5% glycerol, 10 mM $MgCl_2$ 1 mM DTT, 10 mM ATP) containing 66 nM g-^{32}P-ATP and incubated at 30 ˚C for 30 minutes. Kinase treatments with unlabeled ATP were performed by washing kinetochores into kinase buffer with or without ATP and incubated at 30 ˚C for 30 minutes.

GST-Mps1 was purified as described (Holinger et al., 2009). 2 mL of purified protein was added to kinase reactions. Phosphatase reactions were performed with 1 mM $MnCl_2$ and 1.25 U PP1 (NEB) in lysis buffer at 23 ˚C for 20 minutes unless otherwise indicated. Phosphatase inhibitors, consisting of 1 mM sodium pyrophosphate, 2 mM Na-beta-glycerophosphate, 0.1 mM NA_3VO_4, 5 mM NaF, 100 nM microcystin-LR, were used in negative phosphatase control reactions.

Immunological techniques

Immunoprecipitations were carried out in the same conditions as the kinetochore purifications (Akiyoshi et al., 2009). Immunoblotting was performed as described (Biggins et al., 1999). Commercial antibodies used for immunoblotting were: 9E10 (Covance) at a 1:10,000 dilution for the Myc tag, anti-Flag antibodies (Sigma-Aldrich) at 1:3,000, and anti-V5 antibodies (Invitrogen) at 1:5,000. Silver-staining was performed using 4-12 % NuPAGE Novex Bis-Tris gels (Invitrogen) and a SilverQuest silver-staining kit (Invitrogen).

Mass spectrometry

Kinetochore particles were purified via Mtw1-3Flag (SBY8564) to enhance elution of Dsn1 protein with Repigest (Waters) relative to Dsn1-3Flag. Particles were treated with phosphatase, kinase buffer, and incubated with lysate (rebinding conditions, Chapter III) in preparation for mass spectrometry as in Chapter III.

Figures

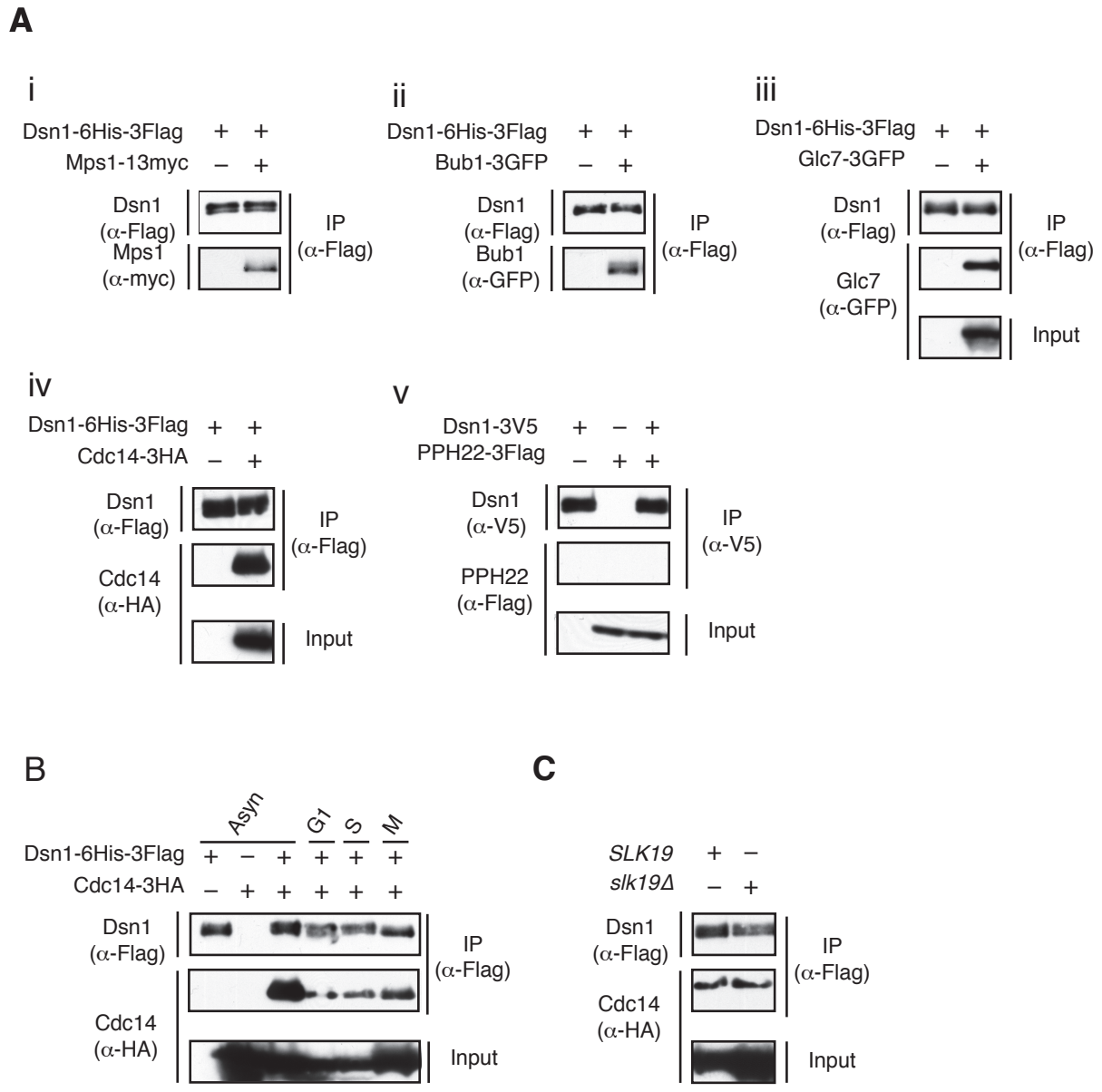

Figure II.1 Mitotic kinase and phosphatase association with purified kinetochores by CoIP

(A) Kinetochores were immunoprecipitated through the Flag epitope from lysate of asynchronously grown cells and analyzed for the associated protein in i-v. In panel v, a 3V5-tagged form of Dsn1, which yields equivalent analytical purifications to Dsn1-6His-3Flag (data not shown) was used for the IP. Proteins were detected by SDS-PAGE followed by Western blotting with the indicated antibodies. (B) Cultured cells were untreated (Asyn) or arrested by treating for 2.5 hours each in α-factor (G1), hydroxyurea (HU) for S-

phase (S), or nocodazole for mitosis (M) before harvesting. Kinetochore particles were immunoprecipitated and analyzed as in (A). (C) Asynchronous cells with or without *SLK19* were grown and analyzed for the kinetochore-Cdc14 CoIP as in (A). Strains used: (A) SBY8253, SBY12440, SBY8502, SBY13535, SBY12703, SBY13610, SBY14021, SBY14174, (B) SBY8253, SBY12745, SBY12747, (C) SBY12745, SBY13087.

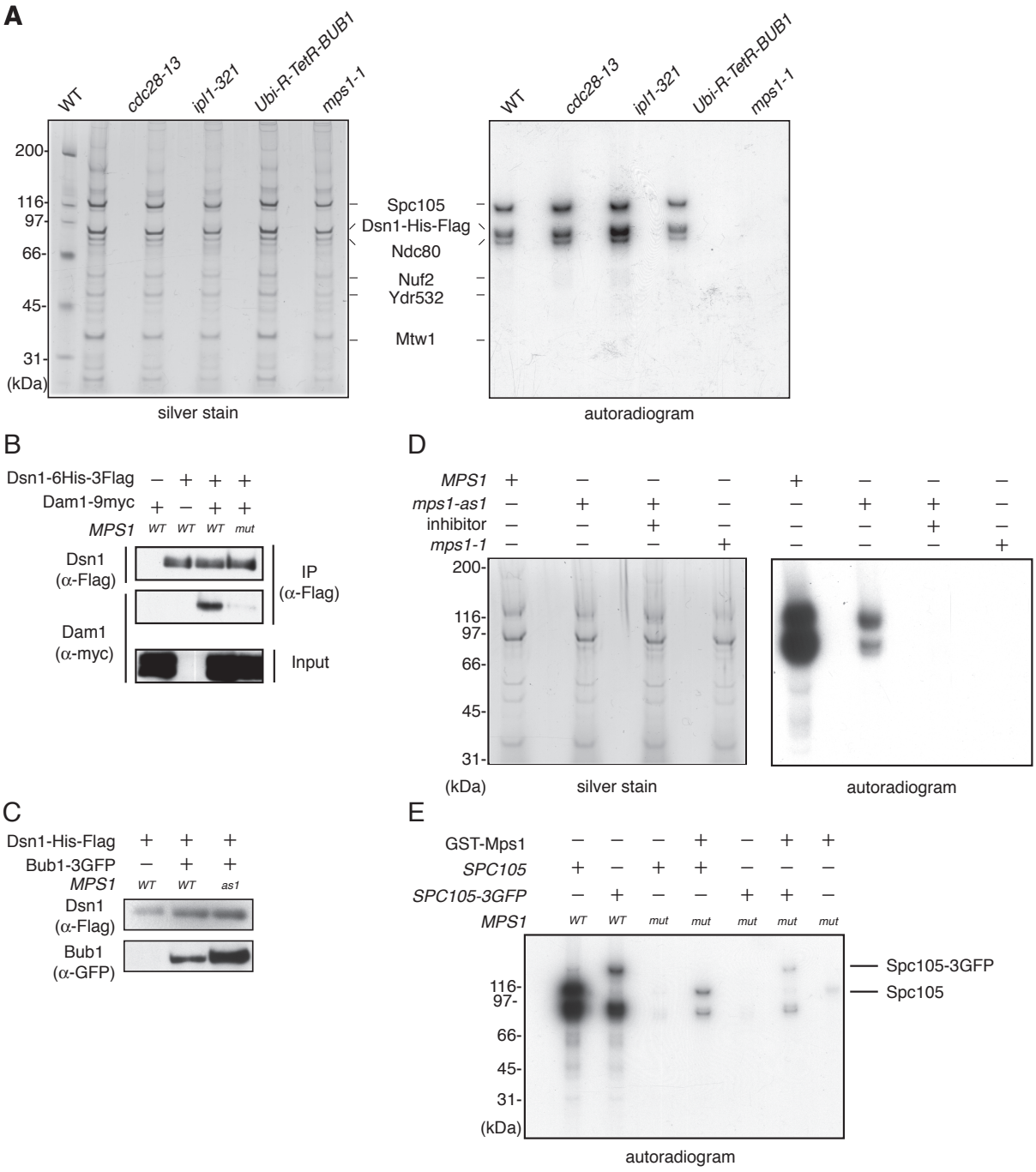

Figure II.2 Active Mps1 copurifies with kinetochore particles

(A) Cells were cultured and temperature shifted to 37° or treated with doxycycline before harvest to inactivate the indicated kinases. Kinetochore particles were immobilized on α-Flag resin, treated with kinase reaction buffer containing radiolabeled ATP, then washed and eluted with Flag peptide. Samples were analyzed by silver stain SDS-PAGE and autoradiography. (B) Cells containing *dam1-9myc* with

MPS1 (*WT*) or *mps1-1* (*mut*) were shifted to 37° before harvest and analyzed as in Fig II.1A. (C) Kinetochores from strains containing Bub1-3GFP and *MPS1* (*WT*) or *mps1-as1* (*as1*) were prepared an analyzed from untreated cells as in Fig II.1A. (D) Kinetochore kinase assays were performed as in (A) for the indicated preparations, except that the inhibitor 1NM-PP1 or DMSO was included in the kinase reaction. (E) As (A) for strains with the indicated composition, where *MPS1* = *WT* and mps1-1 = *mut*. Recombinantly expressed GST-Mps1 was purified and added to the kinase reactions where indicated. The migration shift in the upper species in SPC105-3GFP lanes identifies this band as Spc105. Strains used: (A) SBY8253, SBY8716, SBY8712, SBY8920, SBY8726, (B) SBY2055, SBY8253, SBY10079, SBY8938, (C) SBY8253, SBY8502, SBY10059, (D) SBY8253, SBY8750, SBY8726, SBY9099.

III. Phosphoregulation of Bub1 and Bub3 Recruitment to the Kinetochore

Summary

I identified the core kinetochore component Spc105^{KNL1} as the kinetochore receptor for the Bub1/3 complex. Spc105 contains conserved “MELT-like” repeats, and the threonines within these repeats are targets for the Mps1 kinase. Phosphorylation of these repeats is the biochemical switch that mediates Bub1/3 kinetochore binding, as demonstrated in vivo by mutational analysis and in vitro by biochemical reconstitution. I additionally found that phosphatase activity of PP1^{Glc7} opposes Mps1 activity towards Spc105. This work identified the most upstream phosphorylation event specific to the major signaling pathway that ensures both spindle checkpoint function and error correction.

Introduction

The spindle checkpoint proteins Bub1 and Bub3 are required for a checkpoint response as well as error-correction (Elowe, 2011). Mutants of Bub1 that mislocalize from kinetochores are defective in both of these processes, indicating that the kinetochore interaction is critical for Bub1 function (Kiyomitsu et al., 2007; Klebig et al., 2009). However, Bub1/3 kinetochore localization is dynamic, initially occurring at the onset of mitosis and dramatically decreasing at anaphase onset (Howell et al., 2004). Bub1 is proteolytically degraded at mitotic exit (Qi and Yu, 2006), indicating that its function must be tightly controlled. This localization pattern follows that of Mps1, which is also degraded at anaphase onset (Palframan, 2006). Moreover, Mps1 activity is necessary both for Bub1 localization and for the checkpoint response in other organisms (Ito et al., 2011; Kiyomitsu et al., 2007; Lee et al., 2011; Schittenhelm et al., 2009; Sliedrecht et al., 2010; Vigneron et al., 2004; Zhao and Chen, 2006).

Bub1/3 localization remained a key unresolved question in understanding their function. Structural studies indicated an interaction between human Bub1 and the Spc105 homolog KNL1/Blinkin (Bolanos-Garcia et al., 2011; Kiyomitsu et al., 2007, 2011), although this interaction did not appear to be of high affinity nor was it clear how this interaction could be regulated (Krenn et al., 2012). Specific

observations did not fit with a direct Bub1-Spc105 recruitment model, including the requirements for Bub3 and for Mps1 kinase activity for Bub1 kinetochore localization (which are not required for Spc105 localization). Additionally, a motif on Spc105^{Knl1} that interacts directly with Bub1 is only present in metazoans, whereas Bub1 kinetochore localization is universal (Bolanos-Garcia et al., 2011; Kiyomitsu et al., 2011; Krenn et al., 2012). I therefore sought to illuminate Bub1 kinetochore localization by investigating the requirement for Mps1. I began by identifying Mps1 substrates at the kinetochore that might be responsible. Using purified kinetochores, I determined Mps1 phosphorylation on conserved repeat sequence of Spc105 to be the requirement signal for a Bub1/3 complex. Furthermore, I found that the phosphatase Glc7^{PP1} opposes Mps1 phosphorylation, consistent with its role in checkpoint silencing.

Results

Mps1 mediates Bub1 and Bub3 kinetochore localization

To determine whether Mps1 activity was necessary for Bub1 localization in budding yeast, as had been observed in other organisms, I utilized an analog-sensitive allele of *MPS1* (*mps1-as1*), the activity of which can be specifically inhibited by treatment of cells with the ATP analog 1NM-PP1 (Jones et al., 2005). Because Mps1 inhibition bypasses the spindle checkpoint, leading to mitotic exit, cell were maintained in metaphase by depletion of Cdc20 transcribed from a methionine-repressible promoter. Bub1-3GFP gave high in vivo colocalization with the core-kinetochore protein Mtw1-mCherry upon nocodazole treatment, but this was abolished upon addition of 1NM-PP1 to *mps1-as1* cells (Fig III.1A). In contrast, *MPS1* cells exhibited high Bub1 colocalization with 1NM-PP1 treatment. I next tested the coimmunoprecipitation of Bub1 with kinetochores from cells bearing the temperature-sensitive *mps1-1* allele. Bub1 CoIP'd strongly with *MPS1* kinetochores from asynchronous cultures but did not CoIP with *mps1-1* kinetochores (Fig III.1B), indicating that Mps1 is necessary for Bub1 association that is not due to a mitotic arrest. To ask whether Mps1 has a causative role in Bub1 recruitment, I tested whether *MPS1* overexpression could induce Bub1 localization. Cells were arrested in G1 by α-factor treatment and *MPS1* overexpression was induced with galactose. Strikingly, *pGal-Mps1* cells colocalized Bub1 with the kinetochore marker Mtw1-mCherry, even though Bub1 did not localize in control cells lacking *pGal-Mps1* (Fig III.1C).

The sufficiency of Mps1 activity for Bub1 localization raised the possibility that Mps1 phosphorylation could directly mediate Bub1 binding to the kinetochore. I asked whether the Bub1-kinetochore association was mediated by phosphorylation by immobilizing kinetochores and associated Bub1 on beads. I then incubated these beads with a recombinant phosphatase, PP1, and analyzed the bead-bound material and the soluble material for Bub1. Bub1 was released from kinetochores that were treated with active PP1, but not from kinetochores incubated with PP1 in the presence of phosphatase inhibitors (Fig III.1D). I next asked whether Mps1 phosphorylation of kinetochore-associated substrate(s) could enable Bub1 binding. As before, I immobilized kinetochores on beads, then treated with phosphatase to remove Bub1 and existing phosphorylation. This treatment did not disable copurifying Mps1 activity (data not shown). I next treated the kinetochores with ATP and incubated them with lysate to test whether they could bind Bub1 from the lysate (Fig III.1E, III.1F). ATP-treated kinetochores successfully pulled-down Bub1 from lysate, and this required both ATP treatment and Mps1 activity on kinetochores (Fig III.1F). Together, these experiments established that Mps1 is responsible for Bub1 recruitment and that this occurs through Mps1 phosphorylation on a kinetochore-associated protein.

Bub3 forms a constitutive complex with Bub1, and the two proteins display a corequirement for kinetochore localization (Vanoosthuyse et al., 2004). To ascertain whether Bub1 and Bub3 kinetochore association could be separated in vitro, I first confirmed that Bub3 displayed the same requirement for Mps1 phosphorylation as Bub1. Like Bub1, inhibition of *mps1-as1* abolished Bub3 localization in vivo (Fig III.2A), while inactivation of *mps1-1* abolished the kinetochore-Bub3 CoIP (Fig III.2B). In vitro phosphatase treatment removed Bub3 from kinetochores (Fig III.2C), and Bub3 binding ability was restored upon subsequent ATP treatment in the lysate rebinding assay (Fig III2.D). These observations are consistent with Bub1 and Bub3 binding to kinetochores as a complex.

Bub1-Spc105 binding is mediated by Mps1 and PP1^{Glc7}

Because Spc105 appeared to be required for Bub1 recruitment, I tested whether Spc105 could CoIP Bub1. I detected the CoIP and found that it was abolished when Mps1 was inactivated (Fig III.3A) which resembled the result obtained for *mps1-1* kinetochores (Fig III.2B). In addition, *MPS1* overexpression promoted the Bub1-Spc105 CoIP in cells arrested in mitosis by Cdc20 depletion or in G1

(Fig III.3B, III.3C, and III.3D). This supported the putative identification of Spc105 as the kinetochore receptor for Bub1.

The ability of Mps1 activity to promote the Bub1-Spc105 interaction, combined with the ability of phosphatase activity to dissociate Bub1 from kinetochores in vitro, suggested that a phosphatase likely promotes Bub1-Spc105 dissociation in vivo. The phosphatase $PP1^{Glc7}$ is required for checkpoint silencing and associates with Spc105 (Liu et al., 2010; Pinsky et al., 2009; Vanoosthuyse et al., 2009), so it is the most likely candidate to oppose the Mps1-mediated Bub1-Spc105 interaction. I found that overexpression of Glc7 by galactose induction increased electrophoretic mobility of Spc105, consistent with dephosphorylation, and abolished the Spc105-Bub1 interaction (Fig III.3B). Glc7 overexpression also abolished Bub1 kinetochore localization in vivo (Fig III.3E). Glc7 activity is therefore capable of opposing Mps1 phosphorylation to prevent the Bub1-Spc015 interaction, consistent with its function in checkpoint silencing.

Spc105 is a novel Mps1 substrate and is targeted on its conserved MELT motifs

To identify the potential Mps1 targets at the kinetochore that could meditate a Bub1-Spc105 interaction, I identified the Mps1 substrates in the kinetochore kinase assay described above (Fig II.2A). Kinase assays on kinetochores with epitope-tagged candidate proteins revealed that the major targets of Mps1 were Spc105 and Dsn1, both novel targets, along with Mps1 and Ndc80, established Mps1 targets (Fig II.2E and data not shown) (Kemmler et al., 2009; Lauzé et al., 1995). I next identified Mps1 candidate phosphorylation sites on kinetochore proteins by analyzing in-vitro phosphorylated kinetochores by mass spectrometry (Table II).

Because Spc105 was implicated both in a Bub1 interaction (Fig 3) (Bolanos-Garcia et al., 2011; Kiyomitsu et al., 2011; Krenn et al., 2012) and in the checkpoint (Pagliuca et al., 2009), I initially focused on determining the Spc105 Mps1 sites. Yeast Spc105 contains approximately six MELT consensus motifs ([M/I]-[E/D]-[I/L/M]-[S/T]), which are highly degenerate but nearly universally conserved among homologous proteins (Fig III.4A) (Vleugel et al., 2012). I detected phosphorylation on three of these six sites in my mass spectrometry data (Table II and Fig III.4A), and generated phosphomutant strains where I mutated the conserved threonines to alanines. Mutation of all six threonines (*spc105-6A*) yielded

kinetochores that had reduced autophosphorylation on Spc105 (54% of wild type) as determined by autoradiography (Fig III.4B). *spc105-6A* cells also exhibited increased sensitivity to benomyl, similar to *bub1-degron* cells (Fig III.4C), as well as an inability to stabilize Pds1 in response to nocodazole treatment (Fig III.4D). Spc105-6A protein and corresponding kinetochores did not CoIP Bub1 (Fig III.4E and III.4F) or permit Bub1 binding upon Mps1 phosphorylation in vitro (Fig III.4G). In vivo localization of Bub1 was also abolished in nocodazole-treated *spc105-6A* cells (Fig III.4H). This data collectively implicates Spc105 as a receptor for Bub1/3 and indicates that this interaction is mediated by Mps1 phosphorylation of Spc105 MELT motifs (Fig III.4I).

Discussion

These findings established a new model for Bub1/3 kinetochore localization that accounts for its dynamic regulation (Fig III.4I). The core kinetochore protein Spc105 was identified as the receptor for Bub1/3, and this has been verified in a structural study characterizing the interaction of a phospho-MELT peptide with Bub3 and a Bub1 peptide (Primorac et al., 2013). Complementary work in fission yeast and human cells has shown that the $MELT^{p}$ recruitment of Bub1/3 is conserved (Shepperd et al., 2012; Yamagishi et al., 2012).

The MELT motifs were originally uncovered as an identifying feature of Spc105 homologs (Cheeseman et al., 2004). This work established their function, but important questions remain. As mentioned above, MELT sequences are highly degenerate across species, with the flanking sequence often showing no apparent conservation. Extensive bioinformatics and mutational analysis has since been performed on this region of human $Spc105^{Knl1}$, and this has led to the model that MELT repeats expand by duplication and are under strong negative selection (Vleugel et al., 2012, 2015). Deletion analysis indicates that MELT motifs may lose their Bub1/3 binding function when key residues are mutated, but a single MELT motif is sufficient to recruit low levels of Bub1 (Vleugel et al., 2013). Still, full function of Bub1 requires multiple MELT motifs. A metazoan-specific set of “KI-motifs” on $Spc105^{Knl1}$ mediate direct interactions with Bub1 or BubR1 and somehow seems to enhance function of the associated Bub1 (Bolanos-Garcia et al., 2011; Kiyomitsu et al., 2011; Krenn et al., 2012, 2014). The reason for the high selective pressure on this region of Spc105 remains unresolved.

Dephosphorylation of the MELT motifs dissociates Bub1/3, and this appears to occur through the activity of $PP1^{Glc7}$ (Fig III.3B and III.3E). Subsequent work has confirmed the importance for $PP1^{Glc7}$ in dephosphorylating the MELT sites in human cells (Nijenhuis et al., 2014; Zhang et al., 2013). Another phosphatase, PP2A, has also been found to function upstream of $PP1^{Glc7}$ in MELT dephosphorylation in human cells (Espert et al., 2014), but it is not clear whether this reflects a function of PP2A in activating $PP1^{Glc7}$ at the kinetochore (Nijenhuis et al., 2014). PP1 is expected to be active at kinetochores when stable microtubule attachments are present (Liu et al., 2010), so this may be one way that kinetochores couple microtubule attachments to checkpoint silencing. On the other hand, specific localization of Bub1/3 during mitosis accords with the localization of Mps1, so Mps1 may exhibit continuous activity towards Spc105 while at the kinetochore. So far, the dynamics of Mps1 and PP1 activity on Spc105 have not been well studied.

Identification of Mps1 as the Spc105 kinase provided one of the first molecular events that explain how Mps1 functions in checkpoint activation and in biorientation. However, Bub1/3 localization is not sufficient for checkpoint activation, whereas *MPS1* overexpression is sufficient to signal the checkpoint. Along with other reasons (discussed below), this suggested that Mps1 may have additional substrates for checkpoint activation.

Numerous important questions remain for future investigation based on this work. It remains unknown what the binding stoichiometry of Bub1/3 to Spc105 is – that is, what proportion of MELT sites are occupied at any time. Variability in Bub1/3 occupancy could account for observed variation in the strength of the downstream checkpoint in response to different triggers (Collin et al., 2013; Dick and Gerlich, 2013). For example, a checkpoint response that is caused by a lack of tension may lead to less Bub1/3 occupancy and therefore a weaker checkpoint (London and Biggins, 2014a; Vleugel et al., 2013). In human cells, $Mad3^{BubR1}$ kinetochore localization is important for the checkpoint, and this depends upon Bub1 recruitment. A recent report indicates that BubR1 recruitment occurs through heterodimerization of BubR1 with Bub1 (Overlack et al., 2015). It will be important to next determine how this interaction is regulated and to understand how this pertains to yeast Mad3 protein function, which does not appear to localize to kinetochores.

Materials and Methods

Yeast strains, plasmids and microbial techniques

Media and genetic and microbial techniques were essentially as described (Rose et al., 1990). The construction of yeast strains and plasmids used in this study and the experimental growth conditions are described in (London et al., 2012). Yeast strains are listed in the strain table.

Yeast growth conditions

Temperature shift, tetracycline, and 1NM-PP1 treatments were as described in Chapter II. Galactose induction was performed on cells grown in either 2% raffinose for microscopy experiments or 2% lactic acid for protein purification experiments by addition of galactose to 2% for one hour. Cdc20 depletion was accomplished in cells containing *pMET-CDC20* by culturing cells to mid-logarithmic phase (OD_{600}=0.3-0.5) in synthetic media without methionine, then washing into YPD media containing methionine and culturing for approximately 4 hours at 23 ˚C. Final concentration of nocodazole was 10 mg/mL. G1 arrests were carried out by adding 1 µg/ml α-factor for 3 hours and cells were released by washing out α-factor as previously described [2]. α-factor was added back with rebudding, about 45 minutes after release, in Pds1 stability experiment. Doxycycline was top-plated to 25 ug/mL on appropriate media in viability experiments.

Kinetochore particle assays

Bead-bound kinetochore particles were treated as in Section II. Ipl1 reactions were performed by treatment with GST-Ipl1 and the GST-Sli15 C-terminus for 30 minutes at 30 ˚C as described (Buvelot, 2003). To test rebinding, bead-bound kinetochore particles were treated with phosphatase then with ATP. Beads were washed twice between each reaction with cold lysis buffer containing phosphatase inhibitors to remove phosphatase and ATP. Beads were then incubated with Bub1-3GFP- or Bub3-3GFP-containing lysate at 4 ˚C for 3 hours, then washed in lysis buffer with protease and phosphatase inhibitors followed by elution into sample buffer. Spc105 protein phosphorylation was quantified by Phosphorimager analysis of SDS-PAGE gels. Spc105 intensity was normalized to other phosphorylated species in the same reaction following background subtraction using ImageQuant TL (GE Healthcare).

Immunological techniques

Immunoprecipitations, immunoblotting and silver staining were as performed in Chapter II. Commercial anti-Pgk1 antibodies (Invitrogen) were used at 1:10,000 and anti-GFP (Roche) antibodies were used at 1,000. Anti-Cse4 antibodies were used at 1:500 (Pinsky et al., 2006). Anti-Spc105 antibodies were used at 1:10,000 (Akiyoshi et al., 2010). Anti-Mif2 (OD2, 1:6,000) and anti-Ctf19 (OD10, 1:15,000) antibodies were kind gifts from Arshad Desai.

Microscopy Techniques

GFP and mCherry epitope-tagged proteins were visualized in fixed cells as described (Biggins et al., 1999) and an Evolv EMCCD 512 camera (Photometrics) was used for pictures.

Preparation of material for mass spectrometry

Mass spectrometry experimental details are reported in (London et al., 2012). Briefly, purified kinetochores were phosphorylated by ATP treatment and either individual bands were purified from SDS-PAGE gels or kinetochore particles were eluted from beads with Rapigest (Waters) Proteins were digested with Trypsin. Peptides were analyzed by LC/ESI MS/MS with a nano2D LC (Eksigent) coupled to an LTQ-OrbiTrap mass spectrometer (ThermoScientific) using a “vented” instrument configuration as described (Licklider et al., 2002). The mass spectrometers were operated in the data-dependent mode, and the 5 most intense ions from the Fourier-transform (FT) full scan were selected in the linear ion trap for fragmentation by collision-induced dissociation. Peptide spectra were searched with X!Tandem (Craig and Beavis, 2004) against the *Saccharomyces Genome Database* protein database using potential monoisotopic mass modifications of 15.995 on methionine (oxidation) and 79.966 on serine, threonine, and tyrosine (phosphorylation).

Figures

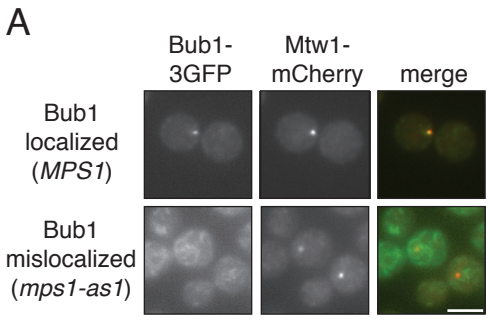

	% colocalization	N
WT - inhibitor	45.9	209
WT + inhibitor	39.5	220
mps1-as1 - inhibitor	49.8	233
mps1-as1 + inhibitor	9.8	214

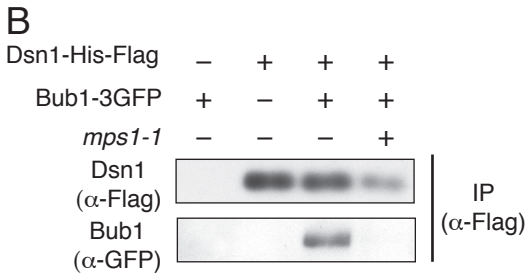

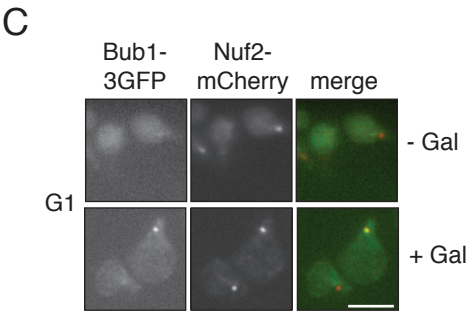

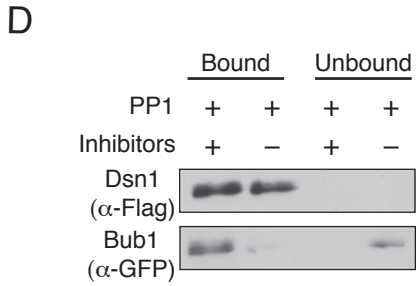

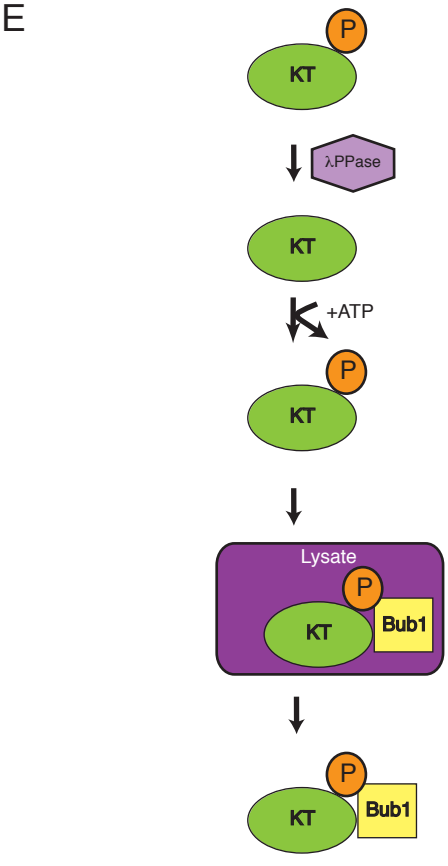

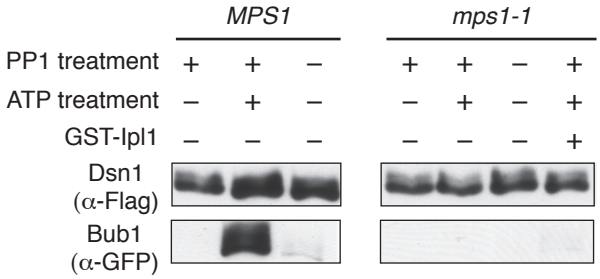

Figure III.1 Mps1 activity localizes Bub1 to kinetochores

(A) Cdc20 depletion was used to arrest cells in metaphase along with nocodazole treatment to stimulate checkpoint signaling. Subsequent treatment with inhibitor (1NM-PP1) was used to inactivate Mps1-as1. The number of cells displaying colocalization of Bub1-3GFP with the kinetochore marker Mtw1-mCherry was quantified. (B) Cells were grown with a 2 hour 37° temperature shift before harvest and kinetochore particles were purified by immunoprecipitation and Flag elution, followed by analysis by SDS-PAGE and immunoblotting. (C) Cells were arrested in G1 with α-factor treatment, then Mps1 was overexpressed by galactose addition or repressed with glucose. The number of cells colocalizing Bub1-3GFP with Mtw1-mCherry was quantified as in (A). (D) Kinetochore particles containing Bub1-3GFP were immobilized on α-Flag resin and treated with PP1 with or without phosphatase inhibitors. Bead-bound and soluble fractions were analyzed. (E) Schematic of kinetochore-Bub1 binding experiment from lysate. (F) Following phosphatase treatment and subsequent ATP incubation, resin-bound kinetochores were incubated with yeast lysate containing tagged Bub1, then washed and analyzed by immunoblotting. Kinetochores were purified from *WT* or *mps1-1* cells. Strains used: (A) SBY10318, SBY10282, (B) SBY8253, SBY3663, SBY8502, SBY9348, (C) SBY10271, (D) SBY8502, (E) SBY8502, SBY9348.

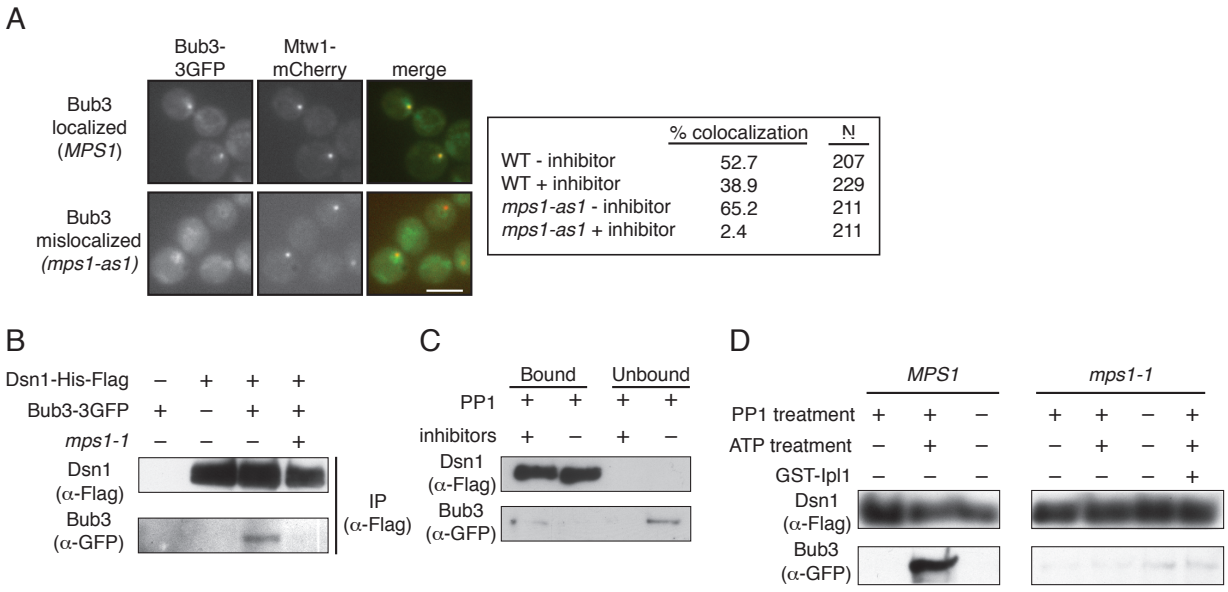

Figure III.2 Mps1 activity localizes Bub3 to kinetochores

(A) Cells were treated as in Fig III.1A and analyzed for colocalization of Bub3-3GFP with Mtw1-mCherry. (B) Kinetochore particles were purified and analyzed for Bub3 association as in Fig III.1B. (C) Bub3-3GFP release from kinetochore particles upon PP1 treatment was monitored as in Fig III.1D. (D) Kinetochore rebinding of Bub3-3GFP from lysate was tested as in Fig III.1F with lysate containing tagged Bub3. Strains used: (A) SBY10282, SBY10318, (B) SBY8882, SBY9347, (C) SBY8882, (D) SBY8882, SBY9347.

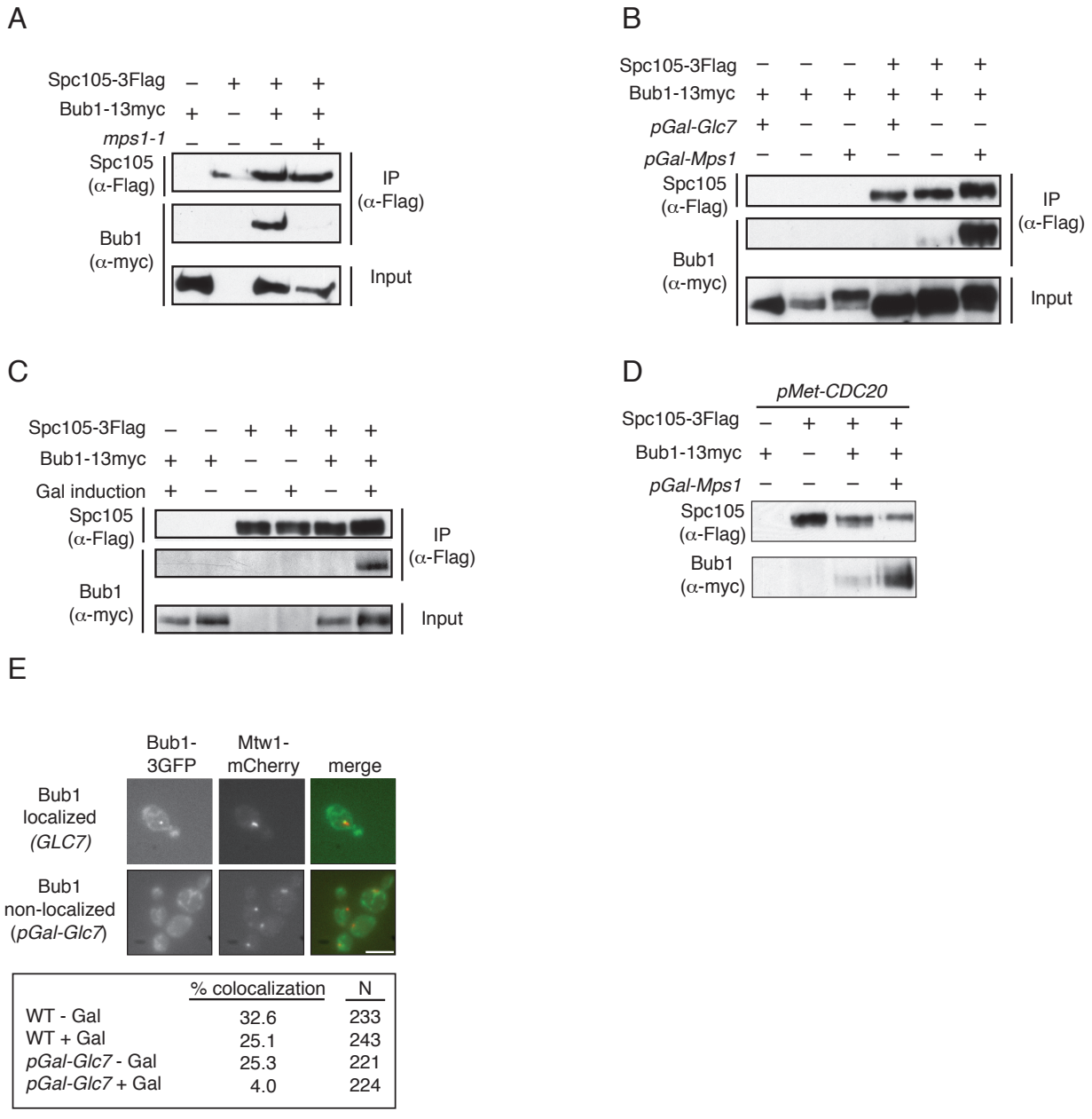

	% colocalization	N
WT - Gal	32.6	233
WT + Gal	25.1	243
pGal-Glc7 - Gal	25.3	221
pGal-Glc7 + Gal	4.0	224

Figure III.3 The Bub1 interaction with Spc105 is mediated by Mps1 and Glc7

(A) Spc105-3Flag was immunoprecipitated from lysate containing Bub1-13myc from *MPS1* or *mps1-1* cells. (B) Spc105-3Flag was immunoprecipitated from cells overexpressing *Glc7* or *Mps1* with galactose induction and immunoblotted to detect Spc105 (α-Flag) or Bub1 (α-myc). (C) Cells were arrested in G1 with α-factor, treated with galactose or glucose, and processed as in (B). (D) Cells were arrested in metaphase by methionine-induced Cdc20 depletion, treated with galactose, and processed as in (B). (E)

Glc7 overexpression was induced with galactose and the percent of cells colocalizing Bub1-3GFP with Mtw1-mCherry was quantified. Strains used: (A) SBY3269, SBY7420, SBY9226, sBY9476, (B) SBY9226, SBY10100, SBY9971, SBY4020, SBY3269, SBY4587. (C) SBY3269, SBY4587, SBY7492, SBY9952, SBY9226, SBY10100. (D) SBY10464, SBY10364, SBY10465, SBY10466, (E)SBY9337, SBY10479.

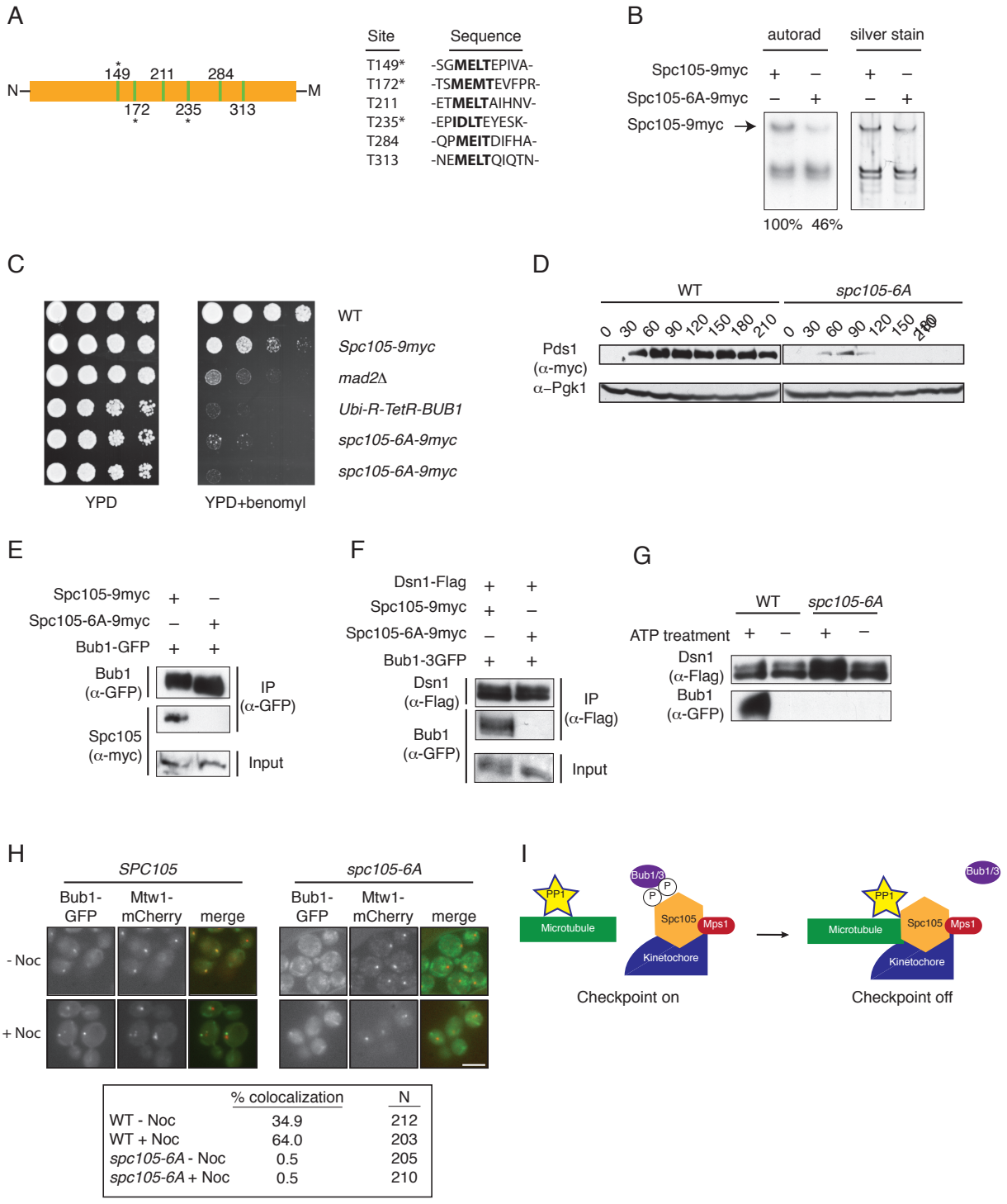

Figure III.4 Spc105 MELT motif phosphorylation recruits Bub1 to kinetochores

(A) Schematic of the N-terminal half of the Spc105 protein and the associated MELT motifs. Phosphorylation (*) was detected on three of six MELT motifs by mass spectrometry. (B) *SPC105* and *spc105-6A* kinetochore particles were treated in a kinetochore kinase assay as in Fig II.2A. ATP

incorporation into Spc105 was measured by autoradiography and normalized against relative protein levels determined by silver staining. (C) Serial dilutions of cultures form the indicated strains were plated into media with doxycycline to repress Bub1 and with or without benomyl. *spc105-6A* lanes correspond to two independently generated strains. (D) Cultures were synchronously released from a G1 α–factor arrest onto media containing nocodazole. Levels of securin (α-myc) and the loading control Pgk1 (α-Pds1) in crude lysate were determined by immunoblotting. (E) Spc105-9myc or Spc105-6A-9myc was immunoprecipitated (α-myc resin) and analyzed for copurifying Bub1-GFP by immunoblotting. (F) Kinetochore particles were immunoprecipitated from *spc105-9myc* or *spc105-6A-9myc* cells and analyzed for copurifying Bub1-3GFP by immunoblotting. (G) Wild type or Spc105-6A kinetochores were assayed for Bub1 rebinding as in III.1E and III.1F. (H) Number of cells displaying Bub1-GFP colocalization with Mtw1-mCherry was quantified in *wild type* or *spc105-6A* cells treated with or without nocodazole. (I) Model for Bub1/3 kinetochore recruitment. Mps1 is present at kinetochores during mitosis and phosphorylates Spc105 on MELT sites, generating a binding site for Bub1/3 and enabling spindle checkpoint function. This phosphorylation is opposed by Glc7, which permits dissociation of Bub1/3 and facilitates checkpoint silencing. Strains used: (B) SBY10265, SBY10267, (C) SBY3, SBY10267, SBY292, SBY8920, SBY10265, SBY10254, (D) SBY10373, SBY10374, (E) SBY104226, SBY10422, (F) SBY10426, SBY10422, (G) SBY10426, SBY10422, (H) SBY10266, SBY10264.

Chapter IV: Mad1 Kinetochore Recruitment

Summary

A major goal in studying the checkpoint is to understand what signals turn on the checkpoint and how those signals activate the established signaling cascade. While Mad1 kinetochore localization is the hallmark molecular event in checkpoint activation, the mechanism of recruitment and binding partners(s) for Mad1 have been unresolved. Budding yeast Mad1 localization requires the checkpoint kinases Mps1 and Bub1. I identified Bub1 as the receptor for Mad1 and found that Bub1-Mad1 binding is regulated by Mps1 phosphorylation of Bub1. This implicates Bub1 phosphorylation as the keystone event in kinetochore activation of the checkpoint.

Introduction

Conformational conversion of Mad2 is believed to be the critical event that activates the checkpoint (Luo and Yu, 2008; Mapelli and Musacchio, 2007), and catalytic conversion appears to be determined by Mad1/2 localization to kinetochores. Consistent with this pivotal role, Mad1 localization is mutually exclusive with bioriented kinetochore attachments (Kops and Shah, 2012). In contrast to Mad1, the upstream checkpoint proteins Mps1, Bub1, and Bub3 localize from prometaphase through anaphase regardless of checkpoint signaling (Howell et al., 2004). Thus, even though Bub1/3 kinetochore localization is required for Mad1/2 localization (Ito et al., 2011; Rischitor et al., 2007; Yamagishi et al., 2012), recruitment of Bub1/3 is not sufficient to explain Mad1/2 localization. While Mad2 turns over rapidly at kinetochore and binds to Mad1 (Howell et al., 2004; Shah et al., 2004), the kinetochore binding partner(s) for Mad1 have remained elusive.

Mad1 has been proposed to interact with several different kinetochore proteins. siRNA depletion of the human Ndc80 kinetochore protein abrogated Mad1 kinetochore localization (Martin-Lluesma et al., 2002), but an interaction between Mad1 and Ndc80 was not detected. Depletion of Ndc80 also reduces Mps1 kinetochore levels (Stucke et al., 2004). Similarly to Ndc80, a requirement for $Spc105^{KNL1}$ was also found in human cells (Varma et al., 2013). Domain analysis of hMad1 further found that distinct fragments

of Mad1 are capable of targeting Mad1 to kinetochores to some degree, indicating Mad1 likely has multiple binding interactions at kinetochores (Kim et al., 2012). Mad1 coimmunoprecipitations have also been reported with the RZZ kinetochore protein complex in *D. melanogaster*, as well as the related protein SPINDLY in *C. elegans* (Défachelles et al., 2015; Yamamoto et al., 2008). RZZ and SPINDLY are stripped from kinetochores upon microtubule binding, and it is unknown whether these interactions correspond to Mad1 recruitment, removal, or both. Additionally, these proteins do not have known homologs in budding yeast. Finally, an interaction between Mad1 and Bub1 was found in budding yeast (Brady and Hardwick, 2000), although this has not been detected in other organisms (Heinrich et al., 2014; Kim et al., 2012; Kruse et al., 2014) excepting a dubious interaction reported between coexpressed human proteins from insect cells (Seeley et al., 1999). It has therefore been unclear what protein(s) Mad1 interacts with at the kinetochore.

Inability to confidently identify the Mad1 receptor(s) has also made it difficult to understand how Mad1 kinetochore localization is dynamically controlled. Although microtubule binding to kinetochores seems to remove Mad1 through a dynein-mediated stripping pathway, this is not the sole mechanism in human cells (Kops and Shah, 2012), and this does not seem to preclude Mad1 kinetochore localization under conditions of *MPS1* overexpression in yeast (Cairo et al., 2012). In contrast, Mps1 activity is strictly required for Mad1 localization (Abrieu et al., 2001).

To understand how Mad1 localizes to kinetochores, I used purified kinetochore particles (Akiyoshi et al., 2010) to identify the kinetochore proteins necessary for Mad1 binding. This led to the identification of Bub1 as the Mad1 receptor, and allowed me to ascertain that Mps1 phosphorylation of Bub1 drives Mad1 binding. Reconstitution using recombinant proteins identified the minimal requirements for this interaction.

Results

Mad1 kinetochore recruitment requires Spc105

Because Mad1 kinetochore association is dynamic, I first tested whether Mad1 could copurify with kinetochores from checkpoint active cells. I found that Mad1 gave a strong CoIP with kinetochores from benomyl-treated cells, but was barely detectable if cells were untreated (Fig IV.1A).

This allowed me to ask what kinetochore components are required for Mad1 binding. Previous work had implicated the outer kinetochore subcomplexes Ndc80 and Spc105 in Mad1 recruitment (Martin-Lluesma et al., 2002; Varma et al., 2013). To test these candidates, I inactivated the kinetochore proteins Spc105, Ndc80, and Dam1 utilizing temperature-sensitive alleles (Enquist-Newman et al., 2001; Nekrasov et al., 2003; Wigge and Kilmartin, 2001). *ndc80-1* kinetochores retained Mad1, while Mad1 levels were significantly increased on *dad-1* kinetochores for an unknown reason (Fig IV.1B and data not shown). Remarkably, *spc105-15* kinetochores did not retain Mad1 even though Ndc80 levels were similar to *wild type*, strongly implying that Spc105, not Ndc80, could be a receptor for Mad1. This result could potentially be explained by a failure of checkpoint activity in *spc105-15* (Pagliuca et al., 2009). Ruling out this possibility, I detected the kinetochore-Mad1 interaction in a checkpoint-null mutant (*mad3*Δ) (Fig IV.1C). I next tested whether Spc105 interacted with Mad1 by CoIP. In contrast to the Ndc80 subcomplex component Nuf2, which gave a very weak association with Mad1, Spc105 strongly copurified Mad1 without Ndc80. (Fig IV.1D). This strongly suggests that Mad1 binds to kinetochores through Spc105.

Bub1 recruits Mad1 to kinetochores

Because Bub1 also copurified with Spc105 and Mad1 from budding yeast (see chapter III), I wondered whether Mad1 binding to Spc105 occurs through Bub1. When I analyzed *spc105-6A* kinetochore particles that cannot bind Bub1 I found that Mad1 was also absent (Fig IV.3B). To ascertain whether the Bub1-Mad1 interaction was necessary for kinetochore recruitment, I generated alleles of Bub1 and of Mad1 that could not interact with each other. A conserved “RLK” motif on Mad1 was reported to be necessary for Bub1 binding (Brady and Hardwick, 2000). Mutation of this Mad1 motif (*mad1-3A*) abolished Mad1 kinetochore association by CoIP (Fig IV.2A). Similarly, the middle region of Bub1 is necessary for checkpoint activity (Klebig et al., 2009; Warren et al., 2002). Deletion of the middle region of Bub1 (*bub1*Δ*M*) also prevented Mad1 association with kinetochores, even though the Bub1ΔM protein remained associated (Fig IV.2B and IV.2C). As expected, *bub1*Δ*M* kinetochores exhibited benomyl sensitivity similar to a *mad1*Δ strain, suggesting it is specifically defective in the checkpoint and not other Bub1 functions (Fig IV.2D). Consistently, *bub1*Δ*M* cells also failed to stabilize securin upon nocodazole

treatment (Fig IV.5B). These experiments show that the middle region of Bub1 and the RLK motif on Mad1 are necessary for kinetochore-Mad1 association.

To test whether Bub1 is sufficient for Mad1 localization, I made translational fusions of the Bub1 middle region Bub1(M), which does not contain the Bub3-binding domain, to either Spc105 or Spc105-6A. This fusion did not recruit endogenous Bub1 or Bub3 to kinetochores (Fig IV.3A). Strikingly, however, the Bub1(M)-Spc105-6A fusion restored the Mad1 CoIP, while the Bub1(M)-Spc105 fusion increased Mad1 association with kinetochores relative to *wild type*, as expected for the presence of additional receptors (Fig IV.3B). Furthermore, *bub1(M)-spc105-6A* cells were able to activate the checkpoint in response to nocodazole treatment, in contrast to *spc105-6A* cells, as determined by securin stabilization (Fig IV.3C). In addition, endogenous Bub1 was not required for the *bub1(M)-spc105-6A* kinetochore-Mad1 CoIP (Fig IV.3D), even though deletion of endogenous Bub1 eliminated the checkpoint response for an unknown reason (data not shown). Together, this indicated that Bub1(M) can function as a Mad1 receptor at kinetochores.

Mps1 phosphorylates Bub1

The observation that Bub1 can localize to kinetochores without Mad1 raised the question of how Bub1-Mad1 binding is regulated. Because phosphorylation is a common mechanism to regulate binding, and because both Bub1 and Mad1 are phosphoproteins, I first tested whether phosphatase treatment could disrupt the interaction in vitro. To test this in the context of kinetochores, I treated Bub1(M)-Spc105-6A kinetochores that had associated Mad1 with λ phosphatase (λPPase). Kinetochores were retained on beads while Mad1 was released with the addition of active λPPase but not inhibited λPPase (Fig IV.4A). To discriminate whether the relevant phosphorylation was present on the Bub1 or Mad1 protein, I purified each protein from yeast in the presence of phosphatase inhibitors. I then incubated the individual proteins separately with or without phosphatase and tested their ability to bind in vitro. Phosphatase or mock treated Mad1 bound to untreated Bub1, but phosphatase-treated Bub1 did not bind to either form of Mad1 (data not shown), indicating that Bub1 phosphorylation mediated Mad1 binding.

Several candidate kinases could potentially target Bub1 to promote Mad1 association. In particular, Bub1 is a reported target of Cdk1 and autophosphorylation (Goto et al., 2011). However,

treatment of Bub1 with these or other candidate kinases did not enable Mad1 binding in vitro (data not shown). Furthermore, deletion of the Bub1 kinase domain did not disrupt the kinetochore-Mad1 CoIP (Fig IV.4B). Bub1 is hyperphosphorylated during spindle checkpoint arrest, conditions under which the kinase Mps1 is active (Brady and Hardwick, 2000). To test whether Mps1 can phosphorylate Bub1, I purified recombinant Bub1(M) and Mps1 and incubated the two proteins together with radiolabeled ATP. MBP-Bub1(M) showed strong phosphorylation while the MBP tag alone did not, indicating that Mps1 can phosphorylate Bub1 in vitro on the region that mediates Mad1 binding (Fig IV.4C). Furthermore, *MPS1* overexpression slowed the electrophoretic mobility of the Bub1 protein, consistent with in vivo phosphorylation of Bub1 by Mps1 (Fig IV.6A).

In order to determine the Bub1 phosphorylation sites, I compiled mass spectrometry data on purified kinetochores that contain Bub1 and found 7 sites had been detected within the Bub1(M) region. I selected these 7 sites as well as 8 adjacent serine or threonine residues for mutation to alanine to prevent phosphorylation, generating *bub1-15A* (Fig IV.4D and Table III Table IV).). I found that Bub1-15A showed faster migration than wild type Bub1, and that this migration was increased further with λPPase treatment, indicating Bub1-15A is less phosphorylated than the wild type protein but also contains additional phosphorylation sites (Fig IV.4E).

Mps1 regulates the Bub1-Mad1 interaction

To address whether Mps1 phosphorylation of Bub1 recruits Mad1 to kinetochores, I first tested the phenotype of *bub1-15A* cells on benomyl media. *bub1-15A* cells grew similarly to *mad2*Δ cells, but significantly better than *bub1*Δ cells, as expected for a checkpoint-specific defect due to Mad1 mislocalization (Fig IV.5A). *bub1-15A* cells also failed to stabilize Pds1 in response to nocodazole treatment, indicating a non-functional checkpoint (Fig IV.5B). To ask whether Mad1 retained kinetochore localization, I purified kinetochore particles from *bub1-15A* cells and found that Mad1 was not associated even though Bub1-15A stayed bound (Fig IV.5C). As an additional test, I generated the 15A mutations in Bub1(M)-Spc105-6A. I also found that Mad1 failed to CoIP with Bub1(M)-15A-Spc105-6A kinetochore particles (Fig IV.5D). Subsequent analysis showed that mutation of the N-terminal three phospho-sites in Bub1(M) (*bub1-3A*) is sufficient to prevent Mad1 binding and checkpoint activation, as is mutation of a

conserved phosphosite upstream of the 15A mutations (Fig IV.5C and IV.5E and Table III and Table IV). This illustrates that multiple phosphorylation sites are required for Mad1 binding.

To test whether Mps1 activity is sufficient to promote Mad1 binding, I first asked whether *MPS1* overexpression could induce Bub1-Mad1 association. Cells were arrested in G1, when the checkpoint is not active, and Mps1 was overexpressed by galactose induction. Bub1 and Mad1 coimmunoprecipitated under these conditions, indicating that Mps1 phosphorylation, but not other mitotic events, promote the Bub1-Mad1 interaction (Fig IV.6A). I next tested whether Mps1 could promote Mad1 binding to kinetochores in vitro. I utilized Bub1(M)-Spc105-6A kinetochores, which retain Mps1 and the Bub1(M) fragment, since it is fused to Spc105-6A, upon phosphatase treatment. These kinetochores were first treated with λPPase to remove existing phosphorylation and Mad1, then rephosphorylated with copurifying Mps1 by addition of ATP and incubated with yeast lysate as a source of Mad1 (Fig IV.6B-E). ATP-treated kinetochores bound to Mad1, and this depended on the presence of the phosphorylation sites on the Bub1(M) fragment as well as activity of Mps1 (Fig IV.6C and 6D). To confirm that endogenous Bub1 and Bub3 were not required for the interaction, I tested the copurifcation of Mad1 with Bub1(M)-Spc105-6A kinetochore particles using lysate from other checkpoint mutants. As expected, endogenous Bub1 and Bub3 were not required in the lysate, but Mad2 was, presumably functioning through its interaction with Mad1 (Fig IV.6E, refs). This contrasts with wild type kinetochores, which require Bub1 and Bub3 to be present in the lysate for Mad1 binding, indicating Mad1 likely associates with these kinetochores through a pre-formed Bub1-Mad1 complex (Fig IV.6E). Cumulatively, these data indicate that Mad1 associates with kinetochores through Mps1-mediated phosphorylation on Bub1.

Bub1 and Mad1 directly interact through Mps1 phosphorylation

To confidently demonstrate a direct recruitment mechanism for Bub1-Mad1 binding, I sought to define the minimal binding requirements. Because yeast protein purifications could contain additional copurifying proteins that facilitate the Mad1-kinetochore interaction, I attempted to reconstitute Bub1-Mad1 binding using recombinant proteins. Due to difficulties expressing full length Bub1 and Mad1, I chose to express the fragments Bub1(M) and the Mad1 C-terminus (Mad1(C)) along with full length Mps1. Because Mad2 was required for kinetochore-Mad1 binding of native yeast proteins (Fig IV.6C), I

also expressed Mad2. First, I coexpressed these four proteins in *E. coli* and tested for stable association by pulldown of S-tagged Bub1(M). Both Mad1 and Bub1 showed significant degradation, and Bub1 migration was highly distorted by extensive phosphorylation. Nonetheless, Mad1(C)/Mad2 formed a complex that clearly copurified with Bub1(M), and this required expression of each individual protein, including Mps1 which was not stably bound to Bub1(M) (Fig IV.7A and IV.7B). Mutation of phosphosites on Bub1(M) prevented Mad1(C)/Mad2 binding, even with Mps1 coexpression (Fig IV.7A). I next tested whether Bub1(M) could bind to Mad1-C/Mad2 in vitro. Consistent with the requirement for Bub1(M) phosphorylation, Bub1(M) was able to bind Mad1-C/Mad2 only when it was coexpressed with Mps1, and this binding was abolished in phosphomutants of Bub1(M) (Fig IV.7C). However, coexpression of Mad1-C/Mad2 with Mps1 did not permit binding to unphosphorylated Bub1(M) (Fig IV.7C). These results show that a Mad1-C/Mad2 complex is sufficient to bind phosphorylated Bub1(M) without contributions from additional proteins or phosphorylation on Mad1(C) or Mad2. I conclude that Mad1 recruitment, the key regulated checkpoint activation step, is determined by Bub1 phosphorylation.

Discussion

The nature of the Mad1-kineotchore interaction has been difficult to ascertain because of in vivo limitations, the complex composition of the kinetochore, and difficulty establishing interactions in vitro. While Ndc80 was a leading candidate for the Mad1 receptor (DeLuca et al., 2003; Martin-Lluesma et al., 2002; McCleland et al., 2003), it now appears likely that the requirement for Ndc80 is instead due to its function in localizing Mps1 (Kemmler et al., 2009; Stucke et al., 2004; Zhu et al., 2013). Because Bub1(M) restores Mad1 localization and function to an *spc105-6A* mutant, my data is consistent with Bub1 as the sole Mad1 kinetochore receptor in yeast. However, Mad1 may have additional or separate binding partners in other organisms, such as the RZZ complex or SPINDLY (Défachelles et al., 2015; Jia et al., 2013; Yamamoto et al., 2008). A Bub1-Mad1 interaction has not been detected in fission yeast, or human cells (Heinrich et al., 2014; Kim et al., 2012; Kruse et al., 2014), but is reported with *C. elegans* proteins (Moyle et al., 2014). Identifying the Mad1 interacting proteins at the kinetochore may also be complicated due to a polyvalent, multi-protein binding mechanism, as proposed for human Mad1 (Kim et al., 2012). In

any case, Bub1 appears to be required for at least part of the Mad1-kinetochore association in humans and *C. elegans*, because Bub1 depletion reduces Mad1 kinetochore levels (Moyle et al., 2014, 2014).

In addition to identifying Bub1 as a receptor for Mad1 in budding yeast, this work identified phosphorylation on Bub1 that regulates this binding. This explains the requirement for Mps1 independently of Bub1/3 recruitment and implicates a molecular target for regulation by microtubule binding. Tethering Mps1 to kinetochores in human cells led to constitutive checkpoint activation, consistent with constitutive Mad1 localization, while similar tethering in fission yeast did not (Ito et al., 2011; Jelluma et al., 2010). This difference may be due to retention of Mps1 regulation when tethered to its natural receptor, Ndc80, in the fission yeast experiments but not when tethered to $Mtw1^{Mis12}$ in the human cell experiment. Mps1 phosphorylation of Ndc80 has been proposed to signal the checkpoint (Kemmler et al., 2009), but I found that a mutant of Ndc80 deficient in Ndc80 phosphorylation could still recruit Mad1 (data not shown).

Because Mps1 activity promotes Bub1/3 localization to kinetochore, it is somewhat surprising that Mps1 also targets Bub1 to recruit Mad1 and activate the checkpoint. This raises the question of why Mps1 does not always phosphorylate Bub1 at the kinetochore. It is probable that Mps1 activity towards Bub1 is specifically regulated in response to microtubule attachment state. Consistent with this idea, fusion of Bub1(M) to Spc105 may be expected to constitutively activate the checkpoint if Mps1 could always phosphorylate Bub1 at the kinetochore. However, this fusion permits viability and appears to have a mostly normal checkpoint response (Fig IV.3D). Such regulation of Mps1 could occur through any number of mechanisms, including microtubule occlusion of Bub1, dissociation or inactivation of Mps1, upregulation of opposing phosphatase activity, or others. Determining such a mechanism will be a key next step in understanding checkpoint activation.

Materials and Methods

Strain and plasmid construction

All strains are isogenic with the W303 background and standard genetic crosses were performed to introduce temperature sensitive kinetochore alleles. Strains used in this study are listed in supplementary tables. Additional information on strain and plasmid construction is reported in (London and Biggins,

2014b).

Yeast methods and purifications

Media and microbial techniques were as described (Rose et al., 1990). Kinetochore particle and Flag-tagged protein purifications from yeast were performed essentially as described in Chapter II. Kinetochore particles were purified from cells expressing Dsn1-6His-3Flag as described (Akiyoshi et al., 2009). Bed-beating lysis (Ranjitkar et al., 2010) was used for Pds1 stability, *pGAL-MPS1* induction, and Bub1 *in vivo* phosphorylation shift experiments. Immunoprecipitated proteins were washed three times in lysis buffer (consisting of 25 mM HEPES, pH 8.0, 150 mM KCl, 0.1% NP-40, 2 mM $MgCl_2$, 0.1 mM EDTA, pH 8.0, 0.5 mM EGTA, pH 8.0, and 15% glycerol) with protease and phosphatase inhibitors, twice in lysis buffer alone, and eluted in SDS sample buffer.

Protein binding assays

Kinetochore-Mad1 binding assays using lysates were performed essentially as described (London et al., 2012). Details of other protein purifications, coexpression, and binding experiments are reported in (London and Biggins, 2014b). Briefly, recombinant binding interactions were performed by incubating resin-bound Bub1-S-tag proteins with purified Mad1-3Flag proteins. In vitro binding buffer consisted of PBS with 0.1% Tween-20, 150 mM NaCl, and 300 ng/μL bovine serum albumin (BSA). Approximately equivalent amounts of each test protein were used in reactions at 4° for 1-2 hours. Coexpression experiments used the pET-Duet and pCDF-Duet expression system (Novagen) with IPTG induction (100 μM IPTG for 1 hour at 37°), and purifications were performed with S-protein agarose resin (EMD Millipore) or α-Flag-conjugated Dynabeads. Bacterial bacterial lysis buffer consisted of 2 mM EDTA, 2 mM EGTA, in PBS with 1 mM PMSF and 10 μg/mL each of Leupeptin, Pepstatin, and Chymostatin.

Immunological methods

Immunoblotting was performed using the following antibodies diluted in PBS-Tween buffer: α-myc 9E10 (Covance) at 1:10,000, α-Flag M2 (Sigma- Aldrich) at 1:3,000, α-V5 (Thermo/Pierce) at 1:5,000, α-

GFP (Roche) at 1:1,000 or α-GFP JL-8 (Clontech) at 1:5,000, α-Pgk1 (Invitrogen) at 1:10,000, α-S-tag (Thermo/Pierce) at 1:2,000, α-Spc105 and α-Ndc80 antibodies were both used at 1:10,000 and were kind gifts from Arshad Desai (Akiyoshi et al., 2010). Immunoprecipitations used antibodies conjugated to Protein G Dynabeads. Images shown above are cropped from original immunoblots for clarity.

Mass Spectrometry

Bub1 phosphorylation sites were determined from mass spectrometry data acquired similarly to that described in Chapter III on complete phosphorylated kinetochore preparations (Mtw1-3Flag (SBY8564)) or associated Bub1 and Spc105 (Dsn1-6His-3Flag Mps1-as1 (SBY9192)). Proteins were subjected to Trypsin digestion, SCX fractionation, and mass spectrometry with an LTQ-Orbitrap instrument. Phosphopeptides identified through X!Tandem searching with a < .7% error rate were selected as true positives. See London, 2014 (London and Biggins, 2014b) for details.

Yeast methods

Temperature shifts, Cdc20 depletion arrests, Pds1 timecourses, galactose inductions, and serial dilutions were performed as described above. Benomyl was used at 30 μg/L in liquid cultures.

Phosphatase and Kinase assays

Mad1 phosphatase release and Bub1 phosphoshift experiments were performed as above, where proteins were immobilized on beads and treated with 1 mM $MnCl_2$ and 200 u λPPase for 20 minutes at 30°. Kinetochore λPPase treatments were performed with the same buffer conditions at 23° for 25 minutes. GST-Mps1 kinase reactions were performed at 30° for 20 minutes in kinase buffer (50 mM Tris-HCl pH 7.5, 75 mM NaCl, 5% glycerol, 10 mM $MgCl_2$ 1 mM DTT, 10 μM ATP) diluted into PBS with 55 nM γ-^{32}P-ATP. MBP-Bub1 phosphorylation levels were determined by normalizing Phosphorimager signal to protein levels based on Coomassie staining using ImageJ.

Figures

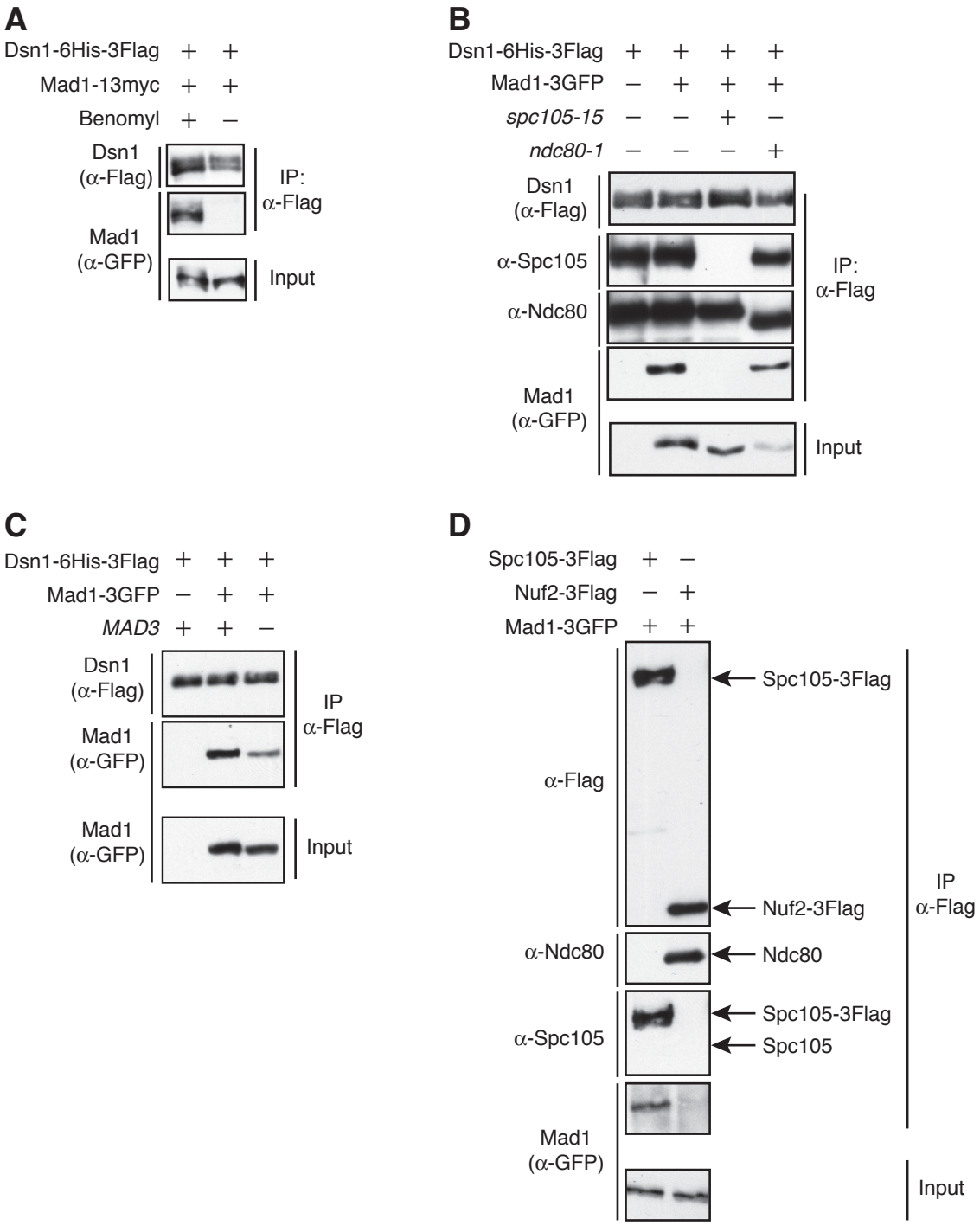

Figure IV.1 Mad1 interacts with kinetochores through Spc105

(A) Benomyl treatment enriches the Mad1 copurification with kinetochores. Kinetochore particles were purified from cells treated with or without benomyl during culture and analyzed for association of Mad1 by

immunoblotting with the indicated antibodies. (B) Mad1 requires Spc105, not Ndc80 function to associate with kinetochores. Cells with the indicated temperature sensitive alleles were shifted to 37° before harvest. Kinetochores were purified and analyzed from these cells as in (A). (C) Downstream checkpoint function is not required for Mad1-kinetochore association. *Wild type* or *mad3*Δ cells were treated with benomyl prior to harvest and analyzed for the kinetochore-Mad1 interaction as in Fig II.1A. (D) The interaction between Spc105 or Nuf2 and Mad1 was assayed from benomyl-treated cells as in Fig II.1A. Strains used: (A) SBY8412, (B) SBY8253, SBY8415, SBY8829, SBY8579, (C) SBY8253, SBY8415, SBY11497, (D) SBY8970, SBY8971.

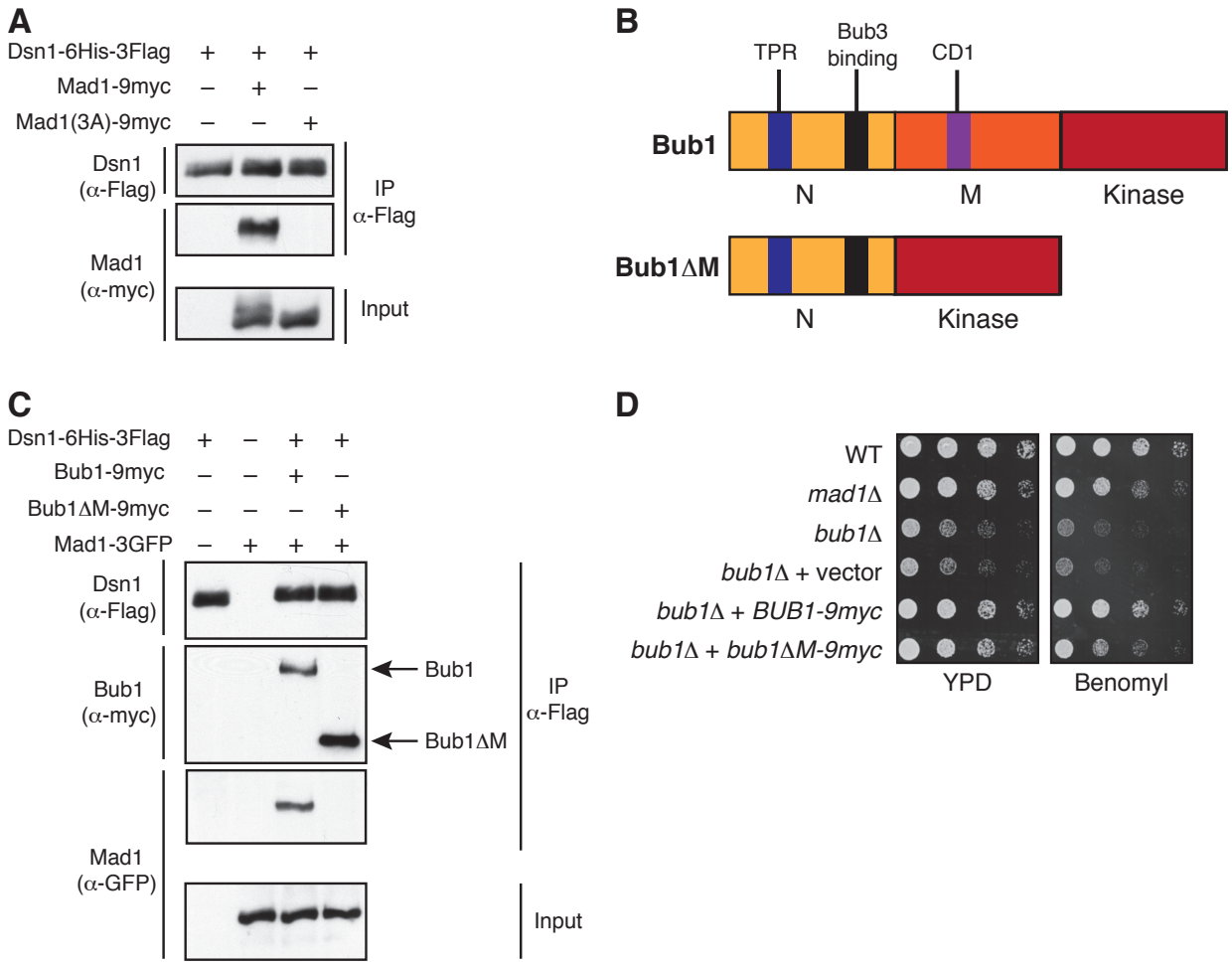

Figure IV.2 A Mad1 RLK motif and the Bub1 middle region are necessary for Mad1 kinetochore recruitment

(A) The Mad1(3A) protein does not associate with kinetochores. Cells containing Mad1-9myc or Mad1(3A)-9myc were treated with benomyl and processed as in Fig IV.1A. (B) Diagram of Bub1 protein domains, including a middle region (residues 369-608) deleted in Bub1ΔM. Also shown are the kinase domain (residues 609-1021), a Bub3-binding domain (residues 315-350) (Larsen et al., 2007), and a tetratricopeptide (TPR) domain (residues 57-171) (Bolanos-Garcia et al., 2009). A conserved domain (CD1) that is necessary for the checkpoint is also present in the middle region (Klebig et al., 2009). (C) Bub1M is necessary for Mad1-kinetochore association. Wild type, Bub1-9myc, or Bub1ΔM-9myc kinetochores were purified and analyzed as in IV.1A. (D) Bub1(M) exhibits a checkpoint-defective growth pattern on benomyl. Serial dilutions of the indicated strains were plated onto media with or without

benomyl and cultured. Strains used: (A) SBY8253, SBY11840, SBY11967, (C) SBY8253, SBY11392, SBY11317, SBY11319, (D) SBY8412, SBY8820, SBY10596, SBY11232, SBY11072, SBY11083.

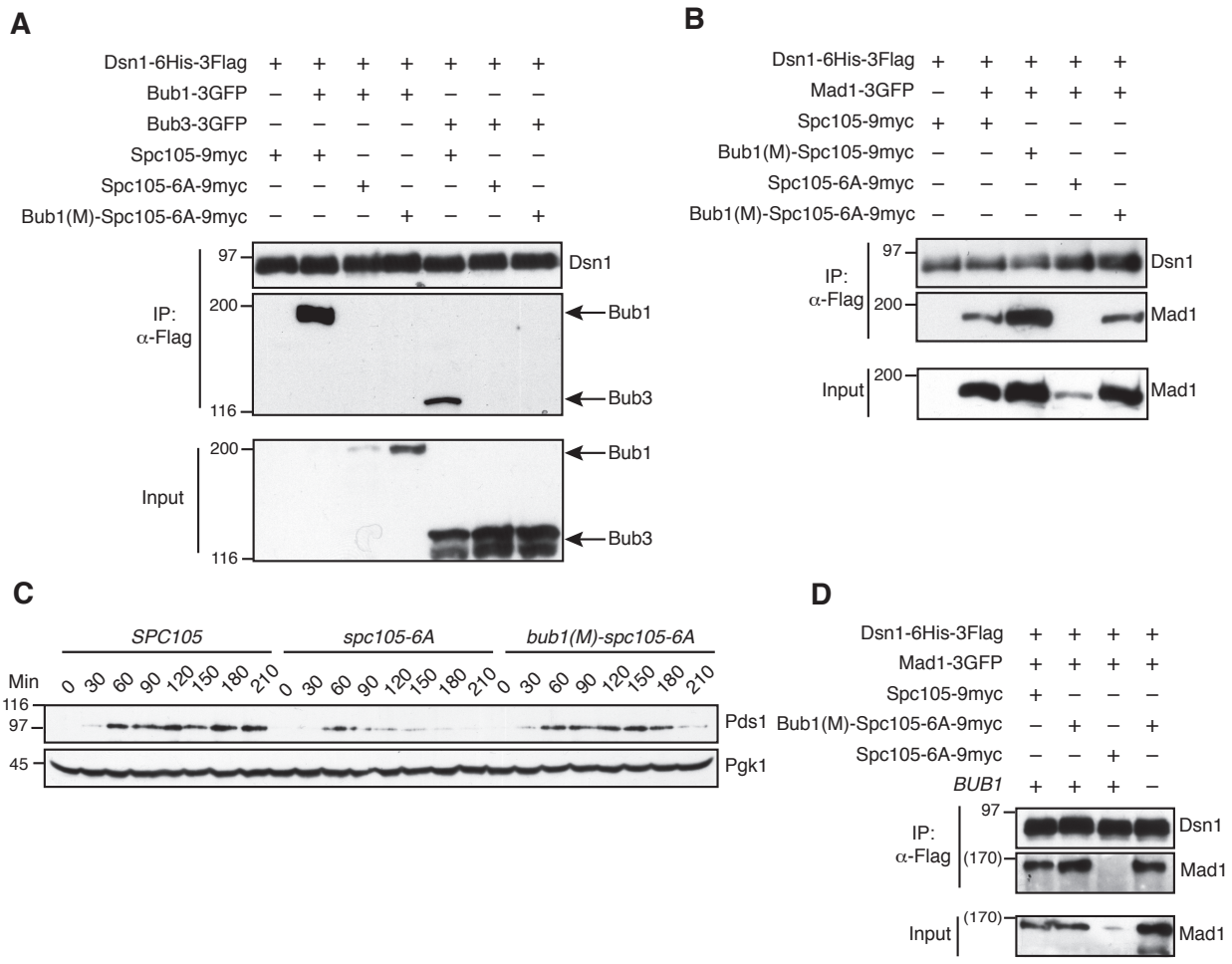

Figure IV.3 Bub1(M) rescues Mad1 association with Spc105-6A kinetochores

(A, B) Bub1(M)-Spc105-6A kinetochore particles do not recruit endogenous Bub1 or Bub3 but do recruit Mad1. Kinetochores from the indicated strains were purified and analyzed as in Fig IV.1A. (C) Bub1(M) fusion restores a checkpoint response to Spc105-6A cells. The indicated strains were assayed for stabilization of secuin (Pds1) in response to nocodazole treatment as in Fig III.4D. (D) Endogenous Bub1 is not required for Mad1 to associate with Bub1(M)-Spc105-6A kinetochores. Kinetochore particles from *BUB1* and *bub1*Δ cells were prepared as in Fig IV.1A. Strains used (A) SBY10267, SBY10347, SBY10422, SBY11725, SBY10372, SBY11637 (B) SBY10267, SBY11207, SBY11208, SBY11210, SBY11209. (C) SBY11892, SBY11893, SBY11894, (D) SBY11207, SBY11209, SBY11210, SBY11303.

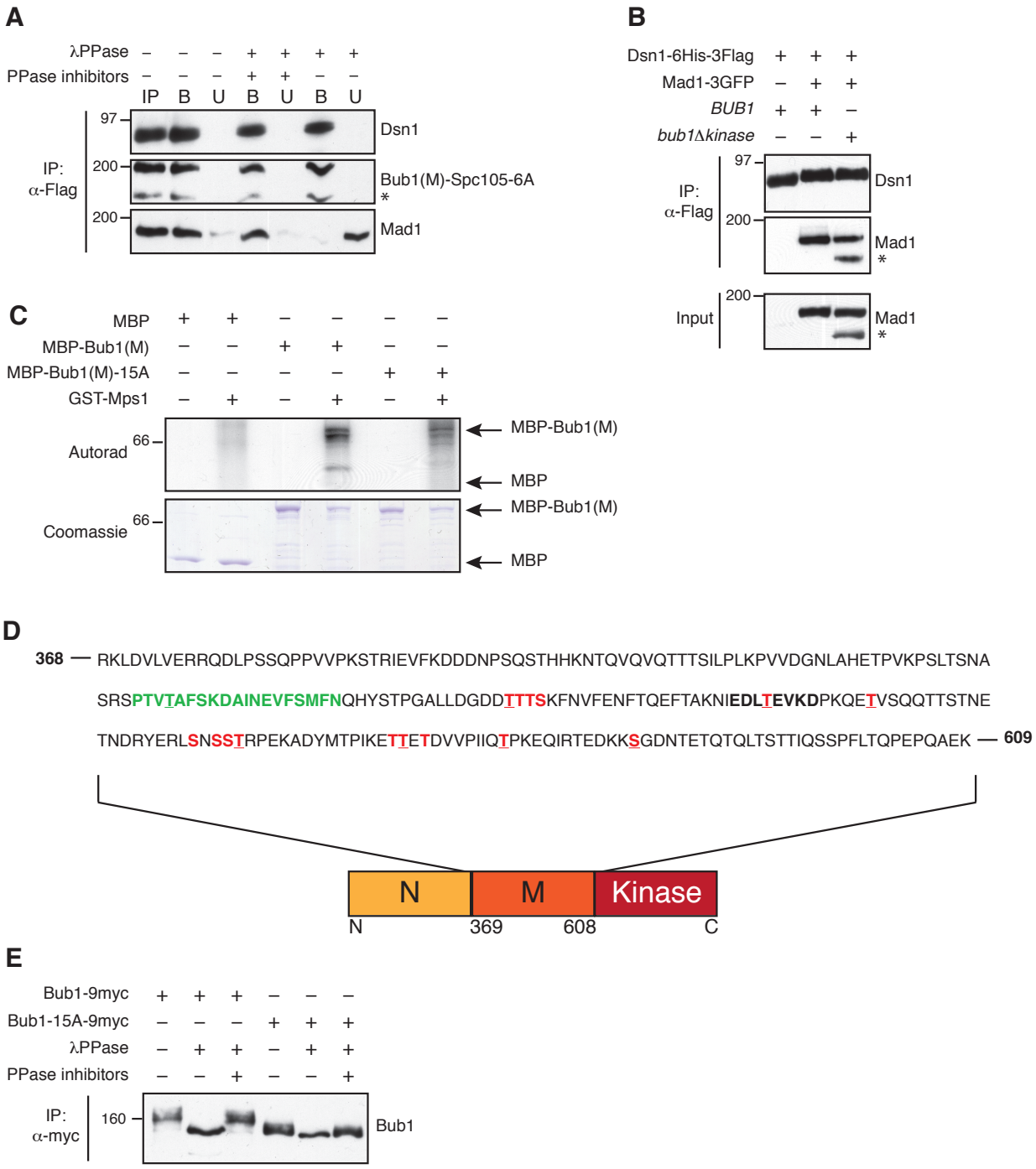

Figure IV.4 Bub1 is a target of Mps1 phosphorylation

(A) Mad1 association with kinetochores is disrupted with phosphatase treatment. Bub1(M)-Spc105-6A kinetochores and copurifying Mad1 were immobilized on α-Flag resin, then incubated in buffer with or without λPPase and with or without phosphatase inhibitors. The bound (B) and unbound (U) fractions

were analyzed by immunoblotting. An untreated control was also included (IP). (B) Bub1 kinase activity is not necessary for Mad1-kinetochore association. Kinetochores from cells with the indicated genotype were prepared as in Fig IV.1A. (*) denotes a degradation produce of Mad1 specific to the strain used. (C) Mps1 phosphorylates Bub1(M) in vitro. Recombinant MBP-Bub1(M) and GST-Mps1 were purified and incubated in buffer containing radiolabeled ATP. Proteins were analyzed by Coomassie staining and autoradiography. (D) Mass spectrometry identified phosphorylation sites on Bub1(M). A set of mass spectrometry data on purified kinetochore particles was analyzed for phosphorylation on the Bub1(M) region. Identified sites are underlined, with the sites selected for mutagenesis in *bub1-15A* in red. CD1 is shown in green, and the best-matching Mps1 consensus site is bolded. (E) Bub1-15A exhibits reduced phosphorylation in vivo. Bub1-9myc and Bub1-15A-9myc proteins from benomyl-treated cells were immobilized on α-myc resin and incubated with λPPase as in (A). Strains used: (A) SBY11209, (B) SBY8253, SBY8415, SBY11006, (E) SBY11764, SBY11766.

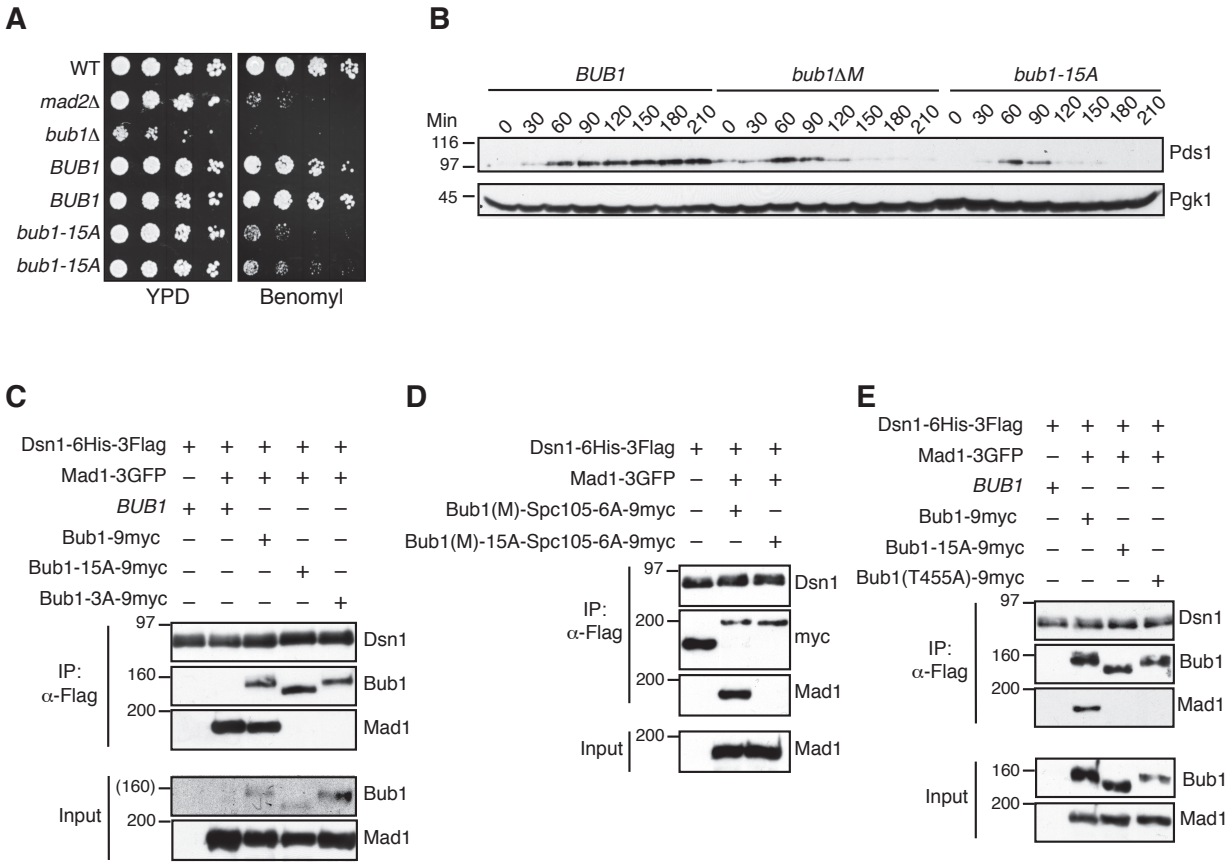

Figure IV.5 Mad1 kinetochore association required Bub1 phosphorylation

(A) Serial dilutions of strains of the indicated genotype were cultured on media with or without benomyl. Two independently generated strains for *BUB1* and *bub1-15A* were plated. (B) *bub1ΔM* and *bub1-15A* cells are checkpoint defective. Cultures were synchronously released into nocodazole media to assay for Pds1 stabilization, as in Fig III.4D. (C, E) Phosphomutant *bub1-15A, bub1-3A,* and *bub1(T455A)* abolish the Mad1-kinetochore association. The indicated strains were processed as in Fig IV.1A. (D) Bub1(15A)-Spc105-6A kinetochores do not copurify Mad1. The indicated strains were processed as in Fig IV.1A. Strains used: (A) SBY8253, SBY292, SBY10596, SBY10596:pSB1983, SBY10596:pSB1984. (B) SBY11340, SBY11341, SBY11342, (C) SBY8253, SBY8415, SBY11764, sBY11766, SBY11751, (D) SBY10267, SBY11209, SBY11415, (E) SBY8253, SBY11764, SBY11766, SBY12068.

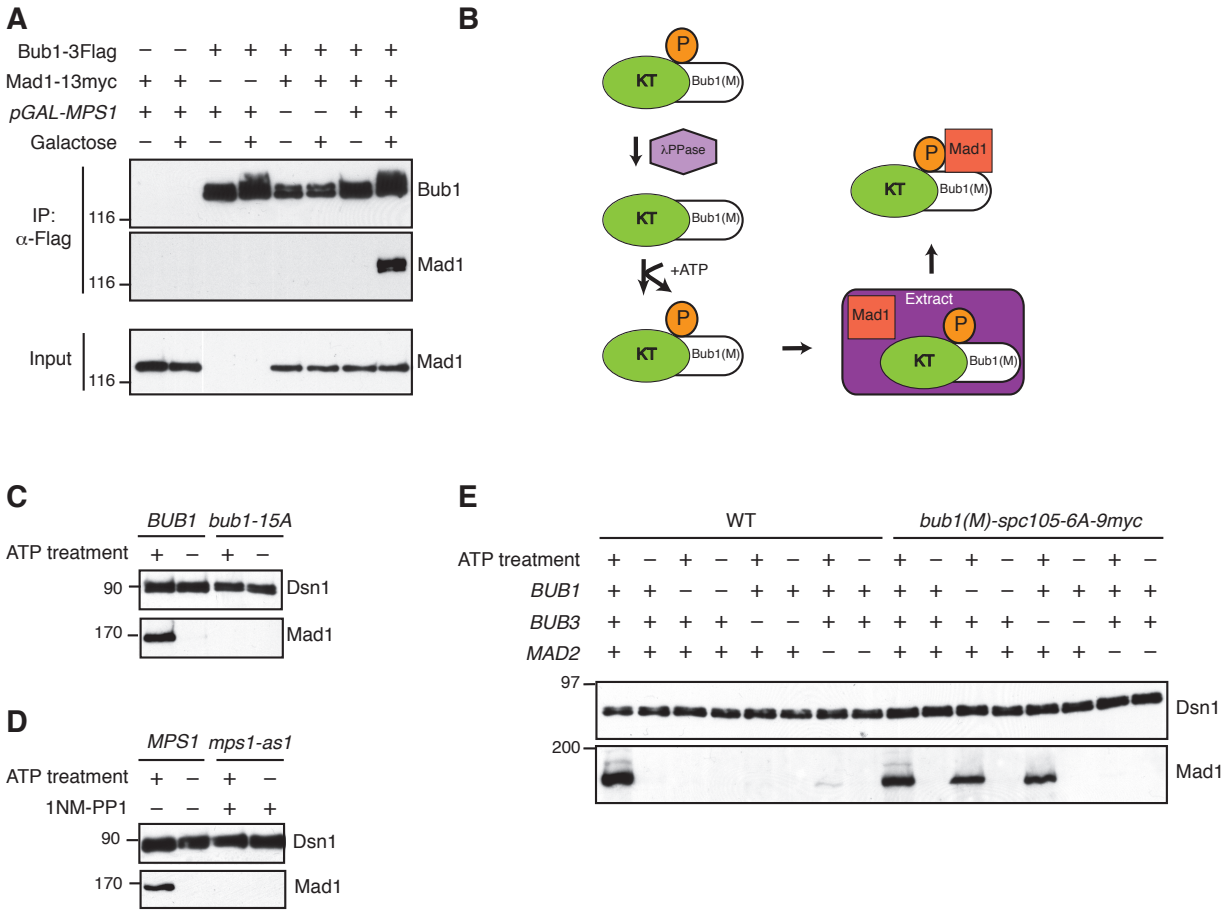

Figure IV.6 Mps1 activity recruits Mad1 to kinetochores

(A) *MPS1* overexpression promotes ectopic Bub1-Mad1 association. Mps1 was overexpressed with galactose in cells containing Bub1-3Flag and Mad1-13myc. Bub1 was immunoprecipitated and analyzed for Mad1 copurification by immunoblotting. (B) Schematic of Bub1(M)-Spc105-6A Mad1-kinetochore rebinding assay. (C,D) Bub1 phosphorylation and Mps1 activity are required for Mad1-kinetochore binding in vitro. Bub1-Spc105-6A-9myc or Bub1-15A-Spc105-6A-9myc kinetochores were immobilized, phosphatase treated, incubated with ATP, then incubated with lysate to assay for Mad1 binding. (E) Bub1(M)-Spc105-6A kinetochores bypass the requirement of endogenous Bub1 and Bub3 for Mad1-kinetochore in vitro binding. Wild type or Bub1(M)-Spc105-6A-9myc kinetochore particles were assayed for Mad1 rebinding as in (B-D), except that the source of lysate was varied. Lysates from *bub1*Δ, *bub3*Δ, and *mad2*Δ cells were used as indicated. Strains used: (A) SBY11541, SBY11490, SBY10532, SBY11488, (C) SBY11149, SBY11325, (D) SBY11149, SBY11486. (E) SBY11149, SBY8253, SBY8416, SBY11464, SBY11418, sBY11389.

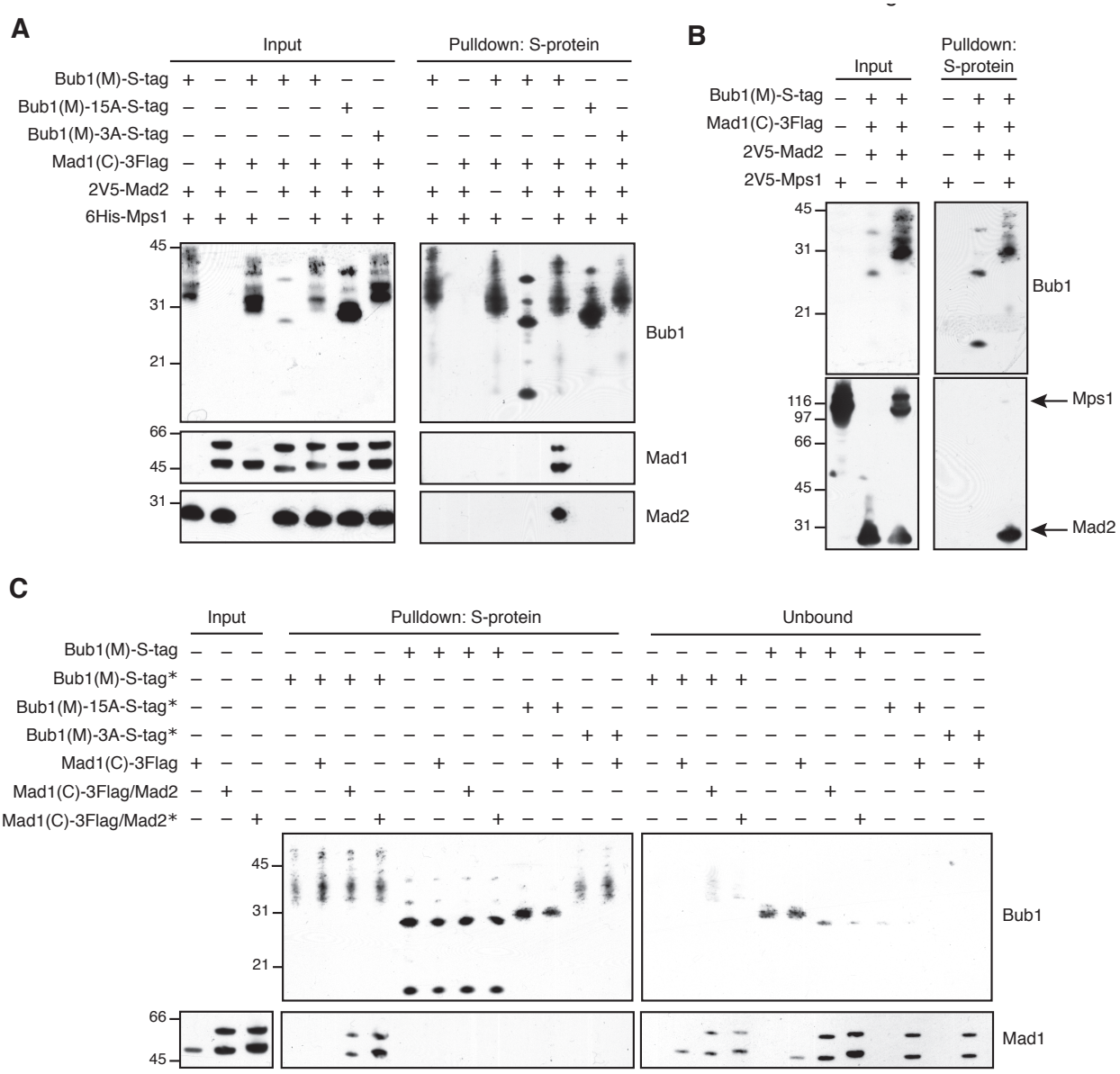

Figure IV.7 The Bub1-Mad1 interaction can be reconstituted in vitro

(A) Bub1 and Mad1 interact when coexpressed with Mps1 and Mad2. The indicated proteins were coexpressed in *E. coli*. Bub1(M)-S-tag proteins were purified from these strains and copurifying proteins were assayed by SDS-PAGE and immunoblotting. Mad1(C) abbreviates Mad1(318-749). (B) Mps1 does not stably associate with Bub1(M)-S-tag. Proteins were coexpressed and analyzed as in (A) with 2V5-Mps1. (C) Purified Bub1(M) and Mad1(C) bind in vitro. (*) indicates Mps1 coexpression with the indicated protein. Mad1-3Flag proteins were purified with α–Flag resin followed by Flag peptide elution. Bub1(M)-S-

tag proteins were immobilized on S-protein resin, then incubated with Mad1-3Flag proteins to test for binding.

Chapter V: Mps1 Phosphorylation of Bub1 is Required to Activate the Spindle Checkpoint Independently of Kinetochores

Summary

Kinetochore recruitment of the checkpoint proteins Mps1, Bub1, Bub3, Mad1, and Mad2 is necessary for spindle checkpoint activation, but it remains unclear precisely why kinetochore localization is required. Surprisingly, the necessity for kinetochores to activate the checkpoint can be bypassed upon *MPS1* overexpression, raising the possibility that kinetochores toggle the checkpoint by regulating Mps1 activity. To better understand the critical signaling events in checkpoint activation, I tested the requirement of specific Mps1 phosphorylation events for the *MPS1* overexpression checkpoint arrest. I found that interaction of the checkpoint proteins with kinetochore proteins through Bub1/3-Spc105 may not be required for this arrest. In contrast, a Bub1-Mad1 interaction, which is mediated by Bub1 phosphorylation, is necessary for this arrest. This supports the concept that the critical function for kinetochores in the checkpoint is to promote checkpoint protein interactions through Mps1 phosphorylation.

Introduction

Kinetochores activate the spindle checkpoint through catalytic production of the MCC. Conformational conversion of Mad2 from “open” (O-Mad2) to “closed” (C-Mad2) occurs at the kinetochore and is the critical biochemical event in MCC production. Mad2 conversion is catalyzed by kinetochores that harbor a template C-Mad2 bound to Mad1 (Luo and Yu, 2008; Mapelli and Musacchio, 2007). Mad1/2 recruitment to kinetochores provides this template, although it is unresolved precisely why Mad1/2 must be recruited to kinetochores in order to promote Mad2 conversion. In addition to conformational conversion of Mad2, C-Mad2 and $Mad3^{BubR1}$ must also associate with Cdc20 for a functional checkpoint, and it is currently unresolved how these binding events are coordinated with Mad2 conformational conversion. Popular models invoke additional poorly defined downstream events to explain Mad2 conversion and MCC assembly (Ballister et al., 2014; Heinrich et al., 2014; Hewitt et al., 2010; Kruse et al., 2014; Kuijt et al., 2014; Maldonado and Kapoor, 2011; Tipton et al., 2013). However,

recent work established that a Bub1-Mad1 interaction is required for the checkpoint in diverse eukaryotes (Brady and Hardwick, 2000; London and Biggins, 2014b; Moyle et al., 2014; Warren et al., 2002), raising the possibility that a Bub1-Mad1 interaction may be critical for triggering Mad2 activation and subsequent MCC formation.

As detailed in chapters III and IV, Mps1 kinase activity recruits Mad1 and Bub1, the Mad1 receptor in budding yeast, to kinetochores and is therefore critical for checkpoint signaling. However, Mps1 may have additional functions in the checkpoint downstream of Mad1 recruitment. For instance, human cells bearing a kinetochore-localization deficient Mps1ΔN protein did not abolish the checkpoint response, suggesting that soluble Mps1 promoted activation (Maciejowski et al., 2010). However, these cells also contained an inactivated form of Mps1 that may nonetheless localize the functional Mps1ΔN protein to kinetochores through dimerization (Nijenhuis et al., 2013). Another study concluded that Mps1 has a downstream role because Mps1 inhibition was initially observed to preserve localization of the Mad1/C-Mad2 template to kinetochores, but abolished localization of O-Mad2 in human cells. This suggested that Mps1 activity is required for cycling of O-Mad2 to C-Mad2, which is necessary for propagation of the checkpoint signal from kinetochores (Hewitt et al., 2010). However, this result may be explained by varying detection limits of conformation-specific Mad2 antibodies that were used because a recent study found Mad1/C-Mad2 dissociated upon Mps1 inhibition, contradicting the earlier observation and explaining O-Mad2 mislocalization (Tipton et al., 2013).

Further evidence supporting a role for Mps1 downstream of the kinetochore came from experiments tethering Mad1 and Mad2 to kinetochores. Forcing Mad1 to localize to kinetochores in human cells, through translational fusion to the Mis12 kinetochore protein, resulted in constitutive checkpoint activation that required activity of Mps1 and Ipl1 and the presence of BubR1 (Maldonado and Kapoor, 2011). (Ipl1 supports Mps1 activation in human cells (Saurin et al., 2011; van der Waal et al., 2012; Zhu et al., 2013) while BubR1 is a structural component of the MCC (see Introduction).) Checkpoint activation also required additional kinetochore components, because tethering Mad1 to chromosome arms did not activate the checkpoint (Maldonado and Kapoor, 2011). Surprisingly, however, similar experiments in fission yeast and human cells revealed that specific regions of Bub1 and Mad1 are also needed for constitutive activation by kinetochore-tethered Mad1. Required are a C-terminal region and an

"RLK" motif of Mad1 (see Fig IV.2A), and a conserved domain within Bub1(M) (Fig IV.2B) (Ballister et al., 2014; Heinrich et al., 2014; Kuijt et al., 2014). Similarly, kinetochore tethering of human Mad2 resulted in constitutive checkpoint activation, but this required Mad1 and the Mad1 C-terminus (Kruse et al., 2014). This is consistent with the necessity of the Mad1-Mad2 interaction for checkpoint activation, even when C-Mad2 is tethered to kinetochores. While this evidence has been interpreted to implicate undefined downstream functions for Mad1 or Mps1 in the checkpoint, all of the mutants tested in these experiments are known or would be expected to disrupt a Bub1-Mad1 interaction (Heinrich et al., 2014; London and Biggins, 2014b and data not shown). These results are therefore consistent with the hypothesis that a Bub1-Mad1 interaction determines Mad2 activation and downstream checkpoint signaling. Finally, the surprising finding that *MPS1* overexpression can activate the checkpoint even when kinetochore assembly is blocked by inactivation of the inner kinetochore protein Ndc10 (Poddar et al., 2005) may suggest that soluble targets of Mps1 in can activate the checkpoint. However, this could also be explained if *MPS1* overexpression leads to Bub1 phosphorylation and Bub1-Mad1 association even in the absence of a kinetochore scaffold. If this is the case, the reported results would all be consistent with a function for a Bub1-Mad1 interaction as a trigger for downstream checkpoint signaling

To investigate the mechanism of Mps1 checkpoint activation, I sought to test whether *MPS1* overexpression-induced checkpoint activation still required the Bub1-Spc105 or Bub1-Mad1 interactions. The identification of Mps1 phosphorylation events that recruit Bub1 to the kinetochore and mediate the Bub1-Mad1 interaction allowed me to test the requirements for these events with phosphomutant alleles (London and Biggins, 2014b; London et al., 2012; Shepperd et al., 2012; Yamagishi et al., 2012). I determined that the Bub1-Mad1 interaction is critical for Mps1-driven checkpoint activation while the Bub1-Spc105 interaction may not be required.

Results

MPS1 overexpression bypasses Spc105 phosphorylation but requires Bub1 phosphorylation to activate the checkpoint

MPS1 overexpression activates the checkpoint in the absence of functional kinetochores in budding yeast, but it remained unclear what Mps1 targets specifically trigger the checkpoint (Poddar et

al., 2005). In order to determine what whether the same checkpoint protein interactions occur under these conditions as upon nocodazole treament, I tested for interactions between Bub1 and Mad1 by coimmunoprecipitation in *pGal-Mps1 ndc10-1* cells. Cultured cells were shifted to 37° to inactivate Ndc10-1, disrupting kinetochores, and treated with galactose to induce *MPS1* overexpression. I found that the Bub1-Mad1 association was not noticeably reduced in *ndc10-1* relative to *NDC10* cells (Fig V.A). This indicated that *MPS1* overexpression can facilitate the Bub1-Mad1 interaction, which requires Bub1 phosphorylation (London and Biggins, 2014b), independently of kinetochores.

I next wanted to determine whether the Bub1-Mad1 interaction is required for the *MPS1* overexpression arrest or if downstream phosphorylation events may be sufficient. The recruitment signal for Bub1/3 at kinetochores is phosphorylation of the MELT motifs on Spc105 (London et al., 2012; Primorac et al., 2013; Shepperd et al., 2012; Yamagishi et al., 2012). I first asked whether phosphorylation on these MELT sites was necessary for the checkpoint when *MPS1* was overexpressed. *spc105-6A* cells are deficient in MELT phosphorylation and cannot activate the checkpoint in response to benomyl treatment (London and Biggins, 2014b). However, *MPS1* overexpression was able to activate the checkpoint in *spc105-6A* cells as determined by securin stabilization in response to nocodazole treatment (Fig V.B). As expected by this result, *MPS1* overexpression also promoted the Bub1-Mad1 coimmunoprecipitation, similarly to *ndc10-1* cells (Fig V.C). These data indicate that Bub1 association with Spc105 may not necessarily be required for checkpoint signaling.

In the potential absence of the Bub1-Spc105 interaction, Mps1 overexpression must target downstream phosphorylation for the mitotic arrest. I next asked whether *MPS1* overexpression could bypass Bub1 phosphorylation, which recruits Mad1 and presumably occurs downstream of Spc105 phosphorylation on *wild type* kinetochores. To do this, I overexpressed *MPS1* in a *bub1* phosphomutant (*bub1-15A*) strain that fails to activate the checkpoint in response to nocodazole treatment. In contrast to *spc105-6A* cells, Pds1 was not stabilized by *MPS1* overexpression in *bub1-15A* cells (Fig V.D). I attempted to test whether Bub1 phosphorylation is sufficient for signaling, but was unable to generate the necessary functional phosphomimetic allele (London and Biggins, 2014b and data not shown). Nonetheless, the phosphodeficient alleles argue that Bub1 phosphorylation is necessary for *MPS1*

overexpression-induced checkpoint arrest, ruling out sufficiency of other possible downstream phosphorylation events, at least in the case of *MPS1* overexpression .

Discussion

Numerous studies have investigated the sufficiency of checkpoint protein function at the kinetochore for checkpoint activity, leading to the consensus conclusion that the proteins Mps1 and potentially Mad1 have critical functions downstream of the kinetochore (Ballister et al., 2014; Heinrich et al., 2014; Hewitt et al., 2010; Kruse et al., 2014; Kuijt et al., 2014; Maldonado and Kapoor, 2011; Tipton et al., 2013). In contrast, my results are consistent with an unappreciated role for an established interaction of these proteins at the kinetochore, and indicate that these functions may be recapitulated instead of bypassed upon *MPS1* overexpression without the kinetochore scaffold. Specifically, phosphorylation of Bub1 mediates a Mad1 interaction, and this interaction is the potential basis for Mad2 activation and downstream events.

It is worth considering existing evidence that indicates other checkpoint protein interactions are also important at the kinetochore. Notably, recent work in human cells has shown the recruitment of Cdc20 through Bub1 and BubR1 is important for a robust checkpoint response, presumably in order to promote binding to Mad2, $Mad3^{BubR1}$, and for incorporation into the MCC (Di Fiore et al., 2015; Lischetti et al., 2014). In Drosophila, the Cdc20-BubR1 interaction has also been reported to be stimulated by Mps1 activity (Conde et al., 2013). Interestingly, however, budding yeast kinetochores do not have reported kinetochore localization of Mad3 and Cdc20 localization appears to be transient (Gillett, 2004; Yang et al., 2015), consistent with rapid turnover with MCC formation. This function for Mps1 therefore may not be conserved in budding yeast. Additionally, Mps1 activity towards Mad2 has been reported in fission yeast, although this may not have an essential checkpoint function (Zich et al., 2012). I was also unable to detect Mps1 phosphorylation of Mad2 with budding yeast proteins, indicating this phosphorylation may not be conserved (data not shown). Similarly, budding yeast lacks a CENP-E homolog and has a divergent BubR1 homolog even though these proteins are important for the checkpoint and may be Mps1 targets in human cells (Espeut et al., 2008; Huang et al., 2008).

Additional work is necessary to test the sufficiency of Bub1 phosphorylation for checkpoint stimulation. To demonstrate this in vivo, it would be necessary to employ a phosphomimetic form of Bub1. However, I was unable to generate functional phosphomimetic substitutions in the Mps1 sites ((London and Biggins, 2014b) and data not shown). In lieu of this, it will be informative to test whether ectopic colocalization of Bub1 with Mps1 can trigger the checkpoint, which would support the concept that kinetochores primarily serve to colocalize Bub1 with Mps1 to initiate signaling. Additionally, it is in principle possible to reconstitute events in vitro to determine what biochemical events are triggered by the Bub1-Mad1 interaction (Han et al., 2013; Kulukian et al., 2009). It will also be critical to understand how the Bub1-Mad1 interaction is negatively regulated. Tension-bearing microtubule attachments presumably oppose the interaction, but it is not known how this would lead to dephosphorylation of Bub1, a seemingly necessary condition for silencing and reactivation. One partial answer may be regulation of Mps1 accessibility to Spc105 and Bub1 through changes in kinetochore structure and architecture upon microtubule binding (Aravamudhan et al., 2015). It is also unclear whether soluble Bub1-Mad1 can cause checkpoint activation or if another scaffold is necessary to facilitate clustering of checkpoint proteins for activation, such as the nuclear pore (Rodriguez-Bravo et al., 2014).

Altogether, this data is consistent with a general model where checkpoint activity is controlled through Bub1-Spc105 by modulating the activity of Mps1. Spc105 may possibly sense microtubule-binding and correspondingly regulate activity of Mps1 towards Bub1 through a number of possible mechanisms including Bub1 displacement, promoting a conformational change in Bub1, or direct occlusion. Understanding how Mps1 activity is coupled to Bub1 phosphorylation at the kinetochore is a major next step.

Materials and Methods

Strain and plasmids

All strains are isogenic with the W303 background. Strains new to this study were generated through standard genetic crossing and transgenic methods.

Immunological methods

Immunoprecipitations and immunoblotting was as described in Chapters II and III.

Yeast methods and purifications

Media and microbial techniques were as described (Rose et al., 1990). Kinetochore particle and Flag-tagged protein purifications from yeast were performed essentially as described in Chapter II. Cells used in Pds1 stability experiments were lysed by bead-beating (Ranjitkar et al., 2010). Immunoprecipitated proteins were washed three times in lysis buffer with protease and phosphatase inhibitors, twice in lysis buffer alone, then eluted in SDS sample buffer prior to analysis. *MPS1* overexpression was induced in cells grown to mid-log phase in 2% raffinose media by addition of galactose to 2%. Pds1 stability experiments were performed by synchronizing cells in G1 with alpha-factor at 10 ug/mL, then releasing into fresh media with or without 2% galactose. Alpha-factor was added back after 40-60 minutes to prevent entry into the next cell cycle. Temperature shifts were accomplished by diluting or washing cells into 37° media and culturing cells in a 37° water bath for 2 hours for IPs or for the length of the timecourse. Cells grown for immunoprecipitation were harvested at an OD_{600} of 1.0-2.0.

Figures

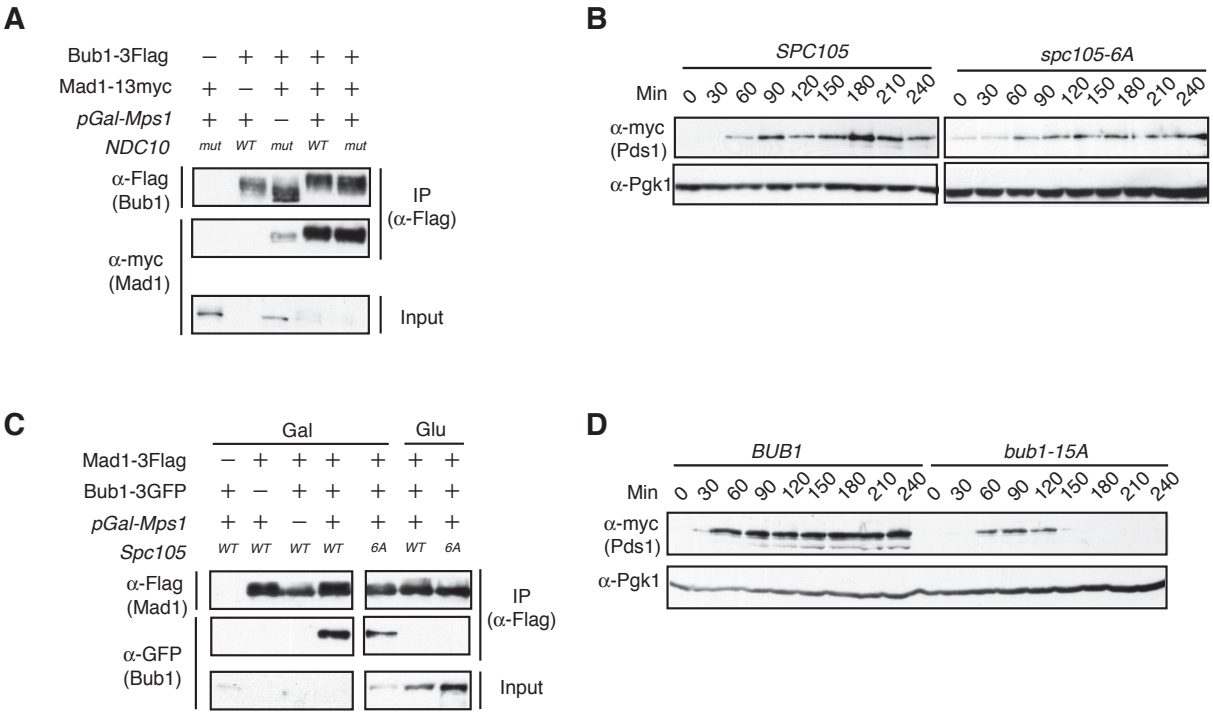

Figure V *MPS1* overexpression requires Bub1 phosphorylation to activate the checkpoint

(A Log phase cells of the indicated genotypes were shifted from RT to 37° and cultured for 2 hours prior to harvest. *MPS1* overexpression was induced or repressed by addition of galactose (Gal) or glucose (Glu), respectively, concomitantly with the temperature shift. Bub1 was immunoprecipitated (α-Flag) and analyzed. Note that Bub1 gave a distinct migration shift upon *MPS1* overexpression. *mut* = *ndc10-1*. (B) *MPS1* overexpression bypasses Spc105 MELT phosphorylation to activate the checkpoint. *SPC105* or *spc105-6A* cells were synchronized in G1 by treatment with alls were synchronized in G1 by treatment with tion to activate the checkpo*MPS1* overexpression. Crude cell lysates from each timepoint were analyzed by Western blotting for Pds1-18myc (α-myc) or the loading control Pgk1 (α-Pgk1). (C) Bub1 CoIPs with Mad1 in *spc105-6A* cell overexpressing *MPS1*. Cells with the indicated genotypes were grown at RT then induced with galactose for 2 hours prior to harvest. Mad1 was immunoprecipitated (α-Flag) and analyzed by immunoblotting. (D) The *MPS1* overexpression arrest depends upon Bub1 phosphorylation. *BUB1* or *bub1-15A* cells were treated as in (A). Strains used: (A) SBY11488, SBY11489, SBY11490, SBY11491, SBY11492, (B) SBY12455, SBY12457, (C) SBY10109, SBY10944, SBY12871, SBY12873, SBY14656, (D) SBY11469, SBY11470.

References

Abrieu, A., Magnaghi-Jaulin, L., Kahana, J.A., Peter, M., Castro, A., Vigneron, S., Lorca, T., Cleveland, D.W., and Labbé, J.-C. (2001). Mps1 is a kinetochore-associated kinase essential for the vertebrate mitotic checkpoint. Cell *106*, 83–93.

Akiyoshi, B., Sarangapani, K.K., Powers, A.F., Nelson, C.R., Reichow, S.L., Arellano-Santoyo, H., Gonen, T., Ranish, J.A., Asbury, C.L., and Biggins, S. (2010). Tension directly stabilizes reconstituted kinetochore-microtubule attachments. Nature *468*, 576–579.

Akiyoshi, B., Nelson, C.R., and Biggins, S. (2013). The Aurora B Kinase Promotes Inner and Outer Kinetochore Interactions in Budding Yeast. Genetics *194*, 785–789.

Aravamudhan, P., Goldfarb, A.A., and Joglekar, A.P. (2015). The kinetochore encodes a mechanical switch to disrupt spindle assembly checkpoint signalling. Nat. Cell Biol. *advance online publication*.

Ballister, E.R., Riegman, M., and Lampson, M.A. (2014). Recruitment of Mad1 to metaphase kinetochores is sufficient to reactivate the mitotic checkpoint. J. Cell Biol. *204*, 901–908.

Biggins, S. (2001). The budding yeast protein kinase Ipl1/Aurora allows the absence of tension to activate the spindle checkpoint. Genes Dev. *15*, 3118–3129.

Biggins, S. (2013). The Composition, Functions, and Regulation of the Budding Yeast Kinetochore. Genetics *194*, 817–846.

Biggins, S., Severin, F.F., Bhalla, N., Sassoon, I., Hyman, A.A., and Murray, A.W. (1999). The conserved protein kinase Ipl1 regulates microtubule binding to kinetochores in budding yeast. Genes Dev. *13*, 532–544.

Bock, L.J., Pagliuca, C., Kobayashi, N., Grove, R.A., Oku, Y., Shrestha, K., Alfieri, C., Golfieri, C., Oldani, A., Dal Maschio, M., et al. (2012). Cnn1 inhibits the interactions between the KMN complexes of the yeast kinetochore. Nat. Cell Biol. *14*, 614–624.

Bolanos-Garcia, V.M., Kiyomitsu, T., D'Arcy, S., Chirgadze, D.Y., Grossmann, J.G., Matak-Vinkovic, D., Venkitaraman, A.R., Yanagida, M., Robinson, C.V., and Blundell, T.L. (2009). The Crystal Structure of the N-Terminal Region of BUB1 Provides Insight into the Mechanism of BUB1 Recruitment to Kinetochores. Structure *17*, 105–116.

Bolanos-Garcia, V.M., Lischetti, T., Matak-Vinković, D., Cota, E., Simpson, P.J., Chirgadze, D.Y., Spring, D.R., Robinson, C.V., Nilsson, J., and Blundell, T.L. (2011). Structure of a Blinkin-BUBR1 Complex Reveals an Interaction Crucial for Kinetochore-Mitotic Checkpoint Regulation via an Unanticipated Binding Site. Structure *19*, 1691–1700.

Brady, D.M., and Hardwick, K.G. (2000). Complex formation between Mad1p, Bub1p and Bub3p is crucial for spindle checkpoint function. Curr. Biol. CB *10*, 675–678.

Buvelot, S. (2003). The budding yeast Ipl1/Aurora protein kinase regulates mitotic spindle disassembly. J. Cell Biol. *160*, 329–339.

Cairo, L.V., Ptak, C., and Wozniak, R.W. (2012). Mitosis-Specific Regulation of Nuclear Transport by the Spindle Assembly Checkpoint Protein Mad1p. Mol. Cell.

Caldas, G.V., and DeLuca, J.G. (2013). KNL1: bringing order to the kinetochore. Chromosoma.

Castillo, A.R., Meehl, J.B., Morgan, G., Schutz-Geschwender, A., and Winey, M. (2002). The yeast protein kinase Mps1p is required for assembly of the integral spindle pole body component Spc42p. J. Cell Biol. *156*, 453–465.

Cheeseman, I.M., Anderson, S., Jwa, M., Green, E.M., Kang, J., Yates III, J.R., Chan, C.S., Drubin, D.G., and Barnes, G. (2002). Phospho-regulation of kinetochore-microtubule attachments by the Aurora kinase Ipl1p. Cell *111*, 163–172.

Cheeseman, I.M., Niessen, S., Anderson, S., Hyndman, F., Yates, J.R., Oegema, K., and Desai, A. (2004). A conserved protein network controls assembly of the outer kinetochore and its ability to sustain tension. Genes Dev. *18*, 2255–2268.

Cheeseman, I.M., Chappie, J.S., Wilson-Kubalek, E.M., and Desai, A. (2006). The Conserved KMN Network Constitutes the Core Microtubule-Binding Site of the Kinetochore. Cell *127*, 983–997.

Collin, P., Nashchekina, O., Walker, R., and Pines, J. (2013). The spindle assembly checkpoint works like a rheostat rather than a toggle switch. Nat. Cell Biol. *15*, 1378–1385.

Conde, C., Osswald, M., Barbosa, J., Moutinho-Santos, T., Pinheiro, D., Guimarães, S., Matos, I., Maiato, H., and Sunkel, C.E. (2013). Drosophila Polo regulates the spindle assembly checkpoint through Mps1-dependent BubR1 phosphorylation. EMBO J. *32*, 1761–1777.

Craig, R., and Beavis, R.C. (2004). TANDEM: matching proteins with tandem mass spectra. Bioinformatics *20*, 1466–1467.

Défachelles, L., Hainline, S.G., Menant, A., Lee, L.A., and Karess, R.E. (2015). A maternal effect rough deal mutation suggesting multiple pathways regulating Drosophila RZZ kinetochore recruitment. J. Cell Sci. jcs.165712.

DeLuca, J.G., Howell, B.J., Canman, J.C., Hickey, J.M., Fang, G., and Salmon, E.D. (2003). Nuf2 and Hec1 Are Required for Retention of the Checkpoint Proteins Mad1 and Mad2 to Kinetochores. Curr. Biol. *13*, 2103–2109.

Diaz-Martinez, L.A., Tian, W., Li, B., Warrington, R., Jia, L., Brautigam, C.A., Luo, X., and Yu, H. (2014). The Cdc20-binding Phe Box of the Spindle Checkpoint Protein BubR1 Maintains the Mitotic Checkpoint Complex during Mitosis. J. Biol. Chem. jbc.M114.616490.

Dick, A.E., and Gerlich, D.W. (2013). Kinetic framework of spindle assembly checkpoint signalling. Nat. Cell Biol. *15*, 1370–1377.

Elowe, S. (2011). Bub1 and BubR1: at the Interface between Chromosome Attachment and the Spindle Checkpoint. Mol. Cell. Biol. *31*, 3085–3093.

Emanuele, M.J., Lan, W., Jwa, M., Miller, S.A., Chan, C.S.M., and Stukenberg, P.T. (2008). Aurora B kinase and protein phosphatase 1 have opposing roles in modulating kinetochore assembly. J. Cell Biol. *181*, 241–254.

Enquist-Newman, M., Cheeseman, I.M., Goor, D.V., Drubin, D.G., Meluh, P.B., and Barnes, G. (2001). Dad1p, Third Component of the Duo1p/Dam1p Complex Involved in Kinetochore Function and Mitotic Spindle Integrity. Mol. Biol. Cell *12*, 2601–2613.

Espert, A., Uluocak, P., Bastos, R.N., Mangat, D., Graab, P., and Gruneberg, U. (2014). PP2A-B56 opposes Mps1 phosphorylation of Knl1 and thereby promotes spindle assembly checkpoint silencing. J. Cell Biol. *206*, 833–842.

Espeut, J., Gaussen, A., Bieling, P., Morin, V., Prieto, S., Fesquet, D., Surrey, T., and Abrieu, A. (2008). Phosphorylation Relieves Autoinhibition of the Kinetochore Motor Cenp-E. Mol. Cell *29*, 637–643.

Espeut, J., Cheerambathur, D.K., Krenning, L., Oegema, K., and Desai, A. (2012). Microtubule binding by KNL-1 contributes to spindle checkpoint silencing at the kinetochore. J. Cell Biol. *196*, 469–482.

Faust, A.M.E., Wong, C.C.L., Yates III, J.R., Drubin, D.G., and Barnes, G. (2013). The FEAR Protein Slk19 Restricts Cdc14 Phosphatase to the Nucleus until the End of Anaphase, Regulating Its Participation in Mitotic Exit in Saccharomyces cerevisiae. PLoS ONE *8*, e73194.

Fernius, J., and Hardwick, K.G. (2007). Bub1 Kinase Targets Sgo1 to Ensure Efficient Chromosome Biorientation in Budding Yeast Mitosis. PLoS Genet *3*, e213.

Di Fiore, B., Davey, N.E., Hagting, A., Izawa, D., Mansfeld, J., Gibson, T.J., and Pines, J. (2015). The ABBA Motif Binds APC/C Activators and Is Shared by APC/C Substrates and Regulators. Dev. Cell *32*, 358–372.

Foley, E.A., and Kapoor, T.M. (2012). Microtubule attachment and spindle assembly checkpoint signalling at the kinetochore. Nat. Rev. Mol. Cell Biol. *14*, 25–37.

Funabiki, H., and Wynne, D.J. (2013). Making an effective switch at the kinetochore by phosphorylation and dephosphorylation. Chromosoma *122*, 135–158.

Gillett, E.S. (2004). Spindle checkpoint proteins and chromosome-microtubule attachment in budding yeast. J. Cell Biol. *164*, 535–546.

Gonen, S., Akiyoshi, B., Iadanza, M.G., Shi, D., Duggan, N., Biggins, S., and Gonen, T. (2012). The structure of purified kinetochores reveals multiple microtubule-attachment sites. Nat. Struct. Mol. Biol. *19*, 925–929.

Goto, G.H., Mishra, A., Abdulle, R., Slaughter, C.A., and Kitagawa, K. (2011). Bub1-Mediated Adaptation of the Spindle Checkpoint. PLoS Genet. *7*, e1001282.

Han, J.S., Holland, A.J., Fachinetti, D., Kulukian, A., Cetin, B., and Cleveland, D.W. (2013). Catalytic Assembly of the Mitotic Checkpoint Inhibitor BubR1-Cdc20 by a Mad2-Induced Functional Switch in Cdc20. Mol. Cell *51*, 92–104.

Han, J.S., Vitre, B., Fachinetti, D., and Cleveland, D.W. (2014). Bimodal activation of BubR1 by Bub3 sustains mitotic checkpoint signaling. Proc. Natl. Acad. Sci.

Heinrich, S., Windecker, H., Hustedt, N., and Hauf, S. (2012). Mph1 kinetochore localization is crucial and upstream in the hierarchy of spindle assembly checkpoint protein recruitment to kinetochores. J. Cell Sci. *125*, 4720–4727.

Heinrich, S., Sewart, K., Windecker, H., Langegger, M., Schmidt, N., Hustedt, N., and Hauf, S. (2014). Mad1 contribution to spindle assembly checkpoint signalling goes beyond presenting Mad2 at kinetochores. EMBO Rep.

Hewitt, L., Tighe, A., Santaguida, S., White, A.M., Jones, C.D., Musacchio, A., Green, S., and Taylor, S.S. (2010). Sustained Mps1 activity is required in mitosis to recruit O-Mad2 to the Mad1-C-Mad2 core complex. J. Cell Biol. *190*, 25–34.

Holinger, E.P., Old, W.M., Giddings, T.H., Wong, C., Yates, J.R., and Winey, M. (2009). Budding Yeast Centrosome Duplication Requires Stabilization of Spc29 via Mps1-mediated Phosphorylation. J. Biol. Chem. *284*, 12949–12955.

Howell, B.J., Moree, B., Farrar, E.M., Stewart, S., Fang, G., and Salmon, E.D. (2004). Spindle checkpoint protein dynamics at kinetochores in living cells. Curr. Biol. *14*, 953–964.

Hoyt, M.A., Totis, L., and Roberts, B.T. (1991). S. cerevisiae genes required for cell cycle arrest in response to loss of microtubule function. Cell *66*, 507–517.

Huang, H., Hittle, J., Zappacosta, F., Annan, R.S., Hershko, A., and Yen, T.J. (2008). Phosphorylation sites in BubR1 that regulate kinetochore attachment, tension, and mitotic exit. J. Cell Biol. *183*, 667–680.

Hwang, L.H., Lau, L.F., Smith, D.L., Mistrot, C.A., Hardwick, K.G., Hwang, E.S., Amon, A., and Murray, A.W. (1998). Budding Yeast Cdc20: A Target of the Spindle Checkpoint. Science *279*, 1041–1044.

Indjeian, V.B., and Murray, A.W. (2007). Budding Yeast Mitotic Chromosomes Have an Intrinsic Bias to Biorient on the Spindle. Curr. Biol. *17*, 1837–1846.

Ito, D., Saito, Y., and Matsumoto, T. (2011). Centromere-tethered Mps1 pombe homolog (Mph1) kinase is a sufficient marker for recruitment of the spindle checkpoint protein Bub1, but not Mad1. Proc. Natl. Acad. Sci. *109*, 209–214.

Jelluma, N., Dansen, T.B., Sliedrecht, T., Kwiatkowski, N.P., and Kops, G.J.P.L. (2010). Release of Mps1 from kinetochores is crucial for timely anaphase onset. J. Cell Biol. *191*, 281–290.

Jia, L., Kim, S., and Yu, H. (2013). Tracking spindle checkpoint signals from kinetochores to APC/C. Trends Biochem. Sci. *38*, 302–311.

Joglekar, A., Bloom, K., and Salmon, E.D. (2009). In vivo protein architecture of the eukaryotic kinetochore with nanometer scale accuracy. Curr. Biol. CB *19*, 694–699.

Joglekar, A.P., Bouck, D., Finley, K., Liu, X., Wan, Y., Berman, J., He, X., Salmon, E.D., and Bloom, K.S. (2008). Molecular architecture of the kinetochore-microtubule attachment site is conserved between point and regional centromeres. J. Cell Biol. *181*, 587–594.

Jones, M.H., Huneycutt, B.J., Pearson, C.G., Zhang, C., Morgan, G., Shokat, K., Bloom, K., and Winey, M. (2005). Chemical genetics reveals a role for Mps1 kinase in kinetochore attachment during mitosis. Curr. Biol. *15*, 160–165.

Kawashima, S.A., Yamagishi, Y., Honda, T., Ishiguro, K. -i., and Watanabe, Y. (2010). Phosphorylation of H2A by Bub1 Prevents Chromosomal Instability Through Localizing Shugoshin. Science *327*, 172–177.

Kemmler, S., Stach, M., Knapp, M., Ortiz, J., Pfannstiel, J., Ruppert, T., and Lechner, J. (2009). Mimicking Ndc80 phosphorylation triggers spindle assembly checkpoint signalling. EMBO J. *28*, 1099–1110.

Kim, S., Sun, H., Tomchick, D.R., Yu, H., and Luo, X. (2012). Structure of human Mad1 C-terminal domain reveals its involvement in kinetochore targeting. Proc. Natl. Acad. Sci. *109*, 6549–6554.

Kim, S.H., Lin, D.P., Matsumoto, S., Kitazono, A., and Matsumoto, T. (1998). Fission Yeast Slp1: An Effector of the Mad2-Dependent Spindle Checkpoint. Science *279*, 1045–1047.

Kiyomitsu, T., Obuse, C., and Yanagida, M. (2007). Human Blinkin/AF15q14 Is Required for Chromosome Alignment and the Mitotic Checkpoint through Direct Interaction with Bub1 and BubR1. Dev. Cell *13*, 663–676.

Kiyomitsu, T., Murakami, H., and Yanagida, M. (2011). Protein Interaction Domain Mapping of Human Kinetochore Protein Blinkin Reveals a Consensus Motif for Binding of Spindle Assembly Checkpoint Proteins Bub1 and BubR1. Mol. Cell. Biol. *31*, 998–1011.

Klebig, C., Korinth, D., and Meraldi, P. (2009). Bub1 regulates chromosome segregation in a kinetochore-independent manner. J. Cell Biol. *185*, 841–858.

Kops, G.J.P.L., and Shah, J.V. (2012). Connecting up and clearing out: how kinetochore attachment silences the spindle assembly checkpoint. Chromosoma *121*, 509–525.

Krenn, V., Wehenkel, A., Li, X., Santaguida, S., and Musacchio, A. (2012). Structural analysis reveals features of the spindle checkpoint kinase Bub1-kinetochore subunit Knl1 interaction. J. Cell Biol. *196*, 451–467.

Krenn, V., Overlack, K., Primorac, I., van Gerwen, S., and Musacchio, A. (2014). KI Motifs of Human Knl1 Enhance Assembly of Comprehensive Spindle Checkpoint Complexes around MELT Repeats. Curr. Biol. *24*, 29–39.

Kruse, T., Larsen, M.S.Y., Sedgwick, G.G., Sigurdsson, J.O., Streicher, W., Olsen, J.V., and Nilsson, J. (2014). A direct role of Mad1 in the spindle assembly checkpoint beyond Mad2 kinetochore recruitment. EMBO Rep.

Kuijt, T.E.F., Omerzu, M., Saurin, A.T., and Kops, G.J.P.L. (2014). Conditional targeting of MAD1 to kinetochores is sufficient to reactivate the spindle assembly checkpoint in metaphase. Chromosoma.

Kulukian, A., Han, J.S., and Cleveland, D.W. (2009). Unattached Kinetochores Catalyze Production of an Anaphase Inhibitor that Requires a Mad2 Template to Prime Cdc20 for BubR1 Binding. Dev. Cell *16*, 105–117.

Lan, W., and Cleveland, D.W. (2010). A chemical tool box defines mitotic and interphase roles for Mps1 kinase. J. Cell Biol. *190*, 21–24.

Larsen, N.A., Al-Bassam, J., Wei, R.R., and Harrison, S.C. (2007). Structural analysis of Bub3 interactions in the mitotic spindle checkpoint. Proc. Natl. Acad. Sci. *104*, 1201–1206.

Lauzé, E., Stoelcker, B., Luca, F.C., Weiss, E., Schutz, A.R., and Winey, M. (1995). Yeast spindle pole body duplication gene MPS1 encodes an essential dual specificity protein kinase. EMBO J. *14*, 1655–1663.

Lee, S., Thebault, P., Freschi, L., Beaufils, S., Blundell, T.L., Landry, C.R., Bolanos-Garcia, V.M., and Elowe, S. (2011). Characterization of Spindle Checkpoint Kinase Mps1 Reveals Domain with Functional and Structural Similarities to Tetratricopeptide Repeat Motifs of Bub1 and BubR1 Checkpoint Kinases. J. Biol. Chem. *287*, 5988–6001.

Li, R., and Murray, A.W. (1991). Feedback control of mitosis in budding yeast. Cell *66*, 519–531.

Licklider, L.J., Thoreen, C.C., Peng, J., and Gygi, S.P. (2002). Automation of nanoscale microcapillary liquid chromatography-tandem mass spectrometry with a vented column. Anal. Chem. *74*, 3076–3083.

Lischetti, T., Zhang, G., Sedgwick, G.G., Bolanos-Garcia, V.M., and Nilsson, J. (2014). The internal Cdc20 binding site in BubR1 facilitates both spindle assembly checkpoint signalling and silencing. Nat. Commun. *5*.

Liu, D., Vleugel, M., Backer, C.B., Hori, T., Fukagawa, T., Cheeseman, I.M., and Lampson, M.A. (2010). Regulated targeting of protein phosphatase 1 to the outer kinetochore by KNL1 opposes Aurora B kinase. J. Cell Biol. *188*, 809–820.

London, N., and Biggins, S. (2014a). Signalling dynamics in the spindle checkpoint response. Nat. Rev. Mol. Cell Biol.

London, N., and Biggins, S. (2014b). Mad1 kinetochore recruitment by Mps1-mediated phosphorylation of Bub1 signals the spindle checkpoint. Genes Dev. *28*, 140–152.

London, N., Ceto, S., Ranish, J.A., and Biggins, S. (2012). Phosphoregulation of Spc105 by Mps1 and PP1 Regulates Bub1 Localization to Kinetochores. Curr. Biol. *22*, 900–906.

Luo, X., and Yu, H. (2008). Protein Metamorphosis: The Two-State Behavior of Mad2. Structure *16*, 1616–1625.

Maciejowski, J., George, K.A., Terret, M.-E., Zhang, C., Shokat, K.M., and Jallepalli, P.V. (2010). Mps1 directs the assembly of Cdc20 inhibitory complexes during interphase and mitosis to control M phase timing and spindle checkpoint signaling. J. Cell Biol. *190*, 89–100.

Maldonado, M., and Kapoor, T.M. (2011). Constitutive Mad1 targeting to kinetochores uncouples checkpoint signalling from chromosome biorientation. Nat. Cell Biol. *13*, 475–482.

Malvezzi, F., and Westermann, S. (2014). “Uno, nessuno e centomila”: the different faces of the budding yeast kinetochore. Chromosoma.

Mapelli, M., and Musacchio, A. (2007). MAD contortions: conformational dimerization boosts spindle checkpoint signaling. Curr. Opin. Struct. Biol. *17*, 716–725.

Maresca, T.J., and Salmon, E.D. (2009). Intrakinetochore stretch is associated with changes in kinetochore phosphorylation and spindle assembly checkpoint activity. J. Cell Biol. *184*, 373–381.

Maresca, T.J., and Salmon, E.D. (2010). Welcome to a new kind of tension: translating kinetochore mechanics into a wait-anaphase signal. J. Cell Sci. *123*, 825–835.

Martin-Lluesma, S., Stucke, V.M., and Nigg, E.A. (2002). Role of Hec1 in Spindle Checkpoint Signaling and Kinetochore Recruitment of Mad1/Mad2. Science *297*, 2267–2270.

Maure, J.-F., Kitamura, E., and Tanaka, T.U. (2007). Mps1 Kinase Promotes Sister-Kinetochore Bi-orientation by a Tension-Dependent Mechanism. Curr. Biol. *17*, 2175–2182.

McCleland, M.L., Gardner, R.D., Kallio, M.J., Daum, J.R., Gorbsky, G.J., Burke, D.J., and Stukenberg, P.T. (2003). The highly conserved Ndc80 complex is required for kinetochore assembly, chromosome congression, and spindle checkpoint activity. Genes Dev. *17*, 101–114.

Meyer, R.E., Kim, S., Obeso, D., Straight, P.D., Winey, M., and Dawson, D.S. (2013). Mps1 and Ipl1/Aurora B Act Sequentially to Correctly Orient Chromosomes on the Meiotic Spindle of Budding Yeast. Science *339*, 1071–1074.

Mok, J., Kim, P.M., Lam, H.Y.K., Piccirillo, S., Zhou, X., Jeschke, G.R., Sheridan, D.L., Parker, S.A., Desai, V., Jwa, M., et al. (2010). Deciphering Protein Kinase Specificity Through Large-Scale Analysis of Yeast Phosphorylation Site Motifs. Sci. Signal. *3*, ra12–ra12.

Moyle, M.W., Kim, T., Hattersley, N., Espeut, J., Cheerambathur, D.K., Oegema, K., and Desai, A. (2014). A Bub1-Mad1 interaction targets the Mad1-Mad2 complex to unattached kinetochores to initiate the spindle checkpoint. J. Cell Biol.

Musacchio, A., and Salmon, E.D. (2007). The spindle-assembly checkpoint in space and time. Nat. Rev. Mol. Cell Biol. *8*, 379–393.

Nekrasov, V.S., Smith, M.A., Peak-Chew, S., and Kilmartin, J.V. (2003). Interactions between Centromere Complexes in Saccharomyces cerevisiae. Mol. Biol. Cell *14*, 4931–4946.

Nijenhuis, W., von Castelmur, E., Littler, D., De Marco, V., Tromer, E., Vleugel, M., van Osch, M.H.J., Snel, B., Perrakis, A., and Kops, G.J.P.L. (2013). A TPR domain-containing N-terminal module of MPS1 is required for its kinetochore localization by Aurora B. J. Cell Biol. *201*, 217–231.

Nijenhuis, W., Vallardi, G., Teixeira, A., Kops, G.J.P.L., and Saurin, A.T. (2014). Negative feedback at kinetochores underlies a responsive spindle checkpoint signal. Nat. Cell Biol. *advance online publication*.

Overlack, K., Primorac, I., Vleugel, M., Krenn, V., Maffini, S., Hoffmann, I., Kops, G.J.P.L., and Musacchio, A. (2015). A molecular basis for the differential roles of Bub1 and BubR1 in the spindle assembly checkpoint. eLife e05269.

Pagliuca, C., Draviam, V.M., Marco, E., Sorger, P.K., and De Wulf, P. (2009). Roles for the Conserved Spc105p/Kre28p Complex in Kinetochore-Microtubule Binding and the Spindle Assembly Checkpoint. PLoS ONE *4*, e7640.

Palframan, W.J. (2006). Anaphase Inactivation of the Spindle Checkpoint. Science *313*, 680–684.

Pinsky, B.A., Kung, C., Shokat, K.M., and Biggins, S. (2006). The Ipl1-Aurora protein kinase activates the spindle checkpoint by creating unattached kinetochores. Nat. Cell Biol. *8*, 78–83.

Pinsky, B.A., Nelson, C.R., and Biggins, S. (2009). Protein Phosphatase 1 Regulates Exit from the Spindle Checkpoint in Budding Yeast. Curr. Biol. *19*, 1182–1187.

Poddar, A., Stukenberg, P.T., and Burke, D.J. (2005). Two Complexes of Spindle Checkpoint Proteins Containing Cdc20 and Mad2 Assemble during Mitosis Independently of the Kinetochore in Saccharomyces cerevisiae. Eukaryot. Cell *4*, 867–878.

Primorac, I., and Musacchio, A. (2013). Panta rhei: The APC/C at steady state. J. Cell Biol. *201*, 177–189.

Primorac, I., Weir, J.R., Chiroli, E., Gross, F., Hoffmann, I., van Gerwen, S., Ciliberto, A., and Musacchio, A. (2013). Bub3 reads phosphorylated MELT repeats to promote spindle assembly checkpoint signaling. Elife *2*.

Qi, W., and Yu, H. (2006). KEN-Box-dependent Degradation of the Bub1 Spindle Checkpoint Kinase by the Anaphase-promoting Complex/Cyclosome. J. Biol. Chem. *282*, 3672–3679.

Ranjitkar, P., Press, M.O., Yi, X., Baker, R., MacCoss, M.J., and Biggins, S. (2010). An E3 Ubiquitin Ligase Prevents Ectopic Localization of the Centromeric Histone H3 Variant via the Centromere Targeting Domain. Mol. Cell *40*, 455–464.

Rieder, C.L., Cole, R.W., Khodjakov, A., and Sluder, G. (1995). The checkpoint delaying anaphase in response to chromosome monoorientation is mediated by an inhibitory signal produced by unattached kinetochores. J. Cell Biol. *130*, 941–948.

Rischitor, P.E., May, K.M., and Hardwick, K.G. (2007). Bub1 Is a Fission Yeast Kinetochore Scaffold Protein, and Is Sufficient to Recruit other Spindle Checkpoint Proteins to Ectopic Sites on Chromosomes. PLoS ONE *2*, e1342.

Rodriguez-Bravo, V., Maciejowski, J., Corona, J., Buch, H.K., Collin, P., Kanemaki, M.T., Shah, J.V., and Jallepalli, P.V. (2014). Nuclear Pores Protect Genome Integrity by Assembling a Premitotic and Mad1-Dependent Anaphase Inhibitor. Cell *156*, 1017–1031.

Rose, M., Winston, F., and Heiter, P. (1990). Methods in Yeast Genetics (Cold Spring Harbor, N.Y.: Cold Spring Harbor Laboratory Press).

Santaguida, S., Tighe, A., D'Alise, A.M., Taylor, S.S., and Musacchio, A. (2010). Dissecting the role of MPS1 in chromosome biorientation and the spindle checkpoint through the small molecule inhibitor reversine. J. Cell Biol. *190*, 73–87.

Sarangapani, K.K., Akiyoshi, B., Duggan, N.M., Biggins, S., and Asbury, C.L. (2013). Phosphoregulation promotes release of kinetochores from dynamic microtubules via multiple mechanisms. Proc. Natl. Acad. Sci. *110*, 7282–7287.

Saurin, A.T., van der Waal, M.S., Medema, R.H., Lens, S.M.A., and Kops, G.J.P.L. (2011). Aurora B potentiates Mps1 activation to ensure rapid checkpoint establishment at the onset of mitosis. Nat. Commun. *2*, 316.

Schittenhelm, R.B., Chaleckis, R., and Lehner, C.F. (2009). Intrakinetochore localization and essential functional domains of Drosophila Spc105. EMBO J. *28*, 2374–2386.

Schleiffer, A., Maier, M., Litos, G., Lampert, F., Hornung, P., Mechtler, K., and Westermann, S. (2012). CENP-T proteins are conserved centromere receptors of the Ndc80 complex. Nat. Cell Biol. *14*, 604–613.

Schutz, A.R., and Winey, M. (1998). New Alleles of the Yeast MPS1 Gene Reveal Multiple Requirements in Spindle Pole Body Duplication. Mol. Biol. Cell *9*, 759–774.

Seeley, T.W., Wang, L., and Zhen, J.Y. (1999). Phosphorylation of Human MAD1 by the BUB1 Kinasein Vitro. Biochem. Biophys. Res. Commun. *257*, 589–595.

Shah, J.V., Botvinick, E., Bonday, Z., Furnari, F., Berns, M., and Cleveland, D.W. (2004). Dynamics of centromere and kinetochore proteins: implications for checkpoint signaling and silencing. Curr. Biol. *14*, 942–952.

Shepperd, L.A., Meadows, J.C., Sochaj, A.M., Lancaster, T.C., Zou, J., Buttrick, G.J., Rappsilber, J., Hardwick, K.G., and Millar, J.B.A. (2012). Phosphodependent Recruitment of Bub1 and Bub3 to Spc7/KNL1 by Mph1 Kinase Maintains the Spindle Checkpoint. Curr. Biol. *22*, 891–899.

Sliedrecht, T., Zhang, C., Shokat, K.M., and Kops, G.J.P.L. (2010). Chemical Genetic Inhibition of Mps1 in Stable Human Cell Lines Reveals Novel Aspects of Mps1 Function in Mitosis. PLoS ONE *5*, e10251.

Stegmeier, F., Visintin, R., and Amon, A. (2002). Separase, Polo Kinase, the Kinetochore Protein Slk19, and Spo12 Function in a Network that Controls Cdc14 Localization during Early Anaphase. Cell *108*, 207–220.

Storchová, Z., Becker, J.S., Talarek, N., Kögelsberger, S., and Pellman, D. (2011). Bub1, Sgo1, and Mps1 mediate a distinct pathway for chromosome biorientation in budding yeast. Mol. Biol. Cell *22*, 1473–1485.

Stucke, V., Baumann, C., and Nigg, E. (2004). Kinetochore localization and microtubule interaction of the human spindle checkpoint kinase Mps1. Chromosoma *113*.

Suijkerbuijk, S.J.E., Vleugel, M., Teixeira, A., and Kops, G.J.P.L. (2012a). Integration of Kinase and Phosphatase Activities by BUBR1 Ensures Formation of Stable Kinetochore-Microtubule Attachments. Dev. Cell *23*, 745–755.

Suijkerbuijk, S.J.E., van Dam, T.J.P., Karagöz, G.E., von Castelmur, E., Hubner, N.C., Duarte, A.M.S., Vleugel, M., Perrakis, A., Rüdiger, S.G.D., Snel, B., et al. (2012b). The Vertebrate Mitotic Checkpoint Protein BUBR1 Is an Unusual Pseudokinase. Dev. Cell *22*, 1321–1329.

Tanaka, T.U., Rachidi, N., Janke, C., Pereira, G., Galova, M., Schiebel, E., Stark, M.J.R., and Nasmyth, K. (2002). Evidence that the Ipl1-Sli15 (Aurora Kinase-INCENP) Complex Promotes Chromosome Bi-orientation by Altering Kinetochore-Spindle Pole Connections. Cell *108*, 317–329.

Tang, Z., Shu, H., Oncel, D., Chen, S., and Yu, H. (2004). Phosphorylation of Cdc20 by Bub1 provides a catalytic mechanism for APC/C inhibition by the spindle checkpoint. Mol. Cell *16*, 387–397.

Thapa, K.S., Oldani, A., Pagliuca, C., Wulf, P.D., and Hazbun, T.R. (2015). The Mps1 Kinase Modulates the Recruitment and Activity of Cnn1 at Saccharomyces cerevisiae Kinetochores. Genetics genetics.115.175786.

Tighe, A., Staples, O., and Taylor, S. (2008). Mps1 kinase activity restrains anaphase during an unperturbed mitosis and targets Mad2 to kinetochores. J. Cell Biol. *181*, 893–901.

Tipton, A.R., Ji, W., Sturt-Gillespie, B., Bekier, M.E., Wang, K., Taylor, W.R., and Liu, S.-T. (2013). Monopolar Spindle 1 (MPS1) Kinase Promotes Production of Closed MAD2 (C-MAD2) Conformer and Assembly of the Mitotic Checkpoint Complex. J. Biol. Chem. *288*, 35149–35158.

Vanoosthuyse, V., Valsdottir, R., Javerzat, J.-P., and Hardwick, K.G. (2004). Kinetochore Targeting of Fission Yeast Mad and Bub Proteins Is Essential for Spindle Checkpoint Function but Not for All Chromosome Segregation Roles of Bub1p. Mol. Cell. Biol. *24*, 9786–9801.

Vanoosthuyse, V., Meadows, J.C., van der Sar, S.J., Millar, J.B., and Hardwick, K.G. (2009). Bub3p facilitates spindle checkpoint silencing in fission yeast. Mol. Biol. Cell *20*, 5096–5105.

Varma, D., Wan, X., Cheerambathur, D., Gassmann, R., Suzuki, A., Lawrimore, J., Desai, A., and Salmon, E.D. (2013). Spindle assembly checkpoint proteins are positioned close to core microtubule attachment sites at kinetochores. J. Cell Biol. *202*, 735–746.

Vigneron, S., Prieto, S., Bernis, C., Labbé, J.-C., Castro, A., and Lorca, T. (2004). Kinetochore localization of spindle checkpoint proteins: who controls whom? Mol. Biol. Cell *15*, 4584–4596.

Vleugel, M., Hoogendoorn, E., Snel, B., and Kops, G.J.P.L. (2012). Evolution and Function of the Mitotic Checkpoint. Dev. Cell *23*, 239–250.

Vleugel, M., Tromer, E., Omerzu, M., Groenewold, V., Nijenhuis, W., Snel, B., and Kops, G.J.P.L. (2013). Arrayed BUB recruitment modules in the kinetochore scaffold KNL1 promote accurate chromosome segregation. J. Cell Biol. *203*, 943–955.

Vleugel, M., Omerzu, M., Groenewold, V., Hadders, M.A., Lens, S.M.A., and Kops, G.J.P.L. (2015). Sequential Multisite Phospho-Regulation of KNL1-BUB3 Interfaces at Mitotic Kinetochores. Mol. Cell.

Van der Waal, M.S., Saurin, A.T., Vromans, M.J.M., Vleugel, M., Wurzenberger, C., Gerlich, D.W., Medema, R.H., Kops, G.J.P.L., and Lens, S.M.A. (2012). Mps1 promotes rapid centromere accumulation of Aurora B. EMBO Rep. *13*, 847–854.

Wan, X., O'Quinn, R.P., Pierce, H.L., Joglekar, A.P., Gall, W.E., DeLuca, J.G., Carroll, C.W., Liu, S.-T., Yen, T.J., McEwen, B.F., et al. (2009). Protein Architecture of the Human Kinetochore Microtubule Attachment Site. Cell *137*, 672–684.

Warren, C.D., Brady, D.M., Johnston, R.C., Hanna, J.S., Hardwick, K.G., and Spencer, F.A. (2002). Distinct Chromosome Segregation Roles for Spindle Checkpoint Proteins. Mol. Biol. Cell *13*, 3029–3041.

Welburn, J.P.I., Grishchuk, E.L., Backer, C.B., Wilson-Kubalek, E.M., Yates III, J.R., and Cheeseman, I.M. (2009). The Human Kinetochore Ska1 Complex Facilitates Microtubule Depolymerization-Coupled Motility. Dev. Cell *16*, 374–385.

Wigge, P.A., and Kilmartin, J.V. (2001). The Ndc80p Complex from Saccharomyces cerevisiae Contains Conserved Centromere Components and Has a Function in Chromosome Segregation. J. Cell Biol. *152*, 349–360.

Winey, M., Mamay, C.L., O'Toole, E.T., Mastronarde, D.N., Giddings, T.H., McDonald, K.L., and McIntosh, J.R. (1995). Three-dimensional ultrastructural analysis of the Saccharomyces cerevisiae mitotic spindle. J. Cell Biol. *129*, 1601–1615.

Wurzenberger, C., and Gerlich, D.W. (2011). Phosphatases: providing safe passage through mitotic exit. Nat. Rev. Mol. Cell Biol. *12*, 469–482.

Yamagishi, Y., Yang, C.-H., Tanno, Y., and Watanabe, Y. (2012). MPS1/Mph1 phosphorylates the kinetochore protein KNL1/Spc7 to recruit SAC components. Nat. Cell Biol. *14*, 746–752.

Yamamoto, T.G., Watanabe, S., Essex, A., and Kitagawa, R. (2008). SPDL-1 functions as a kinetochore receptor for MDF-1 in Caenorhabditis elegans. J. Cell Biol. *183*, 187–194.

Yang, M., Li, B., Liu, C.-J., Tomchick, D.R., Machius, M., Rizo, J., Yu, H., and Luo, X. (2008). Insights into Mad2 Regulation in the Spindle Checkpoint Revealed by the Crystal Structure of the Symmetric Mad2 Dimer. PLoS Biol. *6*, e50.

Yang, Y., Tsuchiya, D., and Lacefield, S. (2015). Bub3 promotes Cdc20-dependent activation of the APC/C in S. cerevisiae. J. Cell Biol. jcb.201412036.

Zhang, G., Lischetti, T., and Nilsson, J. (2013). A minimal number of MELT repeats supports all functions of KNL1 in chromosome segregation. J. Cell Sci. jcs – 139725.

Zhao, Y., and Chen, R.-H. (2006). Mps1 Phosphorylation by MAP Kinase Is Required for Kinetochore Localization of Spindle-Checkpoint Proteins. Curr. Biol. *16*, 1764–1769.

Zhu, T., Dou, Z., Qin, B., Jin, C., Wang, X., Xu, L., Wang, Z., Zhu, L., Liu, F., Gao, X., et al. (2013). Phosphorylation of Microtubule-binding Protein Hec1 by Mitotic Kinase Aurora B Specifies Spindle Checkpoint Kinase Mps1 Signaling at the Kinetochore. J. Biol. Chem. *288*, 36149–36159.

Zich, J., Sochaj, A.M., Syred, H.M., Milne, L., Cook, A.G., Ohkura, H., Rappsilber, J., and Hardwick, K.G. (2012). Kinase Activity of Fission Yeast Mph1 Is Required for Mad2 and Mad3 to Stably Bind the Anaphase Promoting Complex. Curr. Biol. *22*, 296–301.

Table I: Kinetochore copurification of kinases and phosphatases

Protein	Protein probability	Percent coverage	Number of unique peptides	Total independent spectra	Percent share of spectrum IDs
Mps1	**1**	**55.1**	**79**	**219**	**1.802**
Bub1	**1**	**36.1**	**42**	**60**	**0.497**
Cdc14	**1**	**33**	**16**	**18**	**0.146**
Cdc5	**1**	**12.3**	**9**	**9**	**0.077**
Glc7	**1**	**20.5**	**6**	**9**	**0.076**
Ipl1	**0.9883**	**4.1**	**1**	**2**	**0.02**

Representative mass spectrometry data of purified kinetochore particles (Mtw1-3Flag) showing the proportion of total spectra corresponding to mitotic kinases and phosphatases.

Table II. Mps1 phosphorylation sites identified on Spc105 by mass spectrometry

Phosphorylation site	Phosphopeptide	PeptideProphet score
S57	KEVLDG**pS**NTTSR	0.7200
T60	EVLDGSNT**pT**SR	0.5066
S77	RV**pS**FAPDVTLHSFTFVPEQNNEIK	0.9136
T83	VSFAPDV**pT**LHSFTFVPEQNNEIKEPR	0.8749
T143	TAAEEDPD**pT**SGMELTEPIVATPDSNK	0.6381
S144	TAAEEDPDT**pS**GMELTEPIVATPDSNK	0.7644
T149	TAAEEDPDTSGMEL**pT**EPIVATPDSNK	**0.9787**
T155	TAAEEDPDTSGMELTEPIVA**pT**PDSNK	0.9738
T172	ASQHDPTSMEM**pT**EVFPR	**0.9636**
T235	DTVEGEPIDL**pT**EYESKPYVPNSVSR	**0.9354**
S329	DNHHIDE**pS**PSEK	0.9036
T356	LDTVSDYAASVT**pT**PVK	0.9700
T364	D**pT**SGEDNDGDLEMMEK	0.7840
S380	M**pS**PITFSDVDNK	0.9961
T383	MSPI**pT**FSDVDNK	0.3751
S385	MSPITF**pS**DVDNK	0.9296
S886	VHISTQQDY**pS**PSR	0.8822

Spc105 protein was purified from ATP-treated kinetochore particle preparations by gel extraction. Peptide assignments were verified by manual inspection, with a PeptideProphet score of approximately 0.87 corresponding to a 2% false discovery rate. MELT-like sequences are shown in underline and the corresponding sites and PeptideProphet scores are shown in bold.

Table III. List of residues mutated in Bub1-15A

Mutated residue	Mass spec ID
T485	+
T486	-
T487	-
S488	-
T509	+
T518	+
S537	-
S539	-
S540	-
T541	+
T555	-
T556	+
T558	-
T566	+
S578	+

Sites identified as phosphorylated by mass spectrometry (see methods) are indicated by a “+” in the right column.

Table IV. Phenotypic analysis of candidate Bub1 phosphomutants

Allele	**Genotype**	**Benomyl sensitivity**	Plasmid
15A	T485A, T486A, T487A, S488A, T509A, T518A, T537A, S539A, S540A, T541A, T555A, T556A, T558A, T566A, S578A	++	pSB1984
14A	T485A, T486A, T487A, S488A, T509A, T518A, T537A, S539A, S540A, T541A, T555A, T556A, T558A, S578A	++	pSB1988
9A	T537A, S539A, S540A, T541A, T555A, T556A, T558A, T566A, S578A	-	pSB2008
6A	T485A, T486A, T487A, S488A, T509A, T518A	++	pSB2005
5A	T485A, T486A, T487A, S488A, T509A	++	pSB2011
4A	T485A, T486A, T487A, S488A	++	pSB2012
3A	T485A, T509A, T518A	++	pSB2055
2A	T509A, T518A	++	pSB2010
2A	T485A, T509A	++	pSB2048
2A	T485A, T518A	-	pSB2049
1A	T509A	+	pSB2009
1A	T485A	-	pSB2044
1A	T455A	++	pSB1986
15D	T485D, T486D, T487D, T488D, T509D, T518D, T537D, S539D, S540D, T541D, T555D, T556D, T558D, T566D, S578D	++	pSB1977
6D	T485D, T486D, T487D, T488D, T509D, T518D	++	pSB2021
3D	T485D, T509D, T518D	-	pSB2069
2D	T485D, T518D	-	pSB2051
2D	T485D, T509D	-	pSB2050

The contribution of Bub1 phosphorylation sites to checkpoint function was analyzed by mutational analysis followed by testing Bub1 mutant strains for sensitivity to benomyl. The indicated Bub1 mutant alleles were transformed into strains lacking endogenous Bub1. N-terminal sites within the Bub1-15A set were found to confer benomyl sensitivity. T455, a residue within the conserved domain upon which we detected phosphorylation but was not mutated in *bub1-15A*, also conferred sensitivity upon mutation to alanine.

A previously characterized Cdk1 phosphorylation site (T566 (Goto et al., 2011)) was included within Bub1-15A, but this mutation is not necessary for the *bub1-15A* phenotype because reversion of this mutation (*bub1-14A*) did not complement benomyl sensitivity, nor was this mutation present in the minimal Bub1 phosphomutants for the checkpoint defect (this table and Fig IV.5C and IV.5E). - = not benomyl sensitive, + = slightly benomyl sensitive, ++ = similar benomyl sensitivity to *mad1*Δ or *mad2*Δ.

Table V: Strain Table

Strain	Genotype
SBY3	*MAT**a** ura3-1 leu2,3-112 his3-11 trp1-1 ade2-1 LYS2 can1-100 bar1D*
SBY292	*MAT**a** ura3-1 leu2,3-112 his3-11 trp1-1 LYS2 ade2-1 can1-100 mad2::URA3*
SBY3269	*MAT**a** ura3-1 leu2,3-112 his3-11 trp1-1 LYS2 ade2-1 can1-100 bar1-1 BUB1-13myc:TRP1*
SBY4020	*MAT**a** ura3-1::pGAL-GLC7::URA3 leu2,3-112 his3-11 trp1-1 lys2D ade2-1 can1-100 bar1-1 BUB1-13myc::TRP1*
SBY4587	*MAT**a** ura3-1::pGAL-MPS1-myc::URA3 leu2,3-112 his3-11,15 glc7::LEU2 trp1-1::GLC7::TRP1 LYS2 ade2-1 can1-100 bar1-1 BUB1-13myc::TRP1*
SBY7420	*MATa ura3-1 leu2,3-112 his3-11 trp1-1 LYS2 ade2-1 can1-100 bar1-1 SPC105-3Flag::TRP1*
SBY7492	*MAT**a** ura3-1 leu2,3-112 his3-11 trp1-1 LYS2 ade2-1 can1-100 bar1-1 SPC105-3Flag::TRP1*
SBY8253	*MAT**a** ura3-1 leu2,3-112 his3-11 trp1-1 ade2-1 can1-100 LYS2 bar1-1 DSN1-6His-3Flag::URA3*
SBY8415	*MAT**a** ura3-1 leu2,3-112 his3-11 trp1-1 ade2-1 can1-100 bar1-1 DSN1-6His-3Flag::URA3 MAD1-3GFP::HIS3 (pSB1601)*
SBY8416	*MAT**a** ura3-1 leu2,3-112 his3-11 trp1-1 ade2-1 can1-100 bar1-1 MAD1-3GFP::HIS3 (pSB1601)*
SBY8502	*MAT**a** ura3-1 leu2,3-112 his3-11 trp1-1 ade2-1 can1-100 LYS2 bar1-1 DSN1-6His-3Flag::URA3 BUB1-3GFP::HIS3*
SBY8564	*MAT**a** ura3-1 leu2,3-112 his3-11 trp1-1 ade2-1 can1-100 bar1-1 MTW1-3Flag::KANMX*
SBY8579	*MAT**a** ura3-1 leu2,3-112 his3-11 trp1-1 ade2-1 can1-100 bar1-1 DSN1-6His-3Flag::URA3 MAD1-3GFP::HIS3 (pSB1601) ndc80-1*
SBY8712	*MAT**a** ura3-1 leu2,3-112 his3-11 trp1-1 ade2-1 can1-100 LYS2 bar1-1 DSN1-6His-3Flag::URA3 ipl1-321*
SBY8716	*MAT**a** ura3-1 leu2,3-112 his3-11 trp1-1 ade2-1 can1-100 LYS2 bar1-1 DSN1-6His-3Flag::URA3 cdc28-13*

SBY8726 *MAT**a** ura3-1 leu2,3-112 his3-11 trp1-1 ade2-1 can1-100 LYS2 bar1-1 DSN1-6His-3Flag::URA3 mps1-1*

SBY8750 *MAT**a** ura3-1 leu2,3-112 his3-11 trp1-1 ade2-1 can1-100 LYS2 bar1-1 DSN1-6His-3Flag::URA3 SPC105-3GFP::HIS3*

SBY8829 *MAT**a** ura3-1 leu2,3-112 his3-11 trp1-1 ade2-1 can1-100 bar1-1 DSN1-6His-3Flag::URA3 MAD1-3GFP::HIS3 (pSB1601) spc105-15*

SBY8850 *MAT**a** ura3-1 leu2,3-112 his3-11 trp1-1 ade2-1 can1-100 LYS2 bar1-1 BUB3-3GFP::HIS3*

SBY8882 *MAT**a** ura3-1 leu2,3-112 his3-11 trp1-1 ade2-1 can1-100 LYS2 bar1-1 DSN1-6His-3Flag::URA3 BUB3-3GFP::HIS3*

SBY8920 *MAT**a** ura3-1 leu2,3-112 his3-11 trp1-1 ade2-1:: Ubi-R-TetR-BUB1::ADE2 can1-100 LYS2 bar1-1 DSN1-6His-3Flag::URA3 bub1::KanMX*

SBY8970 *MAT**a** ura3-1 leu2,3-112 his3-11 trp1-1 ade2-1 can1-100 bar1-1 SPC105-3Flag::TRP1 MAD1-3GFP::HIS3 (pSB1601)*

SBY8971 *MAT**a** ura3-1 leu2,3-112 his3-11 trp1-1 ade2-1 can1-100 bar1-1 NUF2-3Flag::KANMX MAD1-3GFP::HIS3*

SBY9099 *MAT**a** ura3-1 leu2,3-112 his3-11 trp1-1 ade2-1 can1-100 LYS2 bar1-1 DSN1-6His-3Flag::URA3 SPC105-3GFP::HIS3 mps1-1*

SBY9192 *MAT**a** ura3-1 leu2,3-112 his3-11 trp1-1 ade2-1 can1-100 bar1-1 DSN1-6His-3Flag::URA3 mps1::KANMX::10myc-mps1-as1::TRP1*

SBY9226 *MAT**a** ura3-1 leu2,3-112 his3-11 trp1-1 ade2-1 can1-100 LYS2 bar1-1 SPC105-3Flag::TRP1 BUB1-myc13::TRP1*

SBY9347 *MAT**a** ura3-1 leu2,3-112 his3-11 trp1-1 ade2-1 can1-100 lys2D DSN1-6His-3Flag::URA3 BUB3-3GFP::HIS3 mps1-1*

SBY9348 *MAT**a** ura3-1 leu2,3-112 his3-11 trp1-1 ade2-1 can1-100 LYS2 bar1-1 DSN1-6His-3Flag::URA3 BUB1-3GFP::HIS3 mps1-1*

SBY9476 *MAT**a** ura3-1 leu2,3-112 his3-11 trp1-1 ade2-1 can1-100 LYS2 bar1-1 SPC105-3Flag::TRP1 BUB1-myc13::TRP1 mps1-1*

SBY9478 *MAT**a** ura3-1 leu2,3-112 his3-11 trp1-1 ade2-1 can1-100 LYS2 bar1-1 SPC105-3Flag::TRP1 BUB3-3GFP::HIS3*

SBY9952 *MAT**a** ura3-1::pGAL-MPS1-myc::URA3 leu2,3-112 his3-11 trp1-1 ade2-1 can1-100 LYS2 bar1-1 SPC105-3Flag::TRP1*

SBY9971 *MAT**a** ura3-1::pGAL-GLC7::URA3 leu2,3-112 his3-11 trp1-1 ade2-1 can1-100 lys2D bar1-1 SPC105-3Flag::TRP1 BUB1-13myc::TRP1*

SBY10059 *MAT**a** ura3-1 leu2,3-112 his3-11 trp1-1 ade2-1 can1-100 LYS2 bar1-1 DSN1-6His-3Flag::URA3 mps1D::KAN::10myc-mps1-as1::TRP BUB1-3GFP::HIS3*

SBY10100 *MAT**a** ura3-1::pGAL-MPS1-myc::URA3 leu2,3-112 his3-11 trp1-1 ade2-1 can1-100 LSY2 bar1-1 SPC105-3Flag::TRP1 BUB1-13myc::TRP1*

SBY10116 *MAT**a**/MAT**a** ura3-1/ ura3-1 leu2,3-112/ leu2,3-112 his3-11/ his3-11 trp1-1/ trp1-1 ade2-1/ ade2-1 can1-100/ can1-100 bar1-1/ bar1-1 DSN1-6His-3Flag::URA3/DSN1-6His-3Flag::URA3 SPC105/spc105::TRP1 MTW1/MTW1-mCherry::HYGRO BUB1/BUB1-GFP::KANMX*

SBY10118 *MAT**a** ura3-1 leu2,3-112 his3-11 trp1-1 ade2-1 can1-100 LSY2 bar1-1 SPC105-3Flag::TRP1 BUB3-3GFP::HIS3 mps1-1*

SBY10254 *MAT**a** ura3-1 leu2,3-112 his3-11::spc105-6A-9myc::HIS3 trp1-1 ade2-1 can1-100 LSY2 bar1-1 spc105::TRP1 DSN1-6His-3Flag::URA3*

SBY10264 *MAT**a** ura3-1 leu2,3-112 his3-11::spc105-6A-9myc::HIS3 trp1-1 ade2-1 can1-100 LSY2 bar1-1 spc105::TRP1 DSN1-6His-3Flag::URA3 MTW1-mCherry::HPH BUB1-GFP::KanMX*

SBY10265 *MAT**a** ura3-1 leu2,3-112 his3-11::spc105-6A-9myc::HIS3 trp1-1 ade2-1 can1-100 LSY2 bar1-1 spc105::TRP1 DSN1-6His-3Flag::URA3*

SBY10266 *MAT**a** ura3-1 leu2,3-112 his3-11::SPC105-9myc::HIS3 trp1-1 ade2-1 can1-100 LSY2 bar1-1 spc105::TRP1 DSN1-6His-3Flag::URA3 MTW1-mCherry::HPH BUB1-GFP::KanMX*

SBY10267 *MAT**a** ura3-1 leu2,3-112 his3-11::SPC105-9myc::HIS3 trp1-1 ade2-1 can1-100 LSY2 bar1-1 spc105::TRP1 DSN1-6His-3Flag::URA3*

SBY10268 *MAT**a** ura3-1 leu2,3-112 his3-11::spc105-6A-9myc::HIS3 trp1-1 ade2-1 can1-100 LSY2 bar1-1 spc105::TRP1 DSN1-6His-3Flag::URA3 BUB1-GFP::KanMX*

SBY10271 *MAT**a** ura3-1::pGAL-MPS1-myc::URA3 leu2,3-112 his3-11 trp1-1 ade2-1 can1-100 LSY2 bar1-1 DSN1-6His-3Flag::URA3 BUB1-3GFP::HIS3 NUF2-mCherry::HPH*

SBY10282 *MAT**a** ura3-1 leu2,3-112 his3-11 trp1-1 ade2-1 can1-100 LSY2 bar1-1 mps1::KanMX::10myc-mps1-as1::TRP1 BUB1-3GFP::HIS3 MTW1-mCherry::HPH pMET-CDC20::TRP1*

SBY10318 *MAT**a** ura3-1 leu2,3-112 his3-11 trp1-1 ade2-1 can1-100 LSY2 bar1-1 BUB1-3GFP::HIS3 MTW1-mCherry::HPH pMET-CDC20::TRP1*

SBY10347 *MAT**a** ura3-1 leu2,3-112 trp1-1 ade2-1 can1-100 bar1-1 DSN1-6His-3Flag::URA3 spc105::TRP1 his3-11::SPC105-9myc::HIS3 BUB1-3GFP::LEU2*

SBY10351 *MAT**a** ura3-1 leu2,3-112 his3-11:: SPC105-9myc::HIS3 trp1-1 ade2-1 can1-100 bar1-1 DSN1-6His-3Flag::URA3 spc105::TRP1 BUB3-3GFP::LEU2*

SBY10372 *MAT**a** ura3-1 leu2,3-112 his3-11::spc105-(T149A, T172A, T211A, T235A, T284A, T313A)-9myc::HIS3 trp1-1 ade2-1 can1-100 bar1-1 DSN1-6His-3Flag::URA3 spc105::TRP1 BUB3-3GFP::LEU2*

SBY10373 *MAT**a** ura3-1::SPC105-6His::URA3 leu2,3-112 his3-11 trp1-1 ade2-1 can1-100 LSY2 bar1-1 spc105::TRP1 PDS1-18myc::LEU2*

SBY10374 *MAT**a** ura3-1::spc105-6A-6His::URA3 leu2,3-112 his3-11 trp1-1 ade2-1 can1-100 LSY2 bar1-1 spc105::TRP1 PDS1-18myc::LEU2*

SBY10422 *MAT**a** ura3-1 leu2,3-112 trp1-1 ade2-1 can1-100 bar1-1 DSN1-6His-3Flag::URA3 spc105::TRP1 his3-11::spc105-(T149A, T172A, T211A, T235A, T284A, T313A)-9myc::HIS3 BUB1-3GFP::LEU2*

SBY10532 *MAT**a** ura3-1 leu2,3-112 his3-11 trp1-1 ade2-1 can1-100 bar1-1 BUB1-3Flag::KANMX MAD1-13myc::TRP1*

SBY10596 *MAT**a** ura3-1 leu2,3-112 his3-11 trp1-1 ade2-1 can1-100 bar1-1 DSN1-6His-3Flag::URA3 MAD1-13myc::TRP bub1::KANMX*

SBY11006 *MAT**a** ura3-1 leu2,3-112 his3-11 trp1-1 ade2-1 can1-100 bar1-1 DSN1-6His-3Flag::URA3 MAD1-3GFP::HIS3 (pSB1601) bub1D(608-1021)::HYGRO*

SBY11072 *MAT**a** ura3-1 leu2,3-112 his3-11::BUB1-9myc::HIS3 (pSB1969) trp1-1 ade2-1 can1-100 bar1-1 DSN1-6His-3Flag::URA3 MAD1-13myc::TRP1 bub1::KANMX*

SBY11083 *MAT**a** ura3-1 leu2,3-112 his3-11:: bub1(369-608)-9myc::HIS3 (pSB1970) trp1-1 ade2-1 can1-100 bar1-1 DSN1-6His-3Flag::URA3 MAD1-13myc::TRP1 bub1::KANMX*

SBY11149 *MAT**a** ura3-1 leu2,3-112 his3-11::bub1(369-608)-spc105-(T149A, T172A, T211A, T235A, T284A, T313A)-9myc::HIS3 (pSB1981) trp1-1 ade2-1 can1-100 bar1-1 DSN1-6His-3Flag::URA3 spc105::TRP1*

SBY11207 *MAT**a** ura3-1 leu2,3-112 his3-11:: SPC105-9myc::HIS3 trp1-1 ade2-1 can1-100 bar1-1 DSN1-6His-3Flag::URA3 spc105::TRP1 MAD1-3GFP::LEU2 (pSB1982)*

SBY11208 *MAT**a** ura3-1 leu2,3-112 his3-11::pSPC105-bub1(369-608)-spc105-9myc::HIS3 (pSB1980) trp1-1 ade2-1 can1-100 bar1-1 DSN1-6His-3Flag::URA3 spc105::TRP1 MAD1-3GFP::LEU2 (pSB1982)*

SBY11209 *MAT**a** ura3-1 leu2,3-112 his3-11::pSPC105-bub1(369-608)-spc105-(T149A, T172A, T211A, T235A, T284A, T313A)-9myc::HIS3 (pSB1981) trp1-1 ade2-1 can1-100 bar1-1 DSN1-6His-3Flag::URA3 spc105::TRP1 MAD1-3GFP::LEU2 (pSB1982)*

SBY11210 *MAT**a** ura3-1 leu2,3-112 his3-11:: spc105-(T149A, T172A, T211A, T235A, T284A, T313A)-9myc::HIS3 trp1-1 ade2-1 can1-100 bar1-1 DSN1-6His-3Flag::URA3 spc105::TRP1 MAD1-3GFP::LEU2 (pSB1982)*

SBY11232 *MAT**a** ura3-1 leu2,3-112 his3-11::HIS3 trp1-1 ade2-1 can1-100 bar1-1 DSN1-6His-3Flag::URA3 MAD1-13myc::TRP bub1::KANMX*

SBY11238 *MAT**a** ura3-1 leu2,3-112 his3-11::bub1(T455A)-9myc::HIS3 (pSB1986) trp1-1 ade2-1 can1-100 bar1-1 DSN1-6His-3Flag::URA3 MAD1-13myc::TRP1 bub1::KANMX*

SBY11303 *MAT**a** ura3-1 leu2,3-112 his3-11::pSPC105-bub1(369-608)-spc105-(T149A, T172A, T211A, T235A, T284A, T313A)-9myc::HIS3 (pSB1981) trp1-1 ade2-1 can1-100 bar1-1 DSN1-6His-3Flag::URA3 spc105::TRP1 MAD1-3GFP::LEU2 (pSB1982) bub1::KANMX*

SBY11315 *MAT**a** ura3-1 leu2,3-112 his3-11 trp1-1 ade2-1 can1-100 bar1-1 PDS1-18myc::LEU2 bub1::KANMX*

SBY11317 *MAT**a** ura3-1 leu2,3-112 his3-11::BUB1-9myc::HIS3 (pSB1983) trp1-1 ade2-1 can1-100 bar1-1 DSN1-6His-3Flag::URA3 MAD1-*

3GFP::LEU2::TRP1 (pSB1982) bub1::KANMX

SBY11319 *MAT**a** ura3-1 leu2,3- his3-11:: bub1D(369-608)-9myc::HIS3 (pSB1985) trp1-1 ade2-1 can1-100 bar1-1 DSN1-6His-3Flag::URA3 MAD1-3GFP::LEU2::TRP1 (pSB1982) bub1::KANMX*

SBY11325 *MAT**a** ura3-1 leu2,3-112 his3-11::pSPC105-bub1(369-608)- (T485A, T486A, T487A, S488A, T509A, T518A, T537A, S539A, S540A, T541A, T555A, T556A, T558A, T566A, S578A)-spc105-(T149A, T172A, T211A, T235A, T284A, T313A)-9myc::HIS3 (pSB1998) trp1-1 ade2-1 can1-100 bar1-1 DSN1-6His-3Flag::URA3 spc105::TRP1*

SBY11340 *MAT**a** ura3-1 leu2,3-112 his3-11::BUB1-6His::HIS3 (pSB1989) trp1-1 ade2-1 can1-100 bar1-1 bub1::KANMX PDS1-18myc::LEU2*

SBY11341 *MAT**a** ura3-1 leu2,3-112 his3-11::bub1-(T485A, T486A, T487A, S488A, T509A, T518A, T537A, S539A, S540A, T541A, T555A, T556A, T558A, T566A, S578A)-6His::HIS3 (pSB1990) trp1-1 ade2-1 can1-100 bar1-1 bub1::KANMX PDS1-18myc::LEU2*

SBY11342 *MAT**a** ura3-1 leu2,3-112 trp1-1 ade2-1 can1-100 bar1-1*

bub1::KANMX PDS1-18myc::LEU2

his3-11::bub1D(369-608)-6His::HIS3 (pSB1991)

SBY11368 *MAT**a**/MAT**a** ura3-1/ ura3-1::SPC105-9myc::URA leu2,3-112/ leu2,3-112 his3-11/ his3-11 trp1-1/ trp1-1 ade2-1/ ade2-1 can1-100/ can1-100 bar1-1/ bar1-1 LYS2/lys2D PDS1/PDS1-18myc::LEU2 SPC105/spc105::HYGRO*

SBY11389 *MAT**a** ura3-1 leu2,3-112 his3-11 trp1-1 ade2-1 can1-100 bar1-1 MAD1-3GFP::LEU2 (pSB1982) mad2::KANMX*

SBY11392 *MAT**a** ura3-1 leu2,3-112 his3-11 trp1-1 ade2-1 can1-100 bar1-1 MAD1-3GFP::LEU2 (pSB1982)*

SBY11415 *MAT**a** ura3-1 leu2,3-112 his3-11::pSPC105-bub1(369-608)- (T485A, T486A, T487A, S488A, T509A, T518A, T537A, S539A, S540A, T541A, T555A, T556A, T558A, T566A, S578A)-spc105-(T149A, T172A, T211A, T235A, T284A, T313A)-9myc::HIS3 (pSB1998) trp1-1 ade2-1 can1-100 bar1-1 DSN1-6His-3Flag::URA3 spc105::TRP1 MAD1-3GFP::LEU2 (pSB1982)*

SBY11418 *MAT**a** ura3-1 leu2,3-112 his3-11 trp1-1 ade2-1 can1-100 bar1-1 MAD1-3GFP::LEU2 (pSB1982) bub3::KANMX*

SBY11464 *MAT**a** ura3-1 leu2,3-112 his3-11 trp1-1 ade2-1 can1-100 bar1-1 MAD1-3GFP::LEU2 (pSB1982) bub1::KANMX*

SBY11486 *MAT**a** ura3-1 leu2,3-112 his3-11::pSPC105-bub1(369-608)-spc105-(T149A, T172A, T211A, T235A, T284A, T313A)-9myc::HIS3 (pSB1981) trp1-1 ade2-1 can1-100 bar1-1 DSN1-6His-3Flag::URA3 spc105::TRP1 mps1::KANMX::10myc-mps1-as1::TRP1*

SBY11488 *MAT**a** ura3-1::pGAL-MPS1-myc::URA3 leu2,3-112 his3-11 trp1-1 ade2-1 can1-100 bar1-1 BUB1-3Flag::KANMX MAD1-13myc::TRP1*

SBY11490 *MAT**a** ura3-1::pGAL-MPS1-myc::URA3 leu2,3-112 his3-11 trp1-1 ade2-1 can1-100 bar1-1 BUB1-3Flag::KANMX lys2D*

SBY11497 *MAT**a** ura3-1 leu2,3-112 his3-11 trp1-1 ade2-1 can1-100 bar1-1 DSN1-6His-3Flag::URA3 MAD1-3GFP::LEU2 (pSB1982) mad3::KANMX*

SBY11541 *MAT**a** ura3-1::pGAL-MPS1-myc::URA3 leu2,3-112 his3-11 trp1-1 ade2-1 can1-100 bar1-1 MAD1-13myc::TRP1*

SBY11637 *MAT**a** ura3-1 leu2,3-112 his3-11::pSPC105-bub1(369-608)-spc105-(T149A, T172A, T211A, T235A, T284A, T313A)-9myc::HIS3 (pSB1981) trp1-1 ade2-1 can1-100 bar1-1 DSN1-6His-3Flag::URA3 spc105::TRP1 BUB3-3GFP::LEU2 (pSB1881)*

SBY11725 *MAT**a** ura3-1 leu2,3-112 his3-11::pSPC105-bub1(369-608)-spc105-(T149A, T172A, T211A, T235A, T284A, T313A)-9myc::HIS3 (pSB1981) trp1-1 ade2-1 can1-100 bar1-1 DSN1-6His-3Flag::URA3 spc105::TRP1 BUB1-3GFP::LEU2*

SBY11751 *MAT**a** ura3-1 leu2,3-112 his3-11:: bub1(T485A, T509A, T518A)-9myc::HIS3 (pSB2055) trp1-1 ade2-1 can1-100 bar1-1 DSN1-6His-3Flag::URA3 MAD1-3GFP::LEU2 (pSB1982) bub1::TRP1*

SBY11764 *MAT**a** ura3-1 leu2,3-112 his3-11::BUB1-9myc::HIS3 (pSB1983) trp1-1 ade2-1 can1-100 bar1-1 DSN1-6His-3Flag::URA3 MAD1-3GFP::LEU2 (pSB1982) bub1::TRP1*

SBY11766 *MAT**a** ura3-1 leu2,3-112 his3-11::bub1-(T485A, T486A, T487A, S488A, T509A, T518A, T537A, S539A, S540A, T541A, T555A, T556A, T558A, T566A, S578A)-9myc::HIS3 (pSB1984) trp1-1 ade2-1 can1-100 bar1-1 DSN1-6His-3Flag::URA3 MAD1-3GFP::LEU2*

(pSB1982) bub1::TRP1

SBY11840 *MAT**a** ura3-1::MAD1(D327G)-9myc::URA3 (pSB1935) leu2,3-112 his3-11 trp1-1 ade2-1 can1-100 bar1-1 DSN1-6His-3Flag::URA3 mad1::KANMX*

SBY11853 *MAT**a** ura3-1 leu2,3-112 his3-11:: BUB1-9myc::HIS3 (pSB1983) trp1-1 ade2-1 can1-100 bar1-1 DSN1-6His-3Flag::URA3 bub1::TRP1*

SBY11892 *MAT**a** ura3-1 leu2,3-112 his3-11:: SPC105-2V5::HIS3 (pSB2082) trp1-1 ade2-1 can1-100 bar1-1 PDS1-18myc::LEU2 spc105::HYGRO*

SBY11893 *MAT**a** ura3-1 leu2,3-112 his3-11::spc105-(T149A, T172A, T211A, T235A, T284A, T313A)-2V5::HIS3 (pSB2083) trp1-1 ade2-1 can1-100 bar1-1 PDS1-18myc::LEU2 spc105::HYGRO*

SBY11894 *MAT**a** ura3-1 leu2,3-112 his3-11::pSPC105-bub1(369-608)-spc105-(T149A, T172A, T211A, T235A, T284A, T313A)-2V5::HIS3 (pSB2084) trp1-1 ade2-1 can1-100 bar1-1 PDS1-18myc::LEU2 spc105::HYGRO*

SBY11967 *MAT**a** ura3-1::mad1-(D327G, R653A, L654A, K655A)-9myc::URA3 (pSB1954) leu2,3-112 his3-11 trp1-1 ade2-1 can1-100 bar1-1 DSN1-6His-3Flag::URA3 mad1::KANMX*

SBY12068 *MAT**a** ura3-1 leu2,3-112 his3-11::bub11(T455A)-9myc::HIS3 (pSB1986) trp1-1 ade2-1 can1-100 bar1-1 DSN1-6His-3Flag::URA3 MAD1-3GFP::LEU2 (pSB1982) bub1::TRP1*

All strains are isogenic with the W303 background.

Table VI. Plasmids used in this study

Plasmid	Description
pRS303	*HIS3 (integrating)*
pSB205	*PDS1-18myc, LEU2 (integrating)*
pSB1332	*pSPC105-SPC105-9myc, HIS3 (integrating)*
pSB1601	*mad1(1750-2247)-3GFP, HIS3 (integrating)*
pSB1878	*pSPC105-spc105(T149A, T172A, T211A, T235A, T284A, T313A)-9myc, HIS3 (integrating)*
pSB1880	*bub1(2305-3063)-3GFP, LEU2 (integrating))*
pSB1881	*bub3(501-1023)-3GFP, LEU2 (integrating)*
pSB1935	*pMAD1-MAD1(D327G)-9myc, URA3 (integrating)*
pSB1954	*pMAD1-MAD1(D327G, R653A, L654A, K655A)-9myc, URA3 (integrating)*
pSB1969	*pBUB1-BUB1-9myc, HIS3 (integrating)*
pSB1970	*pBUB1-bub1(D369-608)-9myc, HIS3 (integrating)*
pSB1975	*pBUB1-BUB1(SpeI)-9myc, HIS3 (integrating)*
pSB1976	*pBUB1-bub1(T485A, T486A, T487A, S488A, T509A, T518A, T537A, S539A, S540A, T541A, T555A, T556A, T558A, T566A, S578A)-9myc, HIS3 (integrating)*
pSB1977	*pBUB1-bub1(T485D, T486D, T487D, S488D, T509D, T518D, T537D, S539D, S540D, T541D, T555D, T556D, T558D, T566D, S578D)-9myc, HIS3 (integrating)*
pSB1980	*pSPC105-bub1(369-608)-spc105-9myc, HIS3 (integrating)*
pSB1981	*pSPC105-bub1(369-608)-spc105(T149A, T172A, T211A, T235A, T284A, T313A)-9myc, HIS3 (integrating)*
pSB1982	*mad1(1750-2247)-3GFP, LEU2 (integrating)*
pSB1983	*pBUB1-BUB1-9myc-BUB1-3'-UTR, HIS3 (integrating)*
pSB1984	*pBUB1-bub1(T485A, T486A, T487A, S488A, T509A, T518A, T537A,*

	S539A, S540A, T541A, T555A, T556A, T558A, T566A, S578A)-9myc-BUB1-3'-UTR, HIS3 (integrating)
pSB1985	*pBUB1-bub1(D369-608)-9myc-BUB-3'-UTR, HIS3 (integrating)*
pSB1986	*pBUB1-bub1(T455A)-9myc-BUB1-3'-UTR, HIS3 (integrating)*
pSB1988	*pBUB1-bub1(T485A, T486A, T487A, S488A, T509A, T518A, T537A, S539A, S540A, T541A, T555A, T556A, T558A, S578A)-9myc-BUB1-3'-UTR, HIS3 (integrating)*
pSB1989	*pBUB1-BUB1-6His-BUB1-3'-UTR, HIS3 integrating*
pSB1990	*pBUB1-bub1(T485A, T486A, T487A, S488A, T509A, T518A, T537A, S539A, S540A, T541A, T555A, T556A, T558A, T566A, S578A)-6His-BUB1-3'-UTR, HIS3 (integrating)*
pSB1991	*pBUB1-bub1(D369-608)-6His-BUB1-3'-UTR, HIS3 (integrating)*
pSB1998	*pSPC105-bub1(369-608)(T485A, T486A, T487A, S488A, T509A, T518A, T537A, S539A, S540A, T541A, T555A, T556A, T558A, T566A, S578A)-SPC105(T149A, T172A, T211A, T235A, T284A, T313A)-9myc, HIS3 (integrating)*
pSB2000	*pMal-C2X:MBP-bub1(369-608)*
pSB2002	*pMal-C2X:MBP-bub1(369-608)(T485A, T486A, T487A, S488A, T509A, T518A, T537A, S539A, S540A, T541A, T555A, T556A, T558A, T566A, S578A)*
pSB2005	*pBUB1-bub1(T485A, T486A, T487A, S488A, T509A, T518A)-BUB1-3'-UTR-9myc, HIS3 (integrating)*
pSB2008	*pBUB1-bub1(T537A, S539A, S540A, T541A, T555A, T556A, T558A, T566A, S578A)-BUB1-3'-UTR-9myc, HIS3 (integrating)*
pSB2009	*pBUB1-bub1(T509A)-BUB1-3'-UTR-9myc, HIS3 (integrating)*
pSB2010	*pBUB1-bub1(T509A, T518A)-BUB1-3'-UTR-9myc, HIS3 (integrating)*
pSB2011	*pBUB1-bub1(T485A, T486A, T487A, S488A, T509A)-BUB1-3'-UTR-9myc, HIS3 (integrating)*

pSB2012	*pBUB1-bub1(T485A, T486A, T487A, S488A)-BUB1-3'-UTR-9myc, HIS3 (integrating)*
pSB2021	*pBUB1-bub1(T485D, T486D, T487D, T488D, T509D, T518D)-BUB1-3'-UTR-9myc, HIS3 (integrating)*
pSB2038	*pETDuet-1:6His-MPS1*
pSB2040	*pETDuet-1:6His-MPS1, bub1(369-608)-S-tag*
pSB2041	*pCDFDuet-1:6His-MAD2*
pSB2044	*pBUB1-bub1(T485A)-BUB1-3'-UTR-9myc, HIS3 (integrating)*
pSB2045	*pBub1-bub1(T485D)-BUB1-3'-UTR-9myc, HIS3 (integrating)*
pSB2048	*pBUB1-bub1(T485A, T509A)-BUB1-3'-UTR-9myc, HIS3 (integrating)*
pSB2049	*pBUB1-bub1(T485A, T518A)-BUB1-3'-UTR-9myc, HIS3 (integrating)*
pSB2050	*pBUB1-bub1(T485D, T509D)-BUB1-3'-UTR-9myc, HIS3 (integrating)*
pSB2051	*pBUB1-bub1(T485D, T518D)-BUB1-3'-UTR-9myc, HIS3 (integrating)*
pSB2054	*pCDFDuet-1:6His-MAD2, Mad1(318-749)-3Flag*
pSB2055	*pBUB1-bub1(T485A, T509A, T518A)-BUB1-3'-UTR-9myc HIS3 (integrating)*
pSB2057	*pCDFDuet-1:3Flag*
pSB2058	*pETDuet-1:bub1(369-608)-S-tag*
pSB2062	*pCDFDuet-1:mad1(318-749)-3Flag*
pSB2063	*pETDuet-1:6His-MPS1, bub1(369-608)(T485A, T486A, T487A, S488A, T509A, T518A, T537A, S539A, S540A, T541A, T555A, T556A, T558A, T566A, S578A)-S-tag*
pSB2064	*pETDuet-1:6His-MPS1, bub1(369-608)(T485A, T509A, T518A)-S-tag*
pSB2069	*pBUB1-bub1(T485D, T509D, T518D)-9myc, HIS3 (integrating)*
pSB2082	*pSPC105-SPC105-2V5, HIS3 (integrating)*
pSB2083	*pSPC105-spc105(T149A, T172A, T211A, T235A, T284A, T313A)-2V5, HIS3 (integrating)*
pSB2084	*pSPC105-bub1(369-608)-spc105(T149A, T172A, T211A, T235A,*

	T284A, T313A)-2V5, HIS3 (integrating)
pSB2087	*pCDFDuet-1:2V5-MAD2, mad1(318-749)-3Flag*
pSB2090	*pCDFDuet-1:2V5-MAD2, 3Flag*
pSK1039 (Kemmler et al. 2009)	*pNDC80-ndc80(S4A, T5A, S6A, T21A, S22A, S37A, T38A, T43A, T74, T79, T82, S205A, T248A, T252A)-3HA-KANMX6-NDC80 C-terminus*

VITA

Nitobe London completed his bachelor of science in biochemistry at Western Washington University in 2003, performing research on plant virus replication with Dr. Gerry Prody. He next worked at the Fred Hutchinson Cancer Research Center (FHCRC) as a lab aide and technician in the laboratory of Dr. Jim Priess. Nitobe joined the Molecular and Cellular Biology program at the University of Washington as a graduate student in 2008 and performed his doctoral research work in the laboratory of Dr. Sue Biggins at the FHCRC.